

**POLITECNICO DI  
TORINO**

**Master of Science in Building Engineering  
Green Building specialist track**



**UNIVERSIDAD POLITÉCNICA DE  
CARTAGENA**

**Escuela técnica superior de Arquitectura y Edificación  
Máster en Patrimonio Arquitectónico**

**Towards the 3D cadastre: GIS-BIM  
integration for 3D information management  
of the city of Cehegín**

*Master Thesis*

*Degree session 02.12.2024*

**Supervisor:**

Villa Valentina

**Co- Supervisors:**

Matrone Francesca

Jiménez Vicario, Pedro Miguel

**Candidate:**

Cioce Martina

|  |    |
|--|----|
| Abstract.....  | 4  |
| Introduction .....   | 5  |
| Objectives .....   | 7  |
| 1. State of the art.....   | 8  |
| 1.1. The 2D Cadastre: Management and Limitations .....             | 8  |
| 1.2. The 3D cadastre .....   | 13 |
| 1.3. Advantages of 3D respect to 2D.....                           | 20 |
| 1.4. BIM and GIS in the 3D Cadastre: A Technological Synergy ..... | 21 |
| 1.5. Useful techniques for BIM-GIS integration.....                | 27 |
| 2. Case study: Cehegín, Spain.....                                 | 30 |
| 3. Methodology .....   | 32 |
| 3.1 Data collection.....   | 34 |
| 3.1.1. Accessed by cartographic viewer .....                       | 36 |
| 3.1.2. Accessed by data download and mapping section .....         | 39 |
| 3.2. Data acquisition .....  | 40 |
| 3.3. Data processing .....   | 45 |
| 3.3.1. From the cartographic viewer .....                          | 45 |
| 3.3.2. Alignment of Lidar point cloud scans.....                   | 49 |
| 3.3.3. Point cloud density analysis .....                          | 54 |
| 3.3.4. Georeferencing process for the Lidar point cloud .....      | 61 |
| 3.3.5. Mesh generations .....                                      | 62 |
| 3.4. Data integration and model development.....                   | 64 |
| 3.4.1. Preliminary methodology .....                               | 65 |
| 3.4.2. From the cadastral data to LOD1.....                        | 67 |
| 3.4.3. From the point clouds to LOD2 .....                         | 73 |
| 3.4.4. From the scan to BIM to LOD3.....                           | 79 |
| 3.4.5. Integration analysis.....                                   | 83 |
| 4. Analysis and discussion of the results.....                     | 88 |
| Conclusions .....  | 90 |
| Bibliography .....   | 91 |
| Sitography.....  | 95 |
| List of figures.....   | 97 |

Acknowledgments.....101

# Abstract

Nowadays, the zero land consumption European directives and the ever-increasing multi-story building construction due to urbanisation activities are highlighting the limitations of the bidimensional cadastre. From this context, the 3D cadastre could make a key contribution to managing the future built environment and cities.

In this framework, the thesis aims to understand the potentialities of the 3D cadastre and proposes a methodology to ease its generation through rapid mapping techniques.

Italy and Spain have been analysed as case studies, and it emerged that they have yet to develop their own and complete 3D cadastral systems. A deep investigation and study of one of the most advanced in Europe, the Netherlands, has been therefore carried out.

Nevertheless, it is important to consider that the transition from 2D to 3D cadastre will increasingly be based on the BIM-GIS integration, in which the main data are usually derived from high-resolution 3D data of the urban scenarios, through photogrammetry and LiDAR techniques.

Due to the compelling necessity for the public administration to update the land register, the following thesis will thus present a methodology focused on the development of a flowing 3D model of a building block located in a historical city centre of Spain: Cehegín. This is achieved by the BIM-GIS integration and using the iPad Pro low-cost LiDAR sensor combined with UAV (Unmanned Aerial Vehicle) point cloud data to create a geometrical model. The outcome is then combined with survey data gathered from a visual analysis conducted during the site survey and cadastral data that was retrieved from the official website to create an informative model.

Levels of detail also ensure a faithful representation of the case study; as a consequence, the methodology has been divided into different phases based on them.

A further goal of this research is to step from the 2D to the 3D cadastre in a time-effective manner. The solution of using the iPad Pro has been investigated since it can produce rapid 3D scanning with reduced time and costs of the operations during the site survey. The results prove that the iPad Pro produced a highly detailed point cloud but up to a certain height and without georeferencing, which has led to a necessary integration and georeferencing respect to the point cloud derived from the drone. Moreover, the level of detail obtained during the process is equal to LOD3. However, some interoperability problems were found during the integration of cadastral data in the BIM model imported in GIS software. The causes of these criticalities, which led to a partial inclusion of the cadastral data in the BIM model, can be found within the exchange formats and the limitations of multipatch in GIS software. Our hope is that these results and considerations will establish the groundwork for future investigations.

## **Keywords**

*3D cadastre, iPad, drone, LIDAR, photogrammetry, BIM, GIS, historical buildings*



# Introduction

The United Nations predicted in 2011 a dramatic increase of the level of urbanization, from 52% in 2011 to 67% in 2050 (United Nations Department of Economic and Social Affairs/Population Division, 2011). The growth of urban populations and the consequent growth of urban infrastructures and institutions to support this huge growth represent a global discussion topic. Between all the organisations that must be established to predict, keep up with, and facilitate this growth to benefit urban planning and management, the cadastre is the most important. However, since urban areas expand both horizontally and vertically, a renovation of the current cadastral system is necessary (van Oosterom, 2018). In this context, the 3D cadastre born as solution. The 3D cadastre offers a detailed and three-dimensional model of buildings and parcels, facilitating analysis and visualisation of the area. The main goal of the following thesis is to present a methodology for creating a 3D model that is a faithful representation of the reality, useful for the 2D cadastre transformation. Before reaching this goal, a discussion of the 2D cadastre in Italy and Spain was given, considering the similarities between the two systems. Furthermore, it was conducted scientific research concerning the 3D cadastre considering the limitations of the 2D cadastre. The Italian and Spanish cadastres were at the centre of the study. However, since these nations didn't have introduced a tri-dimensional cadastre, it was presented some pilot projects. Contrary to this scenario, it was presented the Stoter case study, which has brought great improvements within the international scene, showing the 3D cadastre in the Netherlands as the best at present. Furthermore, BIM and GIS and their standard formats was also analysed, as they are an integral part of the transformation process from 2D to 3D cadastre. Particularly, the specific classes of the IFC and CityGML useful for cadastral representation was identified. Photogrammetry and LIDAR was presented as complementary technologies to BIM and GIS and they enabled the 3D representation of buildings in urban contexts. From this discussion, it was possible to deal with the other goal of this research: the reduction of the process for the transformation of the 2D in 3D cadastre. This specific goal was achieved with the introduction of the iPad Pro. iPad Pro, which has been treated as a fast 3D scanning instrument by many researchers in the last period, has led to an improvement in terms of time and cost that far exceeds traditional systems. In addition, the instrument made it possible to obtain a very detailed point cloud of the side walls of the building under study. The obtained point cloud was later integrated with a point cloud acquired by a drone, to have a more detailed representation of the case study. Although there are many advantages, the iPad Pro is a limited tool due to the fact that it cannot exceed 5 meters in height, so it can't be provided as the only solution for scanning buildings.

Based on these considerations, the main goal of the research was achieved. It was based on a methodology, which integrates BIM and GIS, to generate a 3D model of a building in the historic district of Cehegín, Spain. The starting data was obtained through the official sites of the Spanish cadastre and from the site surveys carried out. From a general point of view, the

procedure could be divided into three parts, according to the level of detail obtained. According to CityGML, the first part's level of detail was the LOD1, which based on points derived from the point cloud of the drone and the ground level points allowed the generation of a DTM and a DSM, with subsequent generation of a 3D model on GIS software. Instead, in the second part, a polygon with cadastral data incorporated was generated, starting from cadastral data, distributed in DXF (geometric data) and in excel (descriptive data). Subsequently, a point cloud later transformed into multipatch was inserted into the GIS software. This point cloud is the result of two point clouds: the iPad Pro cloud and the drone cloud. This decision was made because, in addition to being complementary, these two point clouds produced the greatest results at the density level when compared to all other point clouds. Once the multipatch was obtained, the polygon data were transferred to the multipatch generating a 3D model of LOD2. For the last section, the BIM software was introduced. During this part, Scan to BIM procedure was used allowing the generation of a more detailed model of the building. Further information has been added via shared parameters to the building model. The information is derived from a visual analysis carried out during the site survey and from additional cadastral data, traced on the digital cadastre website. This model was later integrated into the GIS software to evaluate the interoperability between BIM and GIS. With this thesis, we hope to have laid the foundations for a future experiment of the iPad Pro within the three-dimensional transformation of the cadastre. Furthermore, we hope the following thesis establishes a foundation for ongoing research into BIM-GIS integration, aimed at creating accurate 3D model representations to support the development of 3D cadastral systems.

# Objectives

The primary goals of the following thesis are to develop a methodology that, by integrating BIM and GIS, can produce a 3D model to assist in the creation of a 3D cadastre and to suggest an efficient method to facilitate the process of converting a 2D cadastre into a 3D cadastre. Secondary goals derived from the main ones:

1. Analysis of the 2D and the 3D cadastre in Italy and Spain. The 2D cadastre is analysed in Italy and in Spain, considering the subdivision of data in the system. Some pivotal researches are presented for the 3D cadastre in Italy and in Spain, based on the absence of the 3D cadastre in these countries. To compare, further research is illustrated that represent the studies at the base of cadastre in Netherlands, considered the most innovative in Europe.
2. Investigation of iPad Pro as an efficient 3D scanning tool for cadastral applications. This study intends to evaluate the iPad Pro's efficacy as a useful tool for producing 3D models rapidly and affordably in comparison to conventional surveying equipment by looking at its speedy 3D data capturing capabilities. In terms of accuracy, effectiveness, and operational reach, this instrument can and cannot replace traditional approaches. Its limits and possible uses in a cadastral context are also reviewed. A density analysis was conducted to demonstrate the quality of iPad point cloud respect to the other point clouds, acquired with terrestrial laser scanner and aerial laser scanner.
3. Testing the interoperability between BIM and GIS systems in the integration of cadastral data and 3D models. The methodology presented to obtain a 3D model based on cadastral data and point clouds allow to examine the interoperability between BIM and GIS, and particularly the interoperability between the standard formats.

The transformation from a 2D to a 3D cadastre, is an essential change for improving land management and administration. This enhancement has important ramifications for reducing the ambiguities and inconsistencies prevalent in 2D representations and providing a more precise and exhaustive representation of the real environment. In this scenario, Building Information Modelling (BIM) and Geographic Information System (GIS) play a fundamental role. However, to fully understand the importance of this transition, it is necessary to analyse how the cadastre is structured and managed, comparing the traditional approach of the 2D cadastre with the more advanced 3D cadastre. In this research, Italian and Spanish cadastres will be examined as prototypes to analyse the 2D cadastre.

# 1. State of the art

## 1.1. The 2D Cadastre: Management and Limitations

A cadastre is the traditional parcel-based system used to register document land ownership, real estate rights, and property borders. A parcel is the basic entity of the cadastre, and it is univocally defined by a cadastral code. The spatial data of properties are represented on a two-dimensional map, as it only displays the horizontal dimensions of land parcels. Furthermore, the cadastre usually contains a geometric description of the land parcels in addition to other records that explain the nature of the interests, who owns or controls them, and often the value of the property and its renovations, as shown in the (fig. 1). As matter of fact, it can be set up for legal (conveyancing), fiscal (value and equitable taxation, for example), administrative (planning and other administrative objectives), or any combination of these (FIG, 1995). Various types of information are recorded in the cadastre such as:

- Boundaries and areas: for land and buildings, the cadastre contains the exact boundaries and total area with geographical coordinates.
- Classification: for each property or land a cadastral category (for example, civil housing, office, agricultural land) and a class are determined, which defines the quality of the property.
- Cadastral rent: each property is associated with a cadastral rent, that is the tax value representing the potential income of the property. This income is used for the calculation of property taxes.
- Intended use: information on the type of use of the property (residential, commercial, agricultural, etc.).

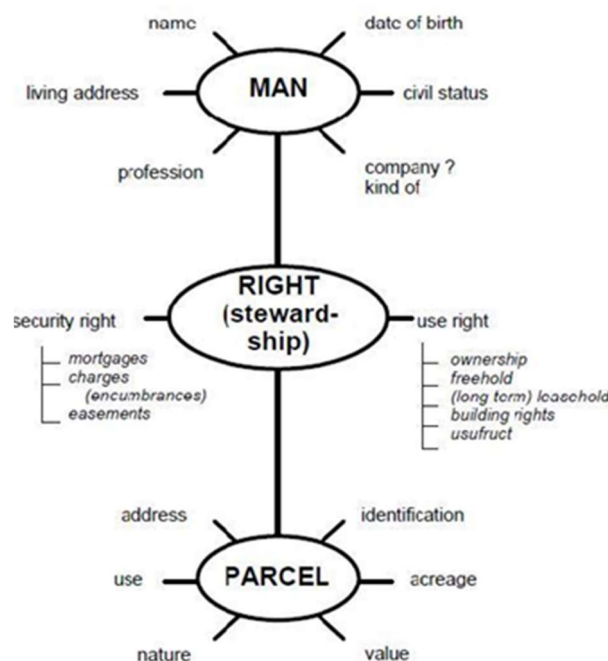


Figure 1 Description of the cadastral system. Source: (Henssen J., 1995)

### **1.1.1. Italy**

The Italian cadastre, an inventory of real estate located on national territory, is divided into land registry and building register. The land register, which includes a list of all agricultural areas, provides information on both the geometrical nature and the technical and economic characteristics of the minimum item in the inventory, the cadastral parcel. The Building Register, instead, established by the enactment of the decree-law of 30 December 1993 is the evolution of the previous Urban Building Register, related only to constructions, and deals with all buildings, both urban and rural. Each property, whether land or building, is identified by a cadastral sheet, which is a map representing a portion of the municipal territory and a parcel number, that is a unique number that identifies a portion of the soil within the sheet. Instead, for the specific case of Building Register, the subaltern is introduced to identify the individual units (e.g. apartments) within a building (Fabrizi C., 2024). Italian cadastre is managed by Agenzia delle Entrate through the Integrated Land System (SIT). The data are catalogued in the Repertorio Nazionale dei Dati Territoriali (RNDT) (AgID, n.d.), established by D.Lgs. 32/2010 following the principles outlined above by the standard of the INSPIRE Directive, INfrastructure for SPatial InfoRmation in Europe (2007/2/EC of 14 March 2007), and subdivided in layers, called Layers, Themes and Classes (fig.2).

**CLASSE: Particella catastale (PART\_CAT - 020190)**

|                                 |            |            |
|---------------------------------|------------|------------|
| <i>Popolamento della classe</i> | <b>NC1</b> | <b>NC5</b> |
|                                 |            |            |

**Definizione**

Questa classe è finalizzata al collegamento logico del Database Geotopografico alla Banca Dati del Catasto. Contiene le particelle catastali al fine di consentire la definizione della classe Corpo Edificato come Corpo Edificato Catastale, utilizzando come criterio principale di aggregazione delle unità volumetriche, o di partizione dei cassoni edilizi, prevalentemente le mappe catastali e, secondariamente, gli elementi architettonico-funzionali previsti dal Catalogo dei Dati Territoriali.

| <i>Attributi</i>  |                   |  |                   | <b>NC1</b> | <b>NC5</b> |
|---|-------------------|--|-------------------|------------|------------|
| <i>Attributi della classe</i>   |                   |  |                   | <b>NC1</b> | <b>NC5</b> |
| <b>02019001</b>   | <b>PART_CAT_C</b> | <b>codice particella catastale</b>                           | <b>String(40)</b> |            |            |
| <b>02019002</b>   | <b>PART_CAT_F</b> | <b>codice identificativo del file cartografico catastale</b> | <b>String(40)</b> |            |            |
| <p>Codice catastale della Particella, costituito dal riferimento al Comune di appartenenza (codice Belfiore), dal codice della Sezione Censuaria, dal numero di Foglio e dal numero di Particella.<br/>Es. H501A001201234, per indicare la Particella 1234, del Foglio 12, sezione censuaria A del comune di Roma.</p> <p>Codice identificativo di 11 caratteri del file cartografico catastale, costituito dal riferimento al Comune di appartenenza (codice Belfiore), dal codice della Sezione Censuaria (es. A, oppure B), dal numero di Foglio, dal codice Allegato (se trattasi di Allegato) e dal codice dello Sviluppo (se trattasi di Sviluppo). Eventuali valori non applicabili del codice Allegato e del codice dello Sviluppo saranno valorizzati con 0.<br/>Ad esempio il file contenente i dati relativi al foglio 1, allegato A della sezione B del comune di Rieti avrà il seguente identificativo: H282B0001A0.</p> |                   |  |                   |            |            |

| <i>Componenti spaziali della classe</i> |                   |                   |  | <b>NC1</b> | <b>NC5</b> |
|---|-------------------|-------------------|--|------------|------------|
| <b>020190101</b>                        | <b>PARCAT_EXT</b> | <b>Estensione</b> | <b>GU_CXSurface2D - Complex Surface 2D</b> |            |            |

**Ruoli**

|                 |   |
|-----------------|---|
| <b>Cedipart</b> | <p>Definisce gli eventuali corpi edificati appartenenti a una specifica particella catastale</p> <p><b>Cedipart [0..*]: CR_EDF <u>inverso</u> Partdice [0..*]</b></p> |
|-----------------|---|

Figure 2 Schema of Rete nazionale dati territoriali. Source: (Gruppo di Lavoro 2 “DB Geotopografici” dell’Agenzia per l’Italia Digitale, 2015)

The layers and themes do not represent a classification but are intended to collect in a simplified and homogeneous way the classes in subsets. The class, on the other hand, defines the representation of a specific type of spatial object. Furthermore, Agenzia delle Entrate offers digital services for consultation of cadastral mapping like the Cadastral Mapping Geoportal, which allows all citizens to freely consult the updated cadastral cartography through the search and dynamic visualization of cadastral parcels. The following information can be obtained by searching the cadastral parcel on the map (fig.3):

- name of the municipality
- possible census section
- map sheet number
- number or letter of the attachment
- number or letter of the development
- number or letter of the parcel

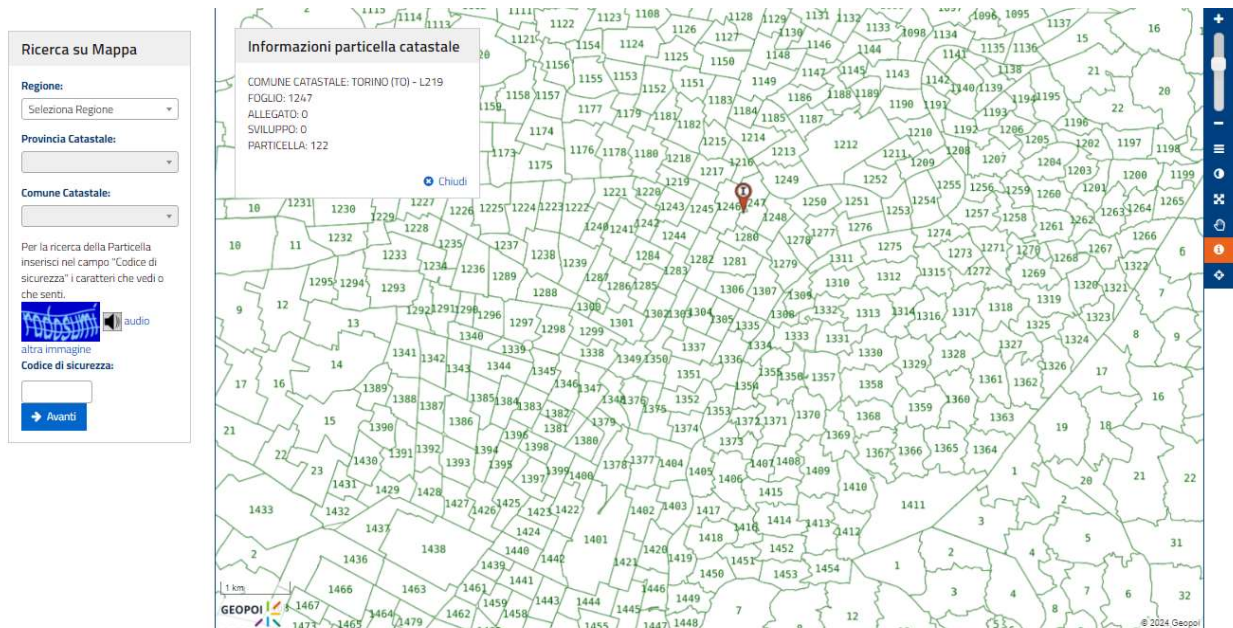


Figure 3 Cadastral map. Source: (Italian Cartography Geoportal, n.d.)

### 1.1.2. Spain

In Spain, the cadastre is managed by the Dirección General del Catastro (General Directorate of the Cadastre) and it is governed by the Real Estate Cadastre Law's Revised Text, which was authorised by Royal Legislative Decree 1/2004 on March 5 (Spanish Cadastre, n.d.). Similarly to other land registry, the Spanish cadastral property is identified by a cadastral code, a physical representation of the property (area, final destination, address and constructive characteristics), cadastral value and information related to the owner. Similar to the Italian data categorisation, Spain's Infraestructura de Datos Espaciales de España (IDEE) organizes all spatial data sets in a tiered framework, as required in the INSPIRE directive, that facilitates easy management, visualisation, and analysis of the information. Specifically, classes (clase), themes (tema), and layers (capas) form the basis of the organisation. Regarding the spatial data sets and services there is the Spanish Regulation (EU) n. 1089/2010 that is derived from INSPIRE directive (2007/2/EC). It is important to consider that the spatial data sets in Spain, as well as in Italy, are organized following the European directive INSPIRE, which is created in order to solve the problem of fragmentation, lack of harmonization and duplication of data sets, information and sources between nations. Considering the cadastral parcels in the INSPIRE directive, the data are organized as follows:

- Basic land unit, part of land defined by specific ownership rights and can include one or more cadastral parcels
- Cadastral boundary, which is the contour line of the cadastral parcel



- Cadastral parcel, which is the area of land that belongs to one or multiple people and is enclosed by a closed line.
- Land use zoning, it is an area used to divide the national territory in cadastral parcels

Furthermore, the Dirección General del Catastro offers digital services for consultation of cadastral mapping like Sede Electrónica del Catastro, which allows all citizens to freely consult the updated cadastral cartography through the search and dynamic visualization of cadastral parcels. Based on the map, it is possible to obtain, as shown in the (fig.4), the followings information by searching the cadastral parcel.

The screenshot displays a web interface titled "Información de parcelas e inmuebles". It features two main sections: "Croquis" (a pink trapezoidal parcel sketch) and "Fotografía fachada" (a street-level photo of a building). Below the sketch, the text reads: "Parcela construida sin división horizontal", "CL DIEGO CHICO DE GUZMAN 15", "CEHEGIN (CEHEGIN) (MURCIA)", and "28 m<sup>2</sup>". A link "Más información de la parcela" with a dropdown arrow is present. An orange banner at the bottom contains "INFORMACIÓN DE LOS INMUEBLES" and an "Excel" download button. A grey box at the very bottom shows the cadastral ID "5473702XH0157C0001KL" and details: "CL DIEGO CHICO DE GUZMAN 15 e/p/p/ /00/OA", "Residencial | 112 m<sup>2</sup> | 100,00% | 1930".

Figure 4 Cadastral information. Source: (Spanish Cadastre, n.d.)

However, the main limitation of the Italian and Spanish cadastre, but in general of the 2D cadastre is that it does not consider vertical dimensions, making it difficult to accurately manage complex situations such as multi-story buildings or underground infrastructures.



## 1.2. The 3D cadastre

Nowadays, the need for vertical space utilisation is rising due to the population expansion. The expansion of the cities, as well as the development of increasingly complex infrastructures above or under the ground level, demands innovative methods to efficiently manage land and rights properties. In this context, the 2D cadastre is considered useless since the two-dimensional dimension doesn't represent and qualify correctly the reality needs. The 3D cadastre, instead, adding the third dimension to include information on height, depth, and volume allows a more precise management of the complex reality. As consequence, the 3D cadastre has become a necessity. In this investigation, the 3D cadastre in Italy and in Spain, will be analysed.

### 1.2.1. Italy

In Italy, the topic of the three-dimensional representation of real estate in the cadastre was studied by (Fronza et al., 2013). In their research, the main goal was creating a methodology to implement three dimensional cadastral units in the land cadastre focusing on the automatic creation of 3D models, in accordance with the CityGML standard. The starting point of their research were cadastral data included in Docfa 4 (Documento Catasto Fabbricati). Docfa 4 is considered the new version of the software Docfa, used by professionals to compile technical and administrative documents of urban properties. This new version has allowed to insert three-dimensional data into the graphics in vector format, which represent the floor plan of each individual building unit, obtaining as result a perfect description of the property. The specific features introduced in DOCFA 4 which have allowed the development of the Fronza's research are:

- Points of origin and orientation of the building: these points indicate the precise orientation and positioning of the Cartesian axis system, which allows to find the correct orientation and position of all building units in the entire building.

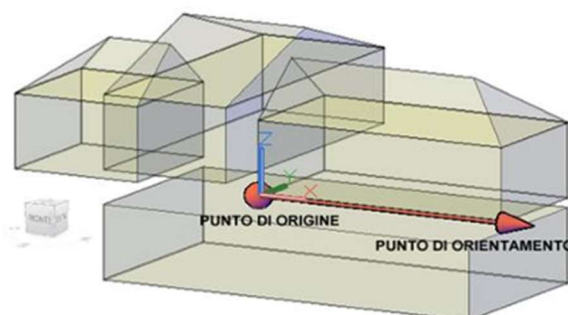


Figure 5 Orientation system of the building. Source: (Fronza et al., 2013)

- Polygons of the building's floor areas referring to the same Real Estate Unit (REU). It is a polygonal representation for each real estate unit, with the specification that multiple polygons should be generated where there are different elevation levels within the same real estate unit.

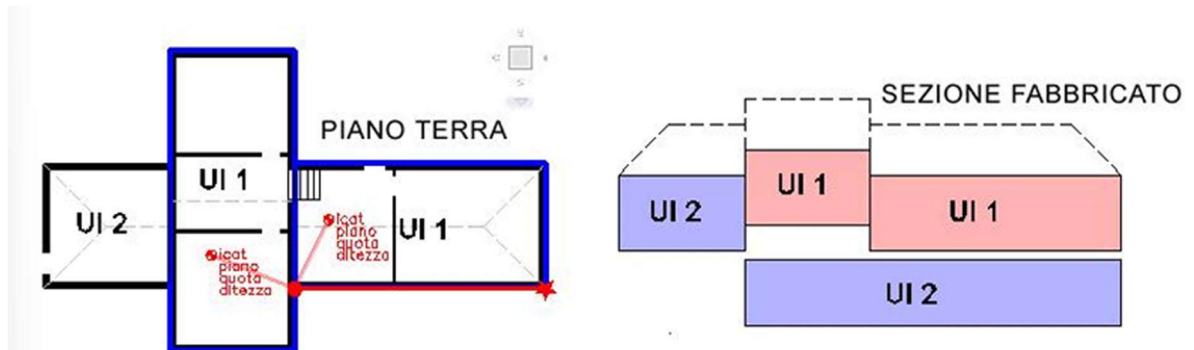


Figure 6 Polygons construction of the real estate unit. Source: (Fronza et al., 2013)

- Portion of Real Estate Unit and its markers. It is the association for each polygon referred to the real estate unit with information on cadastral identifier, reference plan, reference elevation and average height of the polygon.

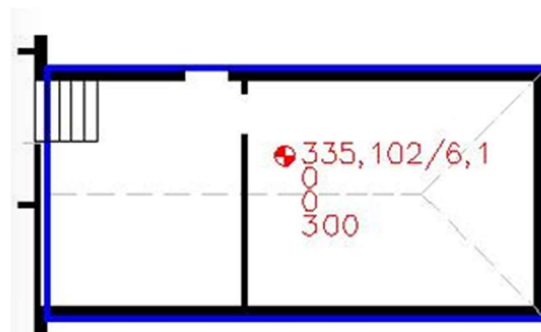


Figure 7 Markers of the subalterno. Source: (Fronza et al., 2013)

- Polygons by type of environment and polygons per room. The polygons by type of environment represent the areas of the real estate unit, including corridors, walls and other ancillary areas, thus providing the gross area to calculate the total available area. Whereas the polygons per room are the internal areas of the unit used, useful for a calculation on the effective useful area.

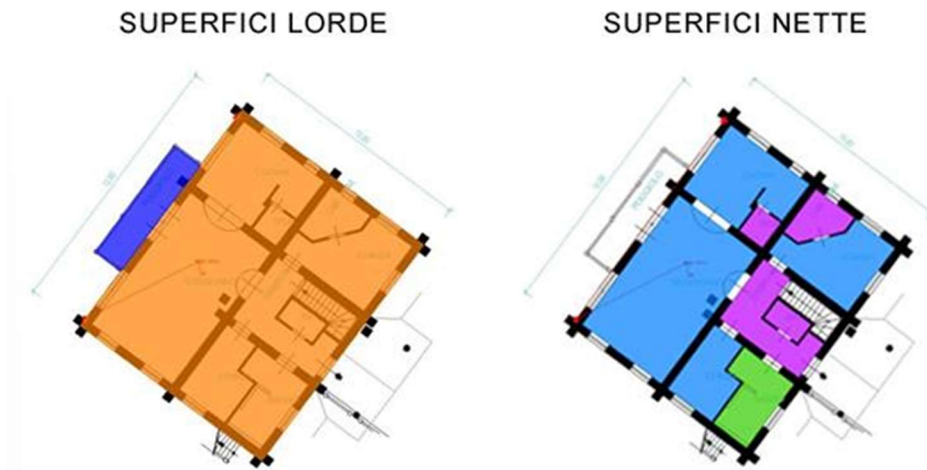


Figure 8 Representation of the net and gross areas. Source: (Fronza et al., 2013)

- Additional elements for modelling. These additional elements are used to represent parts of a complex building, such as an attic, using similar components derived from the modelling.

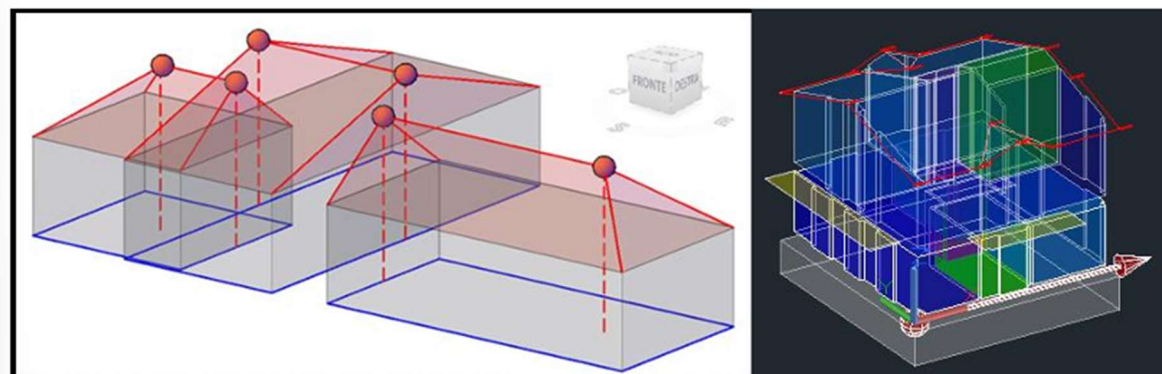


Figure 9 Lines and points of modeling. Source: (Fronza et al., 2013)

- Semantic and quantitative data. The document resulting from the software Docfa 4 is a .pdf file that, in addition to identifying the printing of real estate units, it has an XML file that presents the descriptive part of each unit.

The study of (Fronza et al., 2013), has provided guidance on how to automatically model real estate units using data in the Docfa 4 format. Specifically, temporary tables were created to maintain the characteristics to be allocated to geometric entities from the XML format and polygons of the interior spaces were created based on the DXF format of the visual documents, both included in Docfa 4. Subsequently, the polygons were extruded based on the height reported in the markers and positioned in three dimensions. The dimensions, geometric entity, and orientation of the polygons were obtained from the features of Docfa 4 listed above. Through the integration of Docfa data with the building model, a roto translation matrix was utilised to georeference the model in the UTM coordinate system WGS84. The final model was then automatically generated in CityGML format, imported into PostgreSQL/PostGIS and finally exported for display in Google Earth via KMZ or Collada formats. Based on this methodology, the document Docfa 4's potential for creating 3D models of buildings was assessed, despite the mechanical georeferencing, which was found to be a drawback because it was not mentioned in the document. As a result, despite a pilot project, made by (Fronza et al., 2013), that may have introduced the idea of a three-dimensional land register, the Italian state does not currently have a three-dimensional land register. This is likely because the necessary regulatory framework is lacking, and the costs associated with creating a 3D land register are elevated.



Figure 10 On the left: A three-dimensional representation of the interior of the building derived from Docfa 4 data. On the right: A combined representation of the building's façade (derived from topographic data) and interior (derived from Docfa data). Source: (Fronza et al., 2013)



### 1.2.2. Spain

On the other hand, José Miguel Olivares Garcia and coworkers handled with a pivotal project the 3D cadastre in Spain. Considering as final goal the representation and modelling of three-dimensional component of buildings as objects of cadastral parcels, the research of José Miguel Olivares Garcia proposed two different solutions: a first solution, based on the static representation of the 3D component on the web map service and a second solution that is based on a 3D vector format, modelled by parcel. The first solution implements two different layers in the Web Map Service. A Web Map Service (WMS) is an open geospatial consortium's standard that provides a simple HTTP interface for requesting geo-registered map images from one or more distributed geospatial databases and, as response, it displays one or more geo-registered map images (returned as JPEG, PNG, etc), in a browser application (Open Geospatial Consortium (OGC), n.d.). The first layer provides a shading effect, due to a shift of the buildings above the ground level, to emphasize the building aspect, whereas the second layer gives a Cavalier representation of the building, taking in consideration the sub parcel and the number of plans of each building. The integration between the first and second layers provides a greater understanding of the urban fabric, as shown in the pictures below.



Figure 11 The two layers and the superposition of digital cadastre. Source: (Olivares García et al., 2011)

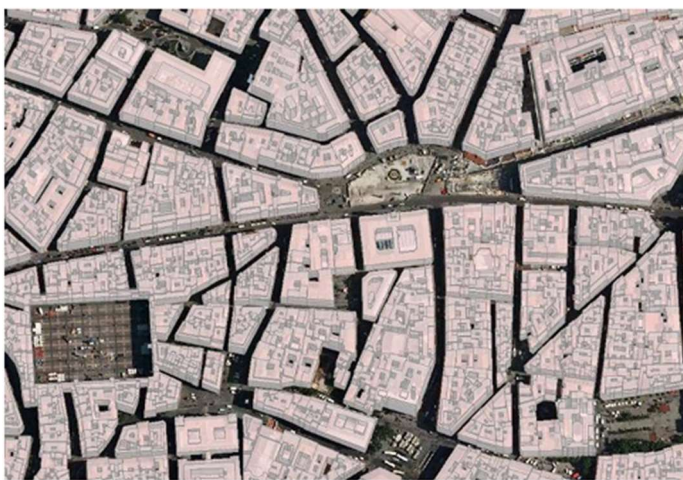


Figure 12 Superposition of the layers with the orthophoto. Source: (Olivares García et al., 2011)

For the second solutions, two products were obtained. The first model was based on the parcel extrusion considering the z value stored in the attribute of the cadastral parcel multiply by an estimated height of 3 meters for floor. On the contrary, the other model based on vector information data in FXCC format for each cadastral parcel, elaborates a 3D representation of the internal parts of the building.

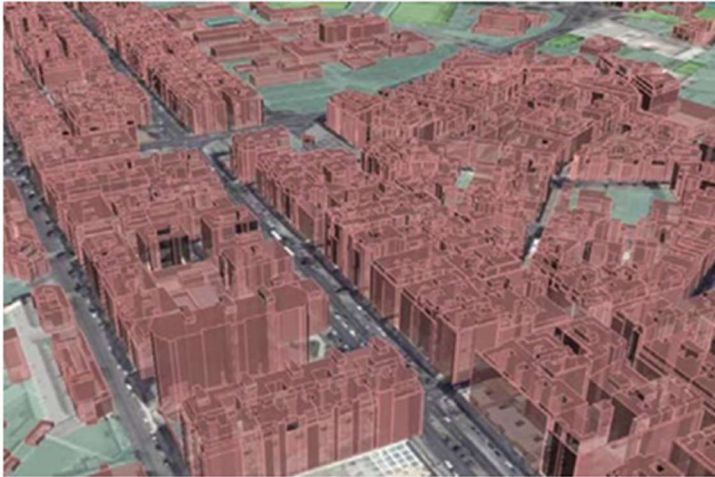


Figure 13 3D model based on parcel extrusion. Source : (Olivares García et al., 2011)

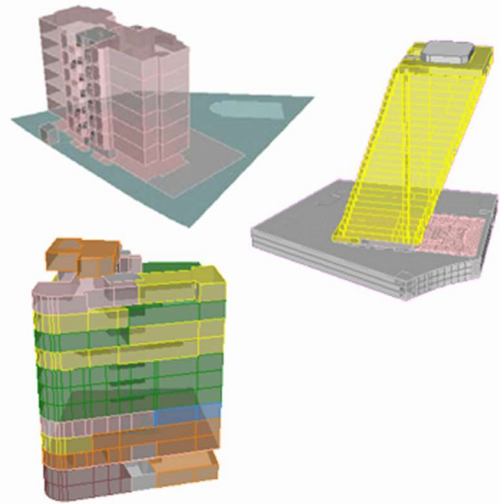


Figure 14 3D representation of the internal parts of the building. Source: (Olivares García et al., 2011)

To sum up, it is possible to denote that, in Italy and in Spain, an integrated 3D cadastre does not exist yet. The reason can be researched in the elevated costs associated to the creation of a 3D land register due to the required use of advanced technology for the scanning, but also it can be attributed to the lack of a technical regulatory framework, even if INSPIRE set the basis there could be some challenges in standardizing data formats across various entities and institutions. Furthermore, the fault could be attributed to cadastral institutions that might be resistant to the substantial resources, training, and operational process adjustments needed to reach a 3D cadastre. Differently Netherlands provides a 3D cadastre that allows to manage multi-level ownerships, underground construction and overlapping properties.

### **1.2.3. Netherlands**

In the Netherlands, a more complex and advanced research is generated from the studies of Stoter and others in the “First 3D Cadastral Registration of Multi-level Ownerships Rights in the Netherlands” in 2016. The research objectives try to overcome the issues related to the difficulty of the representation of the multistorey cadastral owner rights represented in the two dimensional cadastre, addressing a solution that represent adequately the rights connected to 3D volumes. The case study was settled in Delft, and it combined a new railway station and the new city hall, as well as the underground area with railway tunnel, technical installations, bicycle parking and other platforms. The multi layered infrastructure had different owners as can be possible to notice in the pictures 15 and 16.

As matter of a fact, during the first phase of the study of (Stoter J. et al., 2016) they analysed how to represent multi-level property rights in 3D, using the existing cadastre framework. The solution considered the generations of 3D legal volumes on BIM, translated the volumes into interactive 3D PDF files and included them in the deed of the cadastre, which is under the responsibility of the government agency that manages land data, named Kadaster. Building on the previous phase's lessons, the second phase is still in progress and addresses the explicit registration of restricted 3D rights directly in the registration process.

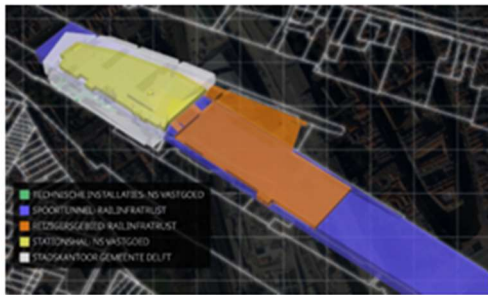


Figure 15 Representation of the different rights.  
Source: (Stoter J. et al., 2016)

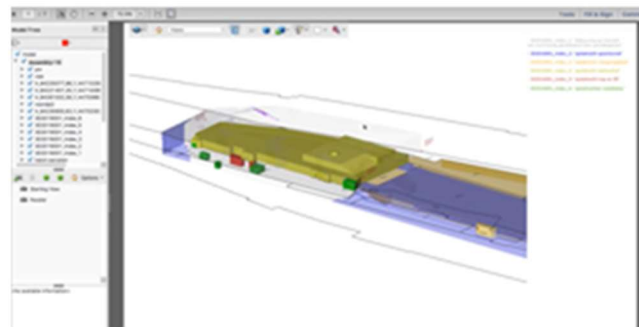


Figure 16 3D model representation based on the different rights. Source: (Stoter J. et al., 2016)

The successful implementation of the research was connected to international standardization of the cadastre in the Netherlands, based on the Land Administration Domain Model (LADM), since it provides a conceptual framework for managing cadastral information, including three-dimensional properties. This model, introduced with ISO19152 in 2012, allows the consistent and interoperable representation of property rights, restrictions, and responsibilities at an international level. LADM model is a crucial factor for enhancing transparency and efficiency in cadastre management. As shown in the (fig. 17), the LADM model is based mainly on four classes (Sun J. et al., 2022):

- LA\_Party: it is represented by a person or an organization.
- LA\_RRR: the acronym of RRR is related to rights, restrictions and responsibilities that a person could have with a LA\_SpatialUnit
- LA\_BAUnit: The basic administrative unit is an administrative entity that is subject to registration (by law) or recordation. It is composed of zero or more spatial units against which (one or more) different and common rights, obligations, or limitations are attached to the entire entity.
- LA\_SpatialUnit: it is the basic spatial unit of the data model. It is an area of land or a volume of space. The structure of spatial units is designed to facilitate the establishment and administration of fundamental administrative entities.

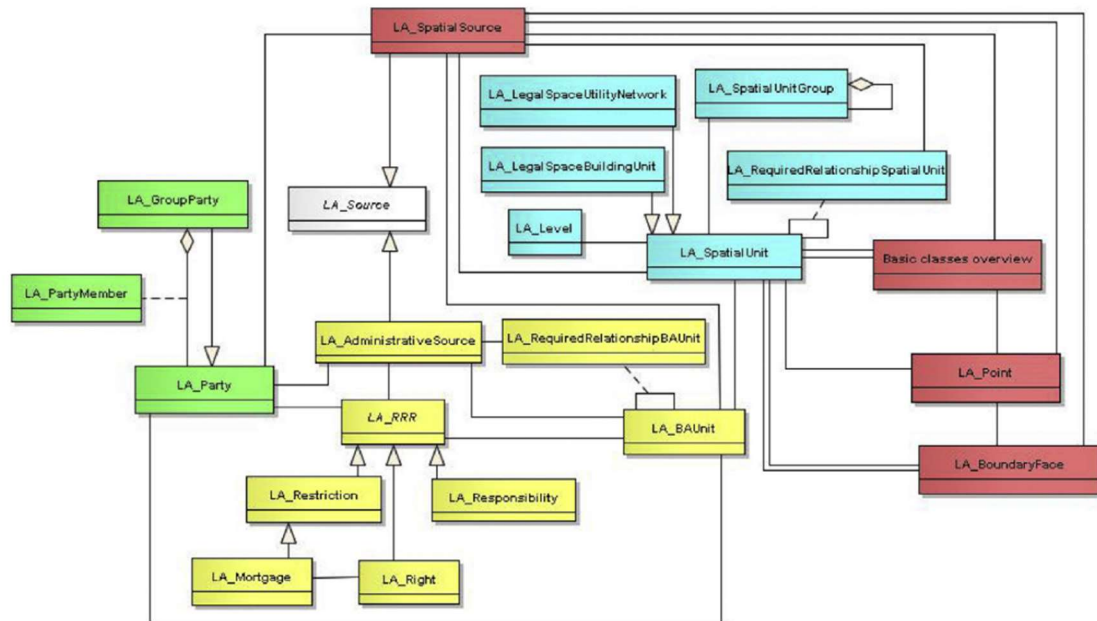


Figure 17 The Land Administration Domain Model. Source: (Lemmen, C. et al., 2015)

### 1.3. Advantages of 3D respect to 2D

The transition from a 2D cadastre to a 3D cadastre brings significant improvements, especially in complex urban environments. Considering the aforementioned case studies, we realize that a 3D cadastre provides a more accurate representation of multi-level properties. Specifically, a 3D cadastre improves management due to the better representation of the structures in the third dimension, but also it improves the accuracy and transparency since it reduces ambiguities caused by overlapping structures. For example, in the case study in Netherlands, for each 3D volumes there were some correspondences with the owner, enhancing clarity in urban planning and management. Another advantage made possible by the 3D cadastre is the possibility to overcome the cumbersome process of describing the complex reality in a two-dimensional description required from the cadastral registration. Also, the utilization of other technologies like GIS and BIM helps to resolve property disputes by clearly defining spatial boundaries in the 3D cadastre.



## 1.4. BIM and GIS in the 3D Cadastre: A Technological Synergy

The 3D cadastre offers a more complete and detailed representation of the cadastral reality. The core of 3D digitisation of the land register is due to the integration of advanced tools such as BIM and GIS, since both systems offer appropriate methods in the representation of the geometry and semantics of 3D objects (Hajji R. et al., 2021).

### 1.4.1. BIM

BIM is a methodology that facilitates the administration and analysis of building data by producing a detailed 3D digital model with rich object-oriented information (Amirebrahimi S. et al., 2016 and Eastman C.M. et al., 2011). In a BIM model, each component is considered as an independent item, characterized by specific attributes such as materials, dimensions and costs. However, it's important to emphasize that BIM final goal is more than merely 3D model, since it is a methodology that allows architects, engineers and other professionals to collaborate together, managing various type of information related to construction process. In this sense, the concept of BIM can be defined as a collaborative and interoperable process (Building Information Modeling) in order to obtain a final detailed and informative product (Building Information Model).

As matter of a fact, the proper use of this comprehensive data structure enhances the management of the entire life cycle of a building, from its initial design and construction to its operation and maintenance, making more sustainable design choices executed with lower costs in the shortest time, compared with the CAD modelling.

A fundamental aspect of BIM is the Level of Development (LOD), defined in the standard UNI 11337 – 4:2017, which includes the geometrical aspects of the element in the project, defined as Level of Graphical (LOG) and the semantical information connected to an object, defined by Level of Information (LOI). Hence, a model can be detailed at various LOD, which provide different degrees of precision. Different numbering systems are used by some nations. For example, in Italy there are the following layers:

- LOD A – Entities are graphically represented through geometric symbols or generic depictions, without geometry constraints. Quantitative and qualitative characteristics are indicative.
- LOD B – Entities are graphically visualized through a generic geometric system or approximate geometry. Quantitative and qualitative characteristics are approximate.
- LOD C – Entities are graphically represented through a defined geometric system, with qualitative and quantitative characteristics defined in a generic manner and compliant with applicable regulations and technical standards, applicable to a variety of similar entities.
- LOD D – Entities having qualitative and quantitative traits unique to a certain range of related products are graphically shown using an advanced geometric system.

Additionally, it details the approximate handling and maintenance clearances as well as the connection with other specific construction systems.

- LOD E – Entities are graphically represented through a specific geometric system, with quantitative and qualitative characteristics specific to a single production system related to the defined product. The level of detail related to manufacturing, assembly, and installation is also defined, including specific clearances for handling and maintenance.
- LOD F – Objects reflect the verified virtualization in the field of a single realized/built production system. Quantitative and qualitative characteristics are specific to the installed product's production system. Management, maintenance, repair, and replacement interventions are also defined to be performed throughout the lifecycle of the project.
- LOD G – Objects represent the updated virtualization of the current state of an entity at a specific time. Management, maintenance, repair, and replacement interventions are also defined to be performed throughout the lifecycle.

The definition of LOD has also been analysed by the American Institute of Architects, or AIA, as five degrees of development (LOD 100-500). In particular, the LOD AIA definition has been adapted to the Spain as follows:

- LOD 100 – Concept: the element is represented generically or with a symbol but does not meet the requirements for LOD 200; further information on the model element may be derived from other elements. Here there are no geometric information in the model elements, only symbols with attached approximate info.
- LOD 200 – Design development: the element is represented with generic quantity, size, shape, position, and orientation, so it may be recognisable object or space allocation for coordination between the disciplines; non-graphic information may also be linked to the element.
- LOD 300 – Documentation: the element is represented with correct size, position, and orientation. For this reason, this level should be suitable for design intent to support processes like costing and bidding. Shop drawings and construction paperwork will be produced using these models.
- LOD 350 – the element is represented with correct size, position and orientation and interfaces correctly with the other elements of the model. So, this level defines proper cross trade coordination and will include connections and interfaces between disciplines.
- LOD 400 – Construction: the element is represented with the correct size, position and orientation, interfaces correctly with the other elements of the model, and reports details of manufacture, assembly, and installation. In this level the contractor will be able to split construction requirements and assign to subcontracts.
- LOD 500 – Facilities Management: the element accurately reflects reality and is a verified representation at the site in terms of geometry and information to support operations and maintenance. It should be as built.

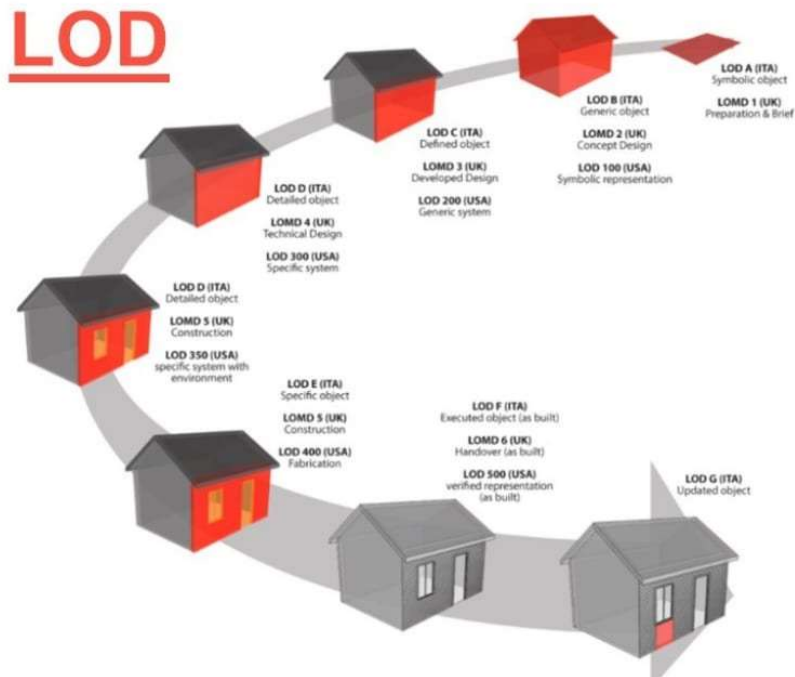


Figure 18 BIM LOD. Source:(Carnevali L. et al., 2019)

BIM uses industry foundation classes (IFC), as the open standard exchange format to share information among software applications by many different stakeholders, allowing the interoperability in the construction industry. IFC is developed by the International Alliance for Interoperability (IAI), now known as buildingSMART. Furthermore, the IFC framework enables the management of the model information in a single data model. (Borrmann A. et al., 2018 and Sun J. et al., 2022) state that IFC, an object-oriented data model, establishes specialisation and generalisation links in the inheritance hierarchy, as shown in the figure below.

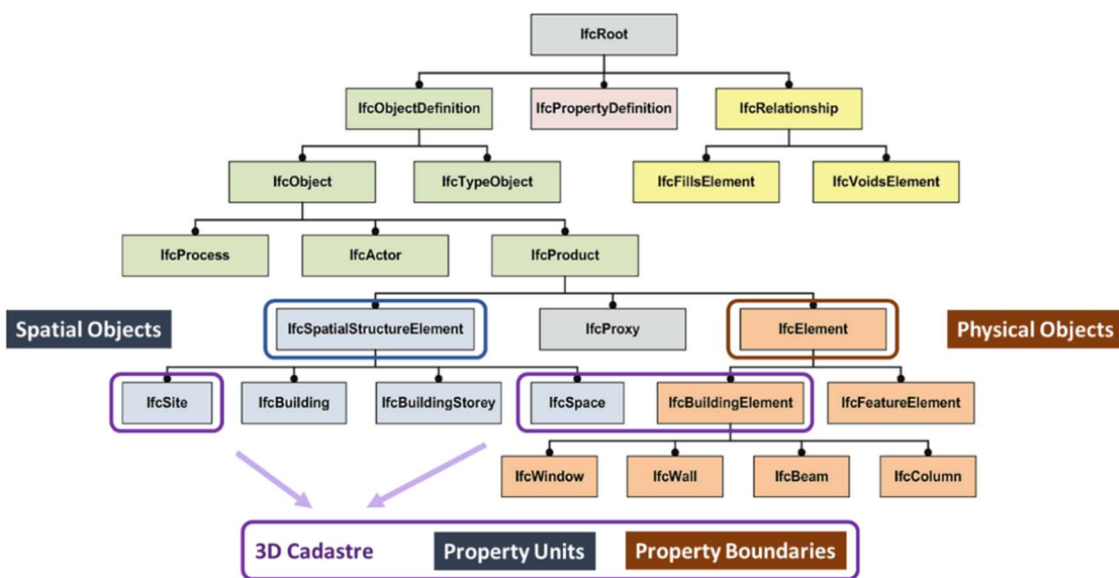


Figure 19 The IFC hierarchical structure and entities mostly integrated with 3D cadastre. Source: (Borrmann et al., 2018)

In the IFC hierarchy, as discussed by (Borrmann et al., 2018), all entities start with the abstract class `IfcRoot`, which branches into three main categories:

- `IfcPropertyDefinition`, which describes the properties and characteristics of the objects
- `IfcRelationship`, which establishes the connection between objects, enabling management and coordination
- `IfcObjectDefinition`, which represents physical, spatial object and conceptual elements, such as building elements, spaces, costs. It includes `IfcProduct`, an abstract class that represents spatial and physical context, which is subsequently divides into subclasses such as `IfcSpatialStructureElement` (that describes non-physical spatial objects) and `IfcElement` (that describes physical objects)

In 3D cadastral systems, the `IfcSpace` class, a subtype of `IfcSpatialStructureElement`, is often associated to define cadastral property units in 3D, by translating the basic geometry from IFC into an equivalent form within CityGML. Instead, the classes of `IfcBuildingElement` are associated to legal property boundaries in 3D.

#### **1.4.2. GIS**

Geographical Information System (GIS) is an information system that manages spatially referenced data in a large scale (Amirebrahimi S. et al., 2016). Hence, 3D models are placed within a broader geographical context by mapping the relationships between buildings and the surrounding territory. GIS utilizes the Geography Markup Language (GML) defined by the Open Geospatial Consortium, which is an XML grammar for expressing geographical features as exchange format (Open Geospatial Consortium (OGC), n.d.). Despite the efficiency of the data structure of GML for storage and exchange of geographic features, a variety of GML “application schemas” have been developed due to its limitation in characterising the semantics of objects. One of these developments is CityGML. The City Geography Markup Language (CityGML) is an open, standardised geometry format based on XML that efficiently facilitates the transmission and archiving of 3D geographical data (Sun J. et al., 2019). It constitutes a more complete GML application schema, and it is represented as the most detailed urban information model for coherent storage and management of the semantic and geometric aspects of urban objects in 3d virtual city models (Döllner J. et al., 2006; Borрман A. et al., 2014). Among CityGML most significant features, there is its modelling support for various Levels of Detail (LOD). Four successive levels of detail (LOD 0-3) are distinguished by the CityGML 3.0 conceptual model, where items get increasingly detailed with increasing LOD in relation to their geometry. The standard designates LOD 0 to denote the landscape, LOD 1 to simplify cubic buildings (up to eaves height or medium height), LOD 2 to encompass roof orientation and shape and LOD 3 to provide a more detailed representation with façade openings and interior spaces.

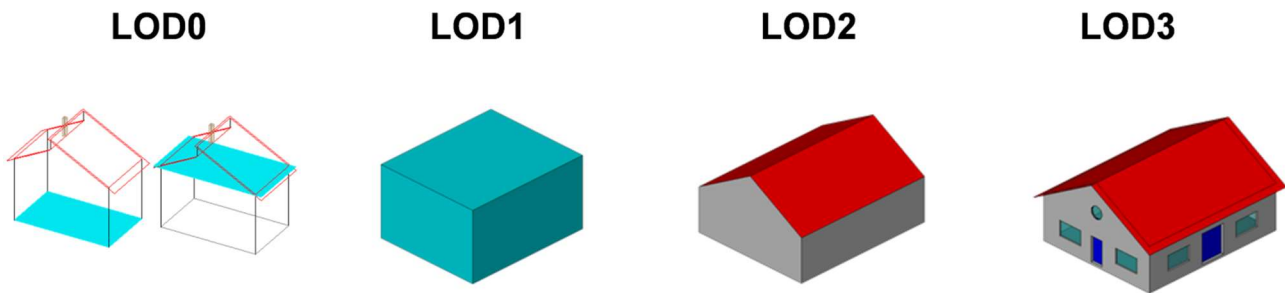


Figure 20 GIS LODs. Source: (Harshit P.C. et al., 2024)

This is the 3.0 CityGML version, standard created to obtain a better interoperation with other standards like IFC, LADM, and IndoorGML which has changed from previous versions due to:

1. Elimination of LOD4: Every kind of object's external and internal constituents can be present in LOD 0-3. For example, the external skin of the building can be in LOD2, while LOD1 can represent the internal contents such as rooms and doors. Likewise, it is also possible to model the outer facade of the Building in LOD1 and the internal Building structure in LOD2 or LOD3 (Konde et al. 2018).
2. Spatial representation: the LODs are not segmented by the semantic approach towards decomposition of the urban object anymore; but merely with its geometric representation. For example, other thematic surfaces and openings such as windows and doors can now be modelled and incorporated in any of the LOD, unlike the past versions that restricted to LOD2 and 3 as bases for modelling.
3. Modularity and simplification: the geometric representations have been moved from the thematic module to the Core module, which has simplified the thematic models. Any objects that are created in the application domain extension (ADE), acquire the spatial representations and the LOD concept within the core module.
4. Spatial representations: the spaces and lower hierarchy (like Buildings and Rooms) can be single point in LOD0, multiple planes in LOD0/2/3, solids in LOD1/2/3 and multiple curves in LOD2/3. The spatial boundaries and their subclasses (such as WallSurfaces and LandUse) can be represented by multiple planes in LOD0/1.

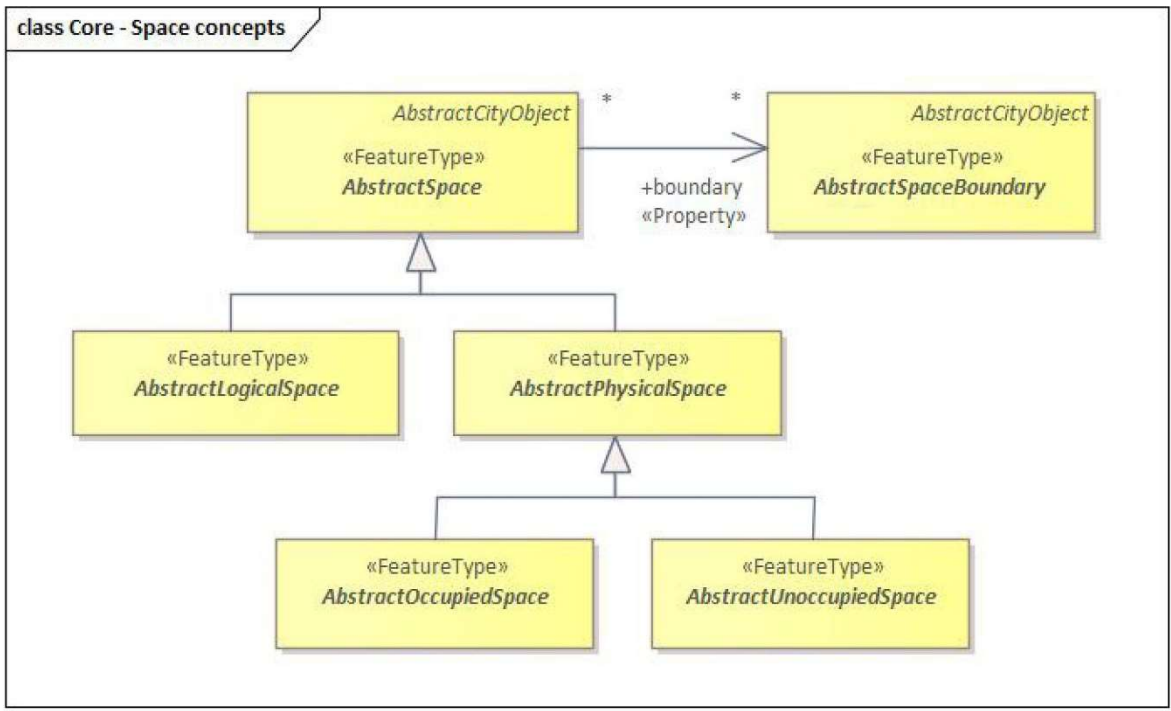


Figure 21 CityGML 3.0 space concepts Source: (Bahram S. et al., 2023)

In 3D cadastre, the class *AbstractLogicalSpace*, shown in the (fig.21), has particularly importance because it allows the modelling of logical spaces, or areas, that don't always have physical boundaries, like legal spaces in a cadastre. Furthermore, the building module of CityGML enables the conversion from IFC to CityGML, allowing constructive components from IFC classes, such as *IfcWall*, *IfcRoof*, and *IfcSlab*, to be mapped into CityGML (Kutzner T. et al., 2018).

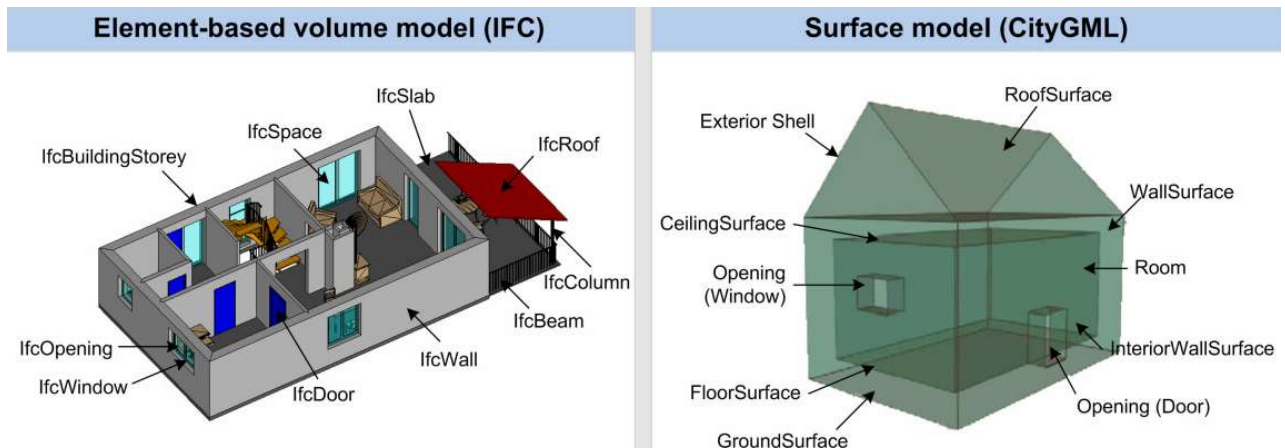


Figure 22 CityGML vs IFC. Source: (Nagel, C. et al., 2007)

## 1.5. Useful techniques for BIM-GIS integration

As matter of a fact, the integration of BIM and GIS is essential to achieve a more accurate representation of the urban reality: 3D cadastre. Essentially, BIM offers detailed models of buildings and infrastructure in a small scale while GIS facilitates the management and analysis of spatial data in a large scale. However, the capture of high-resolution three-dimensional data of the urban reality, made possible by photogrammetry and LiDAR techniques, forms the foundation of the integration between BIM and GIS. Basically, the ability to pass from 2D to 3D cadastre has been made possible by the application of photogrammetry and Lidar techniques.

### 1.5.1. Photogrammetry

The concept of photogrammetry originated from the concept of central projection, which is a geometric procedure that converts the tri-dimensional reality in a two dimensional image. From a theoretical point of view, photogrammetry is the technique used to define the position, shape and size of the objects on the ground. The functioning principle of photogrammetry is based on the image acquisition of an object from different points during a survey. Precisely, it is an indirect survey technique that determines the metrical characteristics of objects starting from at least two different frames, by using homologous points. Homologous points are points on the object's surface that appear in different images and are identified through the comparison of the two images by searching for correspondences among visible features, such as reference points. The evolution of this technique is called Structure from motion (SfM). It allows the generation of a 3D point cloud starting from more pictures obtained during the site survey. The classification of photogrammetry is based on the type of acquisition (aerial, terrestrial, UAV and satellite-based), the type of elaboration (analytical and analogue) and the type of photography (digital and classic) (Cannarozzo et al., 2012). The following research will present a point cloud derived from UAV photogrammetry, which is used for areas that are not particularly large. Unmanned Aerial Vehicle (UAV) is a subcategory of aerial photogrammetry, that uses drones, to obtain a specific survey ensuring more flexibility during the acquisition respect to the traditional aerial photogrammetry.

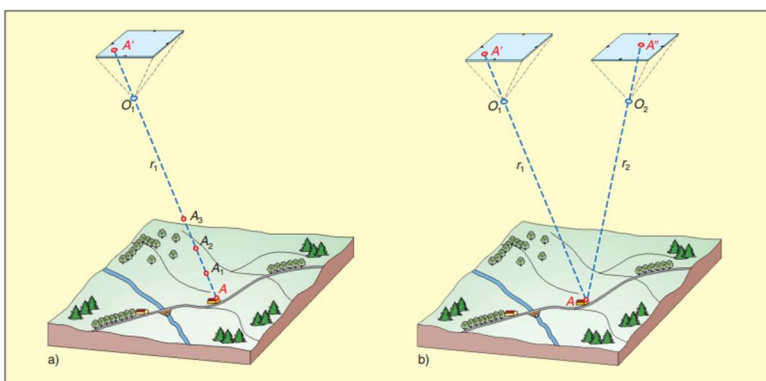


Figure 23 Photogrammetry. Source: (Cannarozzo et al., 2012)

### **1.5.2. LIDAR**

A laser pulse is used in the Light Detection and Ranging (LIDAR) technology to measure the separation between a sensor and an object. The working principle of the LIDAR technique is related to the transmission and the reflection of a laser pulse between the emitter and the object, hit by the pulse. Essentially, the sensor operates by emitting thousands of laser pulses every second, once emitted, each of them hits an object and is reflected back to the sensor emitted. By determining the interval of the time spent between the pulse emission and its reception, these receivers precisely record the distance between the laser pulse's departure from the system and its return. These distance measurements are converted to measurements of the reflected target's actual three-dimensional points in object space when combined with the positioning data (GPS and INS). The data extracted from this acquisition are collected and processed to create a three-dimensional point cloud (Esri, n.d.).

This work presents the use of the iPad Pro for acquiring data. It uses LiDAR sensors that allow for rapid mapping and cost-effective surveys, as shown in the studies of (Spreafico et al., 2021), beating the traditional surveying instruments. As matter of a fact, even if traditional surveying instruments (like Leica Nova MS50), provide high levels of accuracy, as well as present a considerable logistical and budgetary difficulties.

#### **1.5.2.1. iPad Pro**

The LIDAR within an iPad Pro is considered a Direct Time-of-Flight (DToF) sensor, since it measures the necessary time required for the laser light to return to the source after hitting an object. Particularly, the LIDAR sensor emits light from a grid of vertical-cavity surface-emitting lasers (VCSELs) and detects the reflected light using avalanche photodiodes (APDs) or single-photon avalanche diodes (SPADs) (Tontini et al., 2020; Spreafico et al., 2021). The iPad Pro can be defined as a LIDAR built-in instrument, allowing a flexible and lighter instrument during the surveys, particularly suitable for projects that require rapid execution and where budgets are limited (Murtiyoso et al., 2021). Recent studies have demonstrated both the strengths and limitations of the iPad Pro. For example, in (Spreafico et al. 2021) it has been studied the versatility of the iPad Pro in capturing high-quality 3D point clouds, demonstrating that the device could reach an accuracy of 2 cm and a precision of 4 cm, making possible the achievement of 1:200 scale for architectural mapping. Moreover, the (Abbas, Sahar & Abed, Fanar M., 2024) research demonstrated the iPad Pro ability to operate under multiple density levels and resolution settings allowing the instrument to be tailored to different survey needs, particularly when compared to TLS systems. However, one limitation of the LIDAR iPad Pro is the range of 5 meters. This constraint is relievable in terms of small distances, but became relevant as distance increases, since the amount of noise in the generated point clouds tends to rise and the level of detail tends to decrease. This issue, documented in research by (Murtiyoso et al. 2021), affects the quality of the data collected for objects farther from the sensor, limiting its effectiveness in some contexts. The following thesis will avoid the issue of 5 meters, integrating the iPad 3D point cloud with 3D point clouds made by drone. The following research will resolve the 5-meter limitation range of the iPad Pro's LiDAR sensor by integrating



a 3D point cloud acquired by a drone. The combination of two point clouds will ensure a faster, detailed, economic and adaptable solution for developing 3D building scanning in a 3D cadastral environment.

## 2. Case study: Cehegín, Spain

The following research will examine a building settled in the neighbourhood of the city of Cehegín. The city under investigation is a municipality located in the northwestern part of the Murcia region (Spain) and it is declared historic artistic city by the Spanish ministry of culture in 1982. As matter of a fact, it has a history that spans millennia of cultural and historical evolution dominated by various populations, including the Iberians, Romans, Visigoths, Arabs, and Christians.

Furthermore, the city of Cehegín financed and actively collaborated with the research group of the Polytechnic University of Cartagena to elaborate an informed model of the historical centre that will help in management and decision making of the cadastre (Ródenas-López, 2023).



Figure 24 Spain map. Source: (Google Earth, n.d.)



Figure 25 Murcia region map. Source: (Google Earth, n.d.)

The neighbourhood in question is surrounded by two areas designated as archaeological sites, as indicated on the archaeological map of the city. One of these areas, represented in the Ayuntamiento de Cehegín map, has been classified as a property of cultural interest (BIC) and houses the Renaissance church of the conception. The second area is designated as a historical-archaeological protection zone.

The (fig.26) illustrates three distinct groups of protection zones:

- Zone A (red) describes area in which there are monuments classified as historical and cultural assets. In these areas, no modification or construction work is permitted, except for studies and preservation efforts.
- Zone B (blue) represents the boundary areas that are adjacent to the Zone A. Only under certain conditions, in these areas, zonal modifications are allowed.
- Zone C (green) contains all remaining areas that are outside of the Zones A and B, where more flexibility in development or modifications of the archaeological area is permitted.

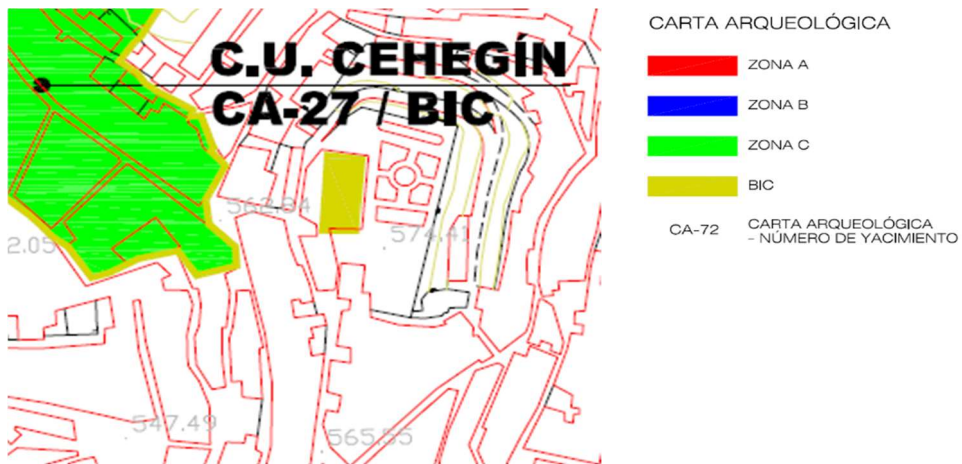


Figure 26 Archaeological map of the study area. Source: (Ayuntamiento de Cehegín, n.d)

In order to gather more data, given the minimal information that was provided, an in-situ acquisition was done, using the Lidar sensor installed in the Apple iPad Pro 11. During the site survey, the Samsung S10 mobile phone was used to capture images of the neighbourhood and a building under investigation (highlighted in red below). The phone's rear camera features a 12.0 MP + 16.0 MP resolution.



Figure 27 In the middle: Cadastral map of the study area. Source: (Sede Electronica del Catastro, n.d.). On the boundary: Picture of the onsite survey. Source: (Author's image, 2024)

The case study presented significant challenges during the on-site survey due to its location within the historic area. This area presented several challenges during the research work of the Polytechnic university of Cartagena, made by (Ródenas-López M. A, 2023), due to the difference altitude of the buildings, variety of roofs with varying slopes, assortment of intricate and distinctive facades and the slope of the ground. Intriguingly, these features also demonstrate the difficulty of creating accurate 3D reconstructions. Some of these problems are common in parts of the old city like the one this study looks at, and the methods described was specifically designed to address them. In particular, the final goal is to obtain a faithful presentation of the reality, which could represent the building in a 3D cadastre. This case study can be applied in comparable historical regions even if it only focuses on one structure in Cehegín.

### 3. Methodology

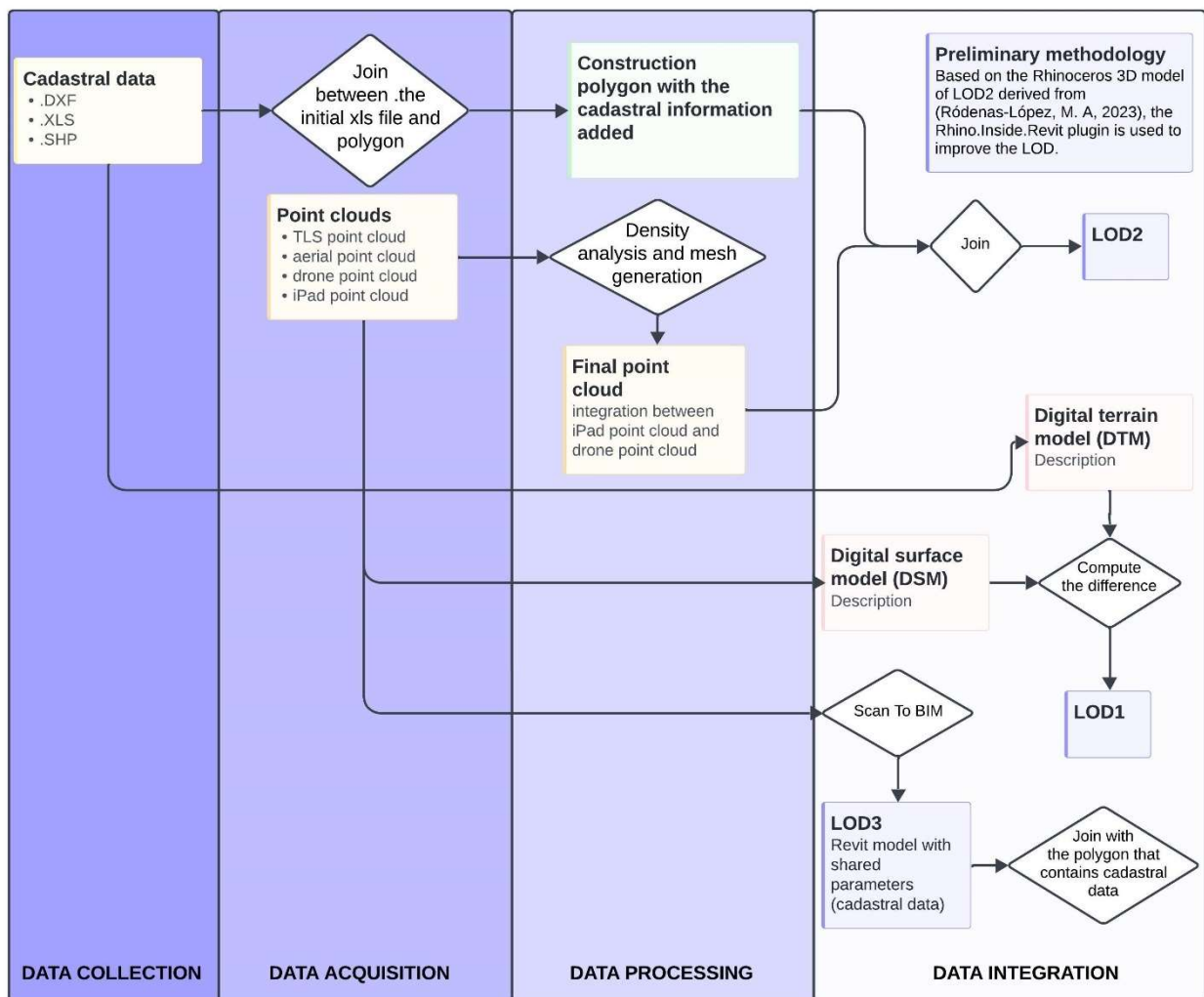


Figure 28 Methodology schema. Source: (Author’s schema, 2024)

The research project's methodological approach serves as the foundation for creating and carrying out the steps necessary to achieve a 3D model faithful to the reality. This process is structured as follows:

- Collection of data available. This section includes a collection analysis conducted on reliable sources to define the types of data useful for the case study. The data were extracted from the Spain's Digital Cadastre, in compliance with the INSPIRE European Directive. Particularly, the geometric data were extracted in .dxf format and the information data such as construction year, final destination in .xls format.
- Acquisition of the point clouds. In this part, there were analysed the acquisition of the point clouds obtained from prior research, made by (Ródenas-López, M. A, 2023) and the acquisition of the point clouds obtained using a rapid 3D mapping system. For this last case, it was used an iPad Pro. It was made a first general scan of the neighbour and then, several scans representing in detail each part of the neighbour, to obtain a detailed final point cloud.
- Processing and post-processing. The cadastral data, geometric and informative ones, was elaborated in GIS software to obtain a polygon with all the information inside of it. Furthermore, the point clouds acquired during the on-site survey with iPad Pro instrument were processed and related problems were analysed. Specifically, an alignment of LIDAR point clouds obtained through iPad Pro acquisition was made. At the end of the process, the point cloud density for each point cloud was analysed to determine the most suitable datasets for enhancing the level of detail. At the end of the process, it was found out that a combination of drone point cloud and iPad Pro point cloud was the most successful for our objectives.
- Data integration and model development. In this section, we attempted to use the Rhinoceros model that was obtained from (Ródenas-López M. A, 2023) with the Rhino for Revit plug-in. The inability to view the building as a single element was the reason this process failed. Thus, an alternative approach was adopted. Following the establishment of the cadastral data and point clouds, the integration process commenced. The integration process could be divided in three main sections based on the three level of detail reached. Initially, the Digital Surface Model (DSM) and Digital Terrain Model (DTM) were built from the cadastral data to create the Level of Detail 1 (LOD1) model for the historic district. The mesh, obtained from the union of the iPad point cloud and drone point cloud, was added to the GIS program. Then, it was changed to multipatch to which the cadastral data were integrated. Based on this procedure, the 3D model can attain a LOD2. However, to create a 3D digital model of LOD3, further geometry and semantics were refined utilising the scan to BIM method and shared parameters in BIM software. At the end, an analysis on the interoperability between BIM and GIS standard formats was performed due to the difficulty of inserting cadastral data in BIM model imported in GIS software.



### 3.1 Data collection

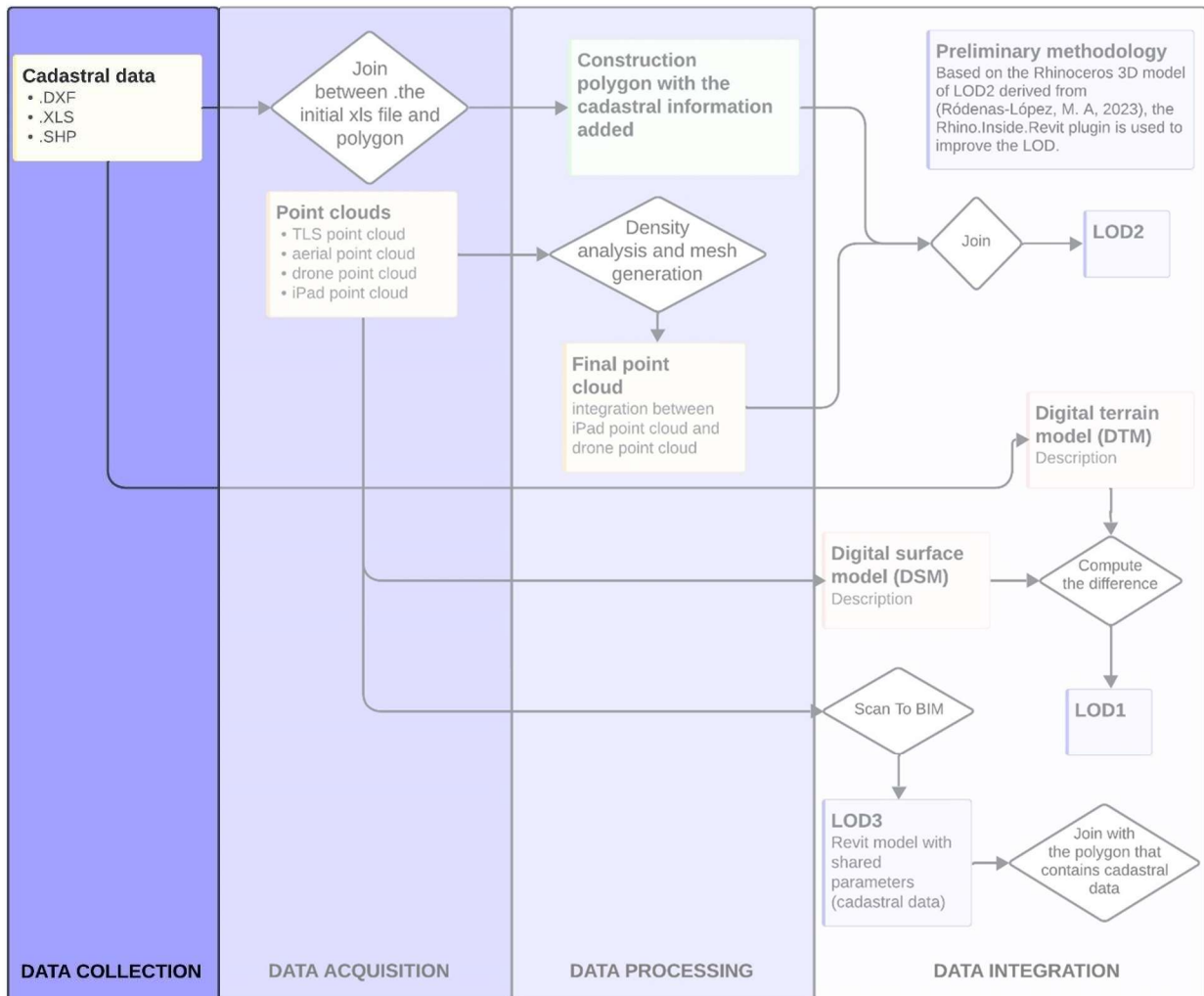


Figure 29 Data collection schema. Source: (Author, 2024)

The research presented in this thesis relies on data currently available within the Spanish digital cadastre site (fig.30). Furthermore, the cadastral information can be accessed and downloaded through three methods: the first includes searching by address or cadastral reference within the cartographic viewer, the second is through the data download and mapping area and the third employs web services (fig.31) (Spanish Cadastre, n.d.). The first two options have been investigated in this examination, as they produced distinct data that were considered necessary for the study. The first method will be the method that will be mainly analysed since it enables the free download of data. The second section will provide reliable and detailed data for the generation of DTM and DSM, as documented in the data integration

section, which was not provided in the previous option.

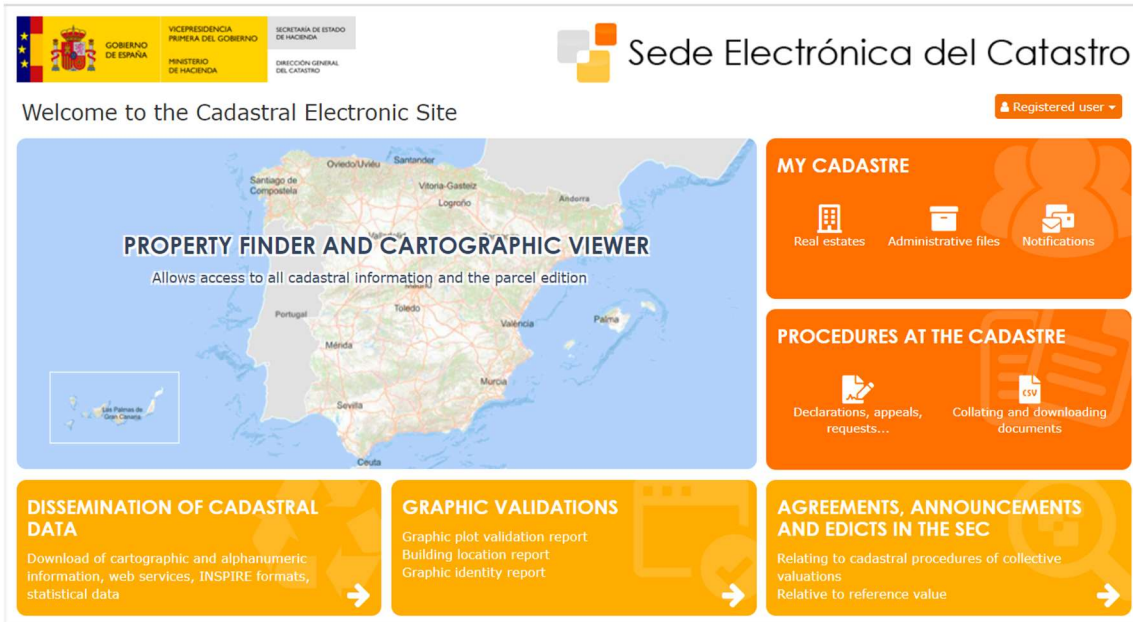


Figure 30 Spanish cadastre website. Source: (Spanish cadastre, n.d.)

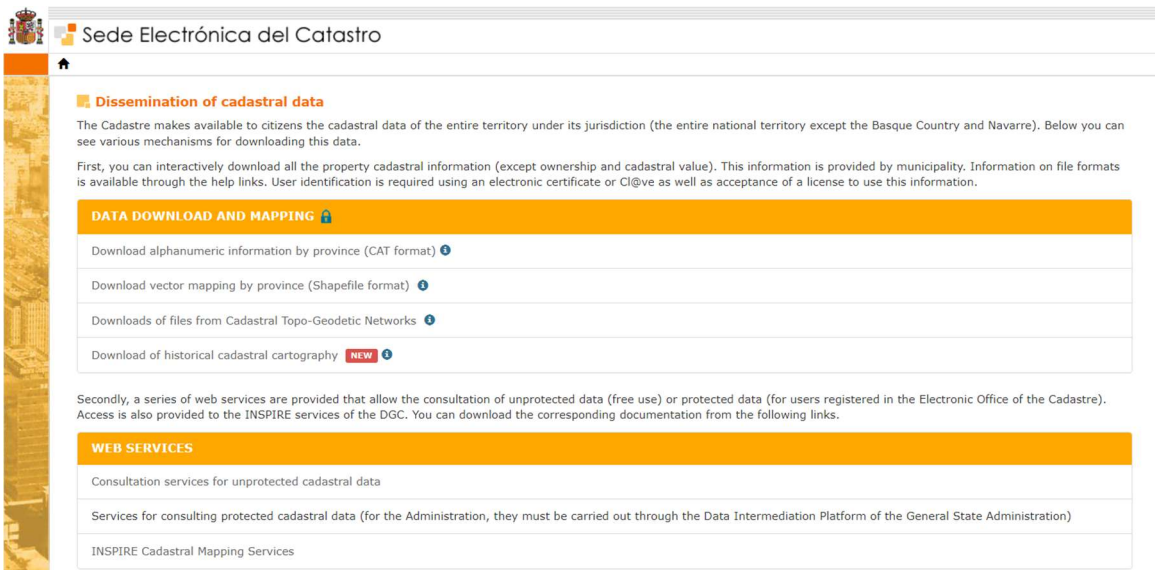


Figure 31 Data download subdivision in the Spanish cadastre. Source: (Spanish cadastre, n.d.)

### 3.1.1. Accessed by cartographic viewer

The data extraction method, based on the first method, involves entering cadastral codes. It is important to notice that the formal and required identifier of property is the cadastral reference. Each property must have a unique cadastral reference that enables it to be identified in the cadastral cartography. This reference is an alphanumeric identifier that is assigned by the cadastre. In the Spanish cadastre, there are a total of twenty characters. The first seven characters identify the parcel or property, the next seven show where on the map sheet it is located, the next four identify the property within the boundaries, and the final two are control characters that let know if the previous eighteen are accurate and help prevent (or detect) recording errors (Ingeoexpert).



Figure 32 Explanation of the cadastral code in Spain. Source: (Ingeoexpert, n.d.)

The area under investigation has been characterised by the utilisation of the following cadastral codes. In particular, the building number 7 is considered as prototype, as the entire procedure which will be detailed in the subsequent sections, can be repeated for the entire area:

|   | Cadastral Reference  | Address                     | Final destination  | Area (m <sup>2</sup> ) | Construction year |
|---|----------------------|-----------------------------|--|------------------------|-------------------|
| 1 | 5473710XH0157C0001JL | CL DIEGO CHICO DE GUZMAN 23 | Suelo sin edif., obras urbaniz., jardinería, constr. ruinosa | 100                    | -                 |
| 2 | 5473706XH0157C0001IL | CL DIEGO CHICO DE GUZMAN 21 | Industrial   | 103                    | 1930              |
| 3 | 5473705XH0157C0001XL | CL SALIENTE 3               | Residencial  | 103                    | 1930              |
| 4 | 5473703XH0157C0001RL | CL DIEGO CHICO DE GUZMAN 13 | Residencial  | 369                    | 1930              |
| 5 | 5473704XH0157C0001DL | CL SALIENTE 5               | Residencial  | 192                    | 1930              |
| 6 | 5473709XH0157C0001SL | CL DIEGO CHICO DE GUZMAN 19 | Residencial  | 171                    | 1900              |



|   |                      |                                      |             |     |      |
|---|----------------------|--------------------------------------|-------------|-----|------|
| 7 | 5473702XH0157C0001KL | CL DIEGO<br>CHICO DE<br>GUZMAN<br>15 | Residencial | 112 | 1930 |
| 8 | 5473701XH0157C0001OL | CL DIEGO<br>CHICO DE<br>GUZMAN<br>17 | Industrial  | 60  | 1930 |
| 9 | 5473708XH0157C0001EL | CL DIEGO<br>CHICO DE<br>GUZMAN<br>23 | Residencial | 324 | 2007 |

The geometric information represented in the cadastral visualization are divided into:

- MASS, urban blocks and rural polygons
- PARCEL, portion of real estate or land owned by the same person or a company
- SUBPARCE, area of uniform cultivation or land use within a parcel
- CONSTRUCTION, urban subparcels representing built volumes within a parcel

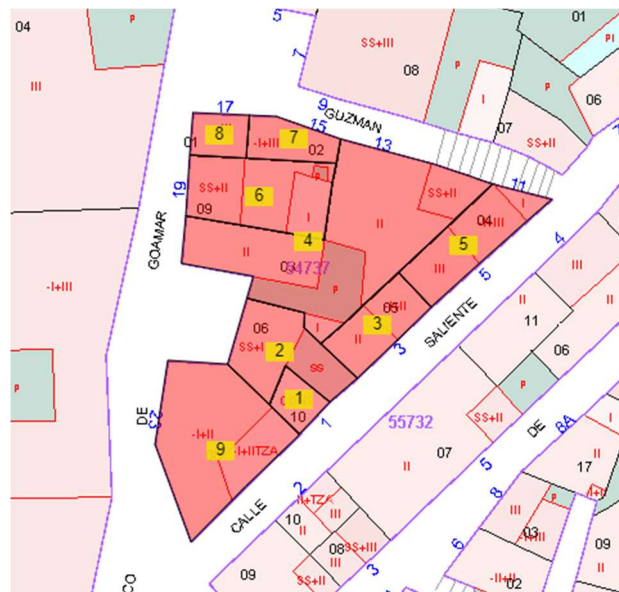


Figure 33 Area of the case study. Source: (Spanish cadastre, n.d.)

However, the sub parcel has a nomenclature that may be observed:

- -I, -II: Volumes below the ground level (1, 2 heights)
- I, II: Volumes over the ground level (1, 2 heights)
- TZA: Terrace
- CONS: under construction
- P: Patio
- SS: Semi-basement

Consequently, the building under investigation, which is number 7 selected in the picture n.33, is characterized by a floor below the ground level and three levels above the ground level. The previously analysed data can be downloaded for free in Excel and DXF formats. Specifically, the geometric data, which is divided into mass, parcel, sub parcel, and construction layers can be downloaded in dxf format, whereas the informative data, which is listed in the table adjacent to the cadastral code, can only be downloaded as an excel file, as shown in the pictures below.



Figure 34 Building under investigation. Source: (Spanish cadastre, n.d.)

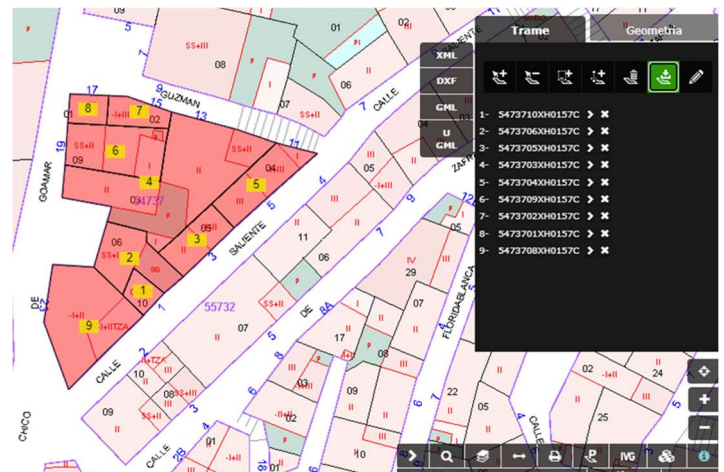


Figure 35 Cartographic viewer of the Spanish cadastre. Source: (Spanish cadastre, n.d.)

The cartographic viewer, shown in the picture 35, is based on National Geographic Institute's (IGN) cartography as default, even if it is also possible to use the most recent orthophotographs of the National Aerial Orthophotography Plan (PNOA) as a base.

Furthermore, estimated economic data for the building's area can be accessed inside the cartographic view (fig.36). This economic value is based on an average case study of the investigating area. Although this value is not specific of the building under research, it is included to provide a broader context within the cadastral study and to comply with the requirements of digital cadastral data, as it will be possible to observe during the data integration section.

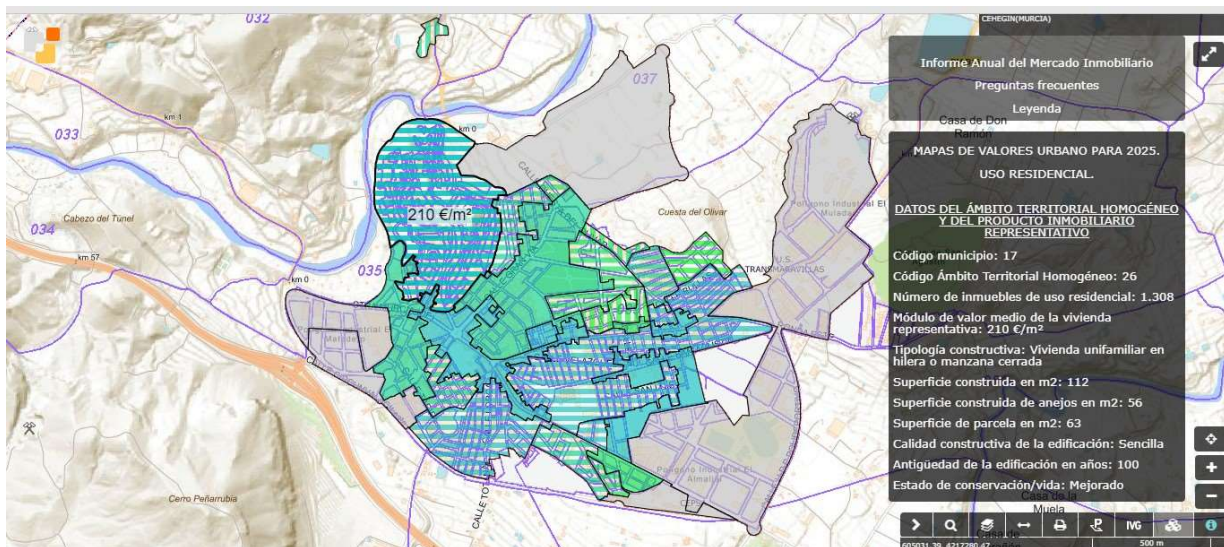


Figure 36 Economic map of the Cehegín municipality. Source: (Spanish cadastre, n.d.)

### 3.1.2. Accessed by data download and mapping section

The “data download and mapping section” of the cadastral site enables the acquisition of the urban map of Cehegín municipality in shapefile format (Spanish Cadastre n.d.). The data that can be extracted, with a digital certificate, from the digital cadastre are the followings:

- ALTIPUN: Points that represents the elevation points.
- CARVÍA : Hydrographic and communication route code description.
- CONSTRU: Built volumes within an urban parcel represented by sub-parcels
- EJES: The axes of linear elements such as routes.
- ELEMLIN: Linear cartographic elements.
- ELEMpun: Point cartographic elements.
- ELEMTEX: Map labels.
- ERRLIN: These are errors and should not exist. In particular, they are open sections in the parcel that are analysed during loading.
- HOJAS: Sheets separating urban cartography.
- LIMITS: These are the territorial divisions used by the government to demarcate regions like cities or urban land.
- MAPA: This stands for unique cartographic representations used to identify different zones. Every municipality usually has several maps for its rural and urban sections. Even though every single map is uniform, there can be a few little differences between them.
- MASA: These are groups of parcels, which can be found in both rural and urban locations.
- PARCELA: a portion of real estate or land owned by the same person and a company
- SUBPARCELA: area of uniform cultivation or land use within a parcel

After acquiring the data, the ALTIPUN shapefile was selected for generating the digital terrain model, as it contains "cota" data, which represents the elevation points in meters above sea level.

### 3.2. Data acquisition

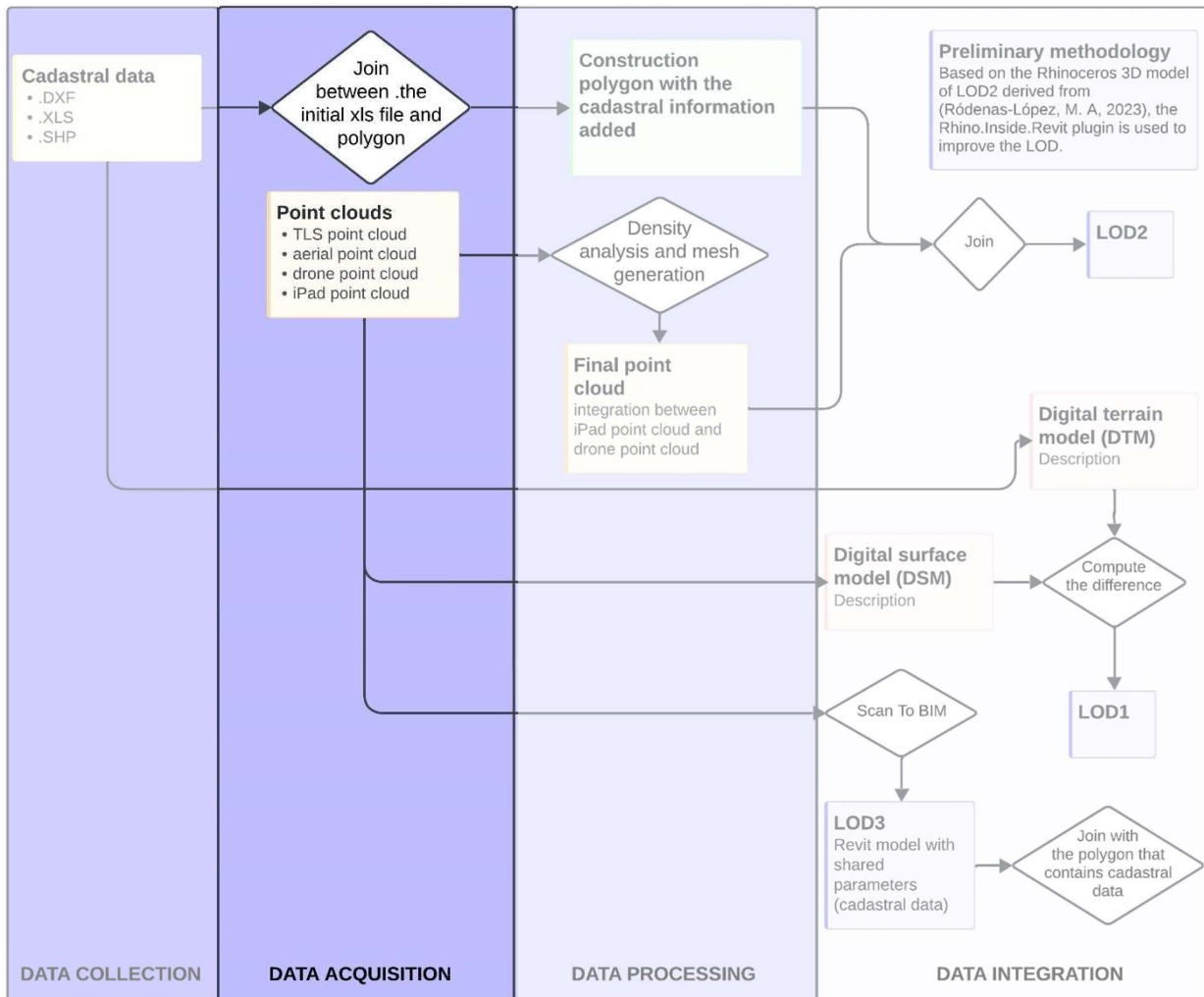
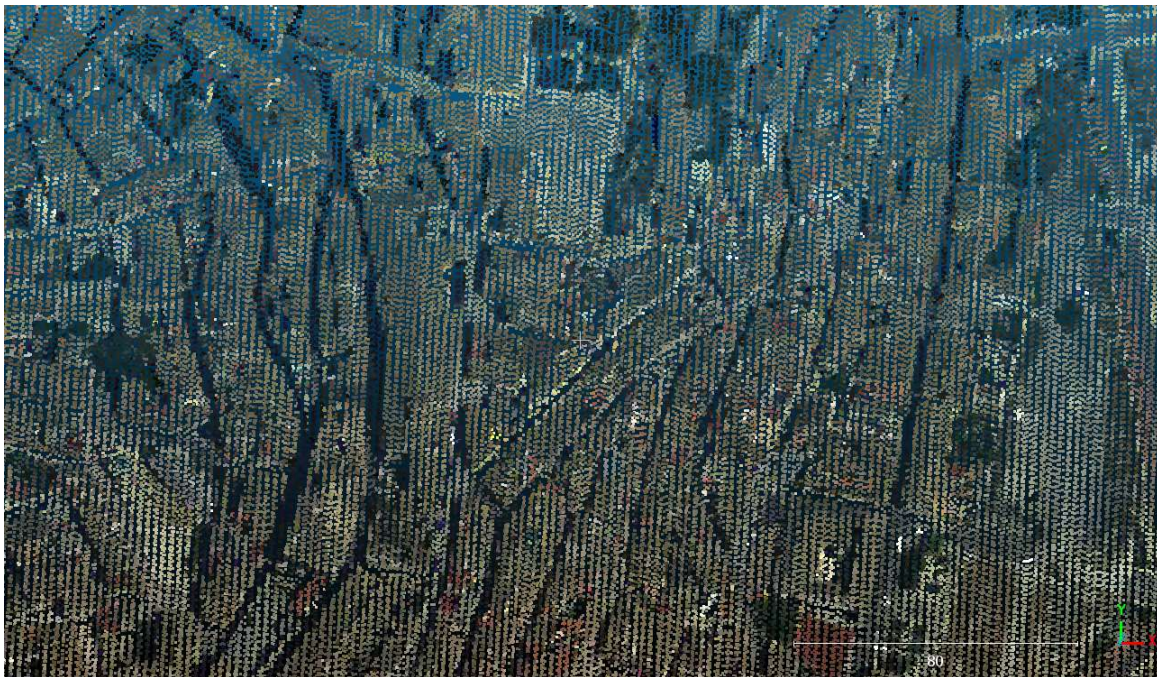


Figure 37 Data acquisition schema. Source: (Author, 2024)



To improve the accuracy and precision of the urban representation, it is necessary to integrate cadastral information with data obtained from site surveys. As a matter of fact, details such as building roofs and openings cannot be determined solely from cadastral information. Therefore, the use of on-site surveys with professional equipment is essential for a more detailed and faithful representation of urban reality. In this regard, three surveys were conducted: one on a large scale and two on a smaller scale. The first large-scale survey, performed in 2016 using aerial photogrammetry technology, was obtained from the National Geographic Institute's website. This survey is part of the National Plan for Aerial Orthophotography (PNOA), a pilot project launched in 2004 with the goal of capturing three-dimensional data on a national scale through aerial instrument (PNOA, n.d.). The coverage density was 0.5 points per square meter, and the data, in LAZ format (compressed from .las), is coloured in RGB and georeferenced in the ETRS 89 coordinate system.



*Figure 38 Lidar Point cloud, obtained by public Lidar sensor flights from 2015 onwards, excluded due to the scarcity of density. Source: (Instituto Geografico Nacional, n.d.)*

A second, smaller-scale survey was carried out by (Ródenas-López, M. A, 2023) as part of a research project aimed at automating the creation of 3D urban models in the historic centre of Cehegín. The survey used a Leica Nova MS50 total station for ground-based scanning (fig. 39). On the contrary, aerial data was collected through photogrammetry using a drone (fig. 40). All the specificities about the drone are unavailable.

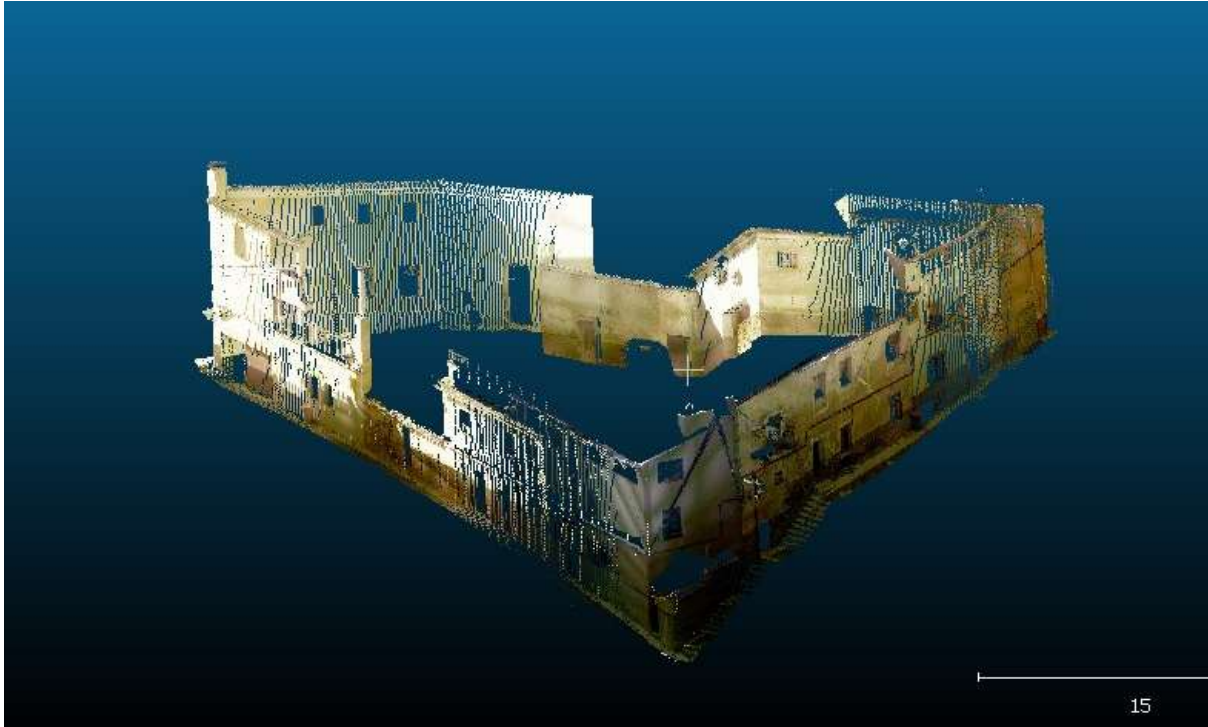


Figure 39 Terrestrial laser scanner acquired using Leica Nova MS50. Source: Cloud Compare



Figure 40 Final drone point cloud. Source: (Cloud Compare)

The data collection process was enriched by a further point cloud generated by using an innovative scanning device: the iPad Pro 11-inch (2nd generation). This choice was driven by the need to obtain high-resolution data in areas that are difficult to access, allowing for quicker and more detailed data collection. The survey was conducted over the course of a few hours during a sunny afternoon, which provided optimal conditions for the analysis of the buildings and a higher time saving compared with traditional instruments. The app used for the Lidar scanning was 3d scanner. During the on-site survey, two distinct resolutions were utilised to effectively capture the characteristics of the area. Initially, a resolution of 50 mm was utilized for a general scan of the study area. Subsequently, a higher resolution of 5 mm was employed for a more detailed scans, particularly focusing on the characteristics of the buildings of the study area. From this procedure a general point cloud of the study area was generated from the 50 mm resolution scan, along with eight additional point clouds derived from the detailed 5 mm scans. The names of the generated point clouds are provided:

- Point cloud of the study area:
  - Scansione 4\_2\_hd
- Point clouds of the buildings within the study area:
  - Scansione 5\_2\_hd
  - Scansione 6\_3\_hd
  - Scansione 7\_3\_hd
  - Scansione 8\_2\_hd
  - Scansione 9\_2\_hd
  - Scansione 10\_2\_hd
  - Scansione 11\_2\_hd
  - Scansione 12\_2\_hd

The scans have been textured in HD, as can be seen from the name, in order to achieve better data quality. It should be noted that one of the eight scans (Scansione 11\_2\_hd) was discarded due to the high level of detail produced by the 5 mm resolution, which rendered the point cloud so intricate that the scanning application encountered difficulties in processing it effectively. Ultimately, the objective of utilizing these varied resolutions was to significantly enhance the point density in areas where data from previous surveys had been insufficient.



*Figure 41 Final point cloud obtained from iPad. Source: (Cloud Compare)*



### 3.3. Data processing

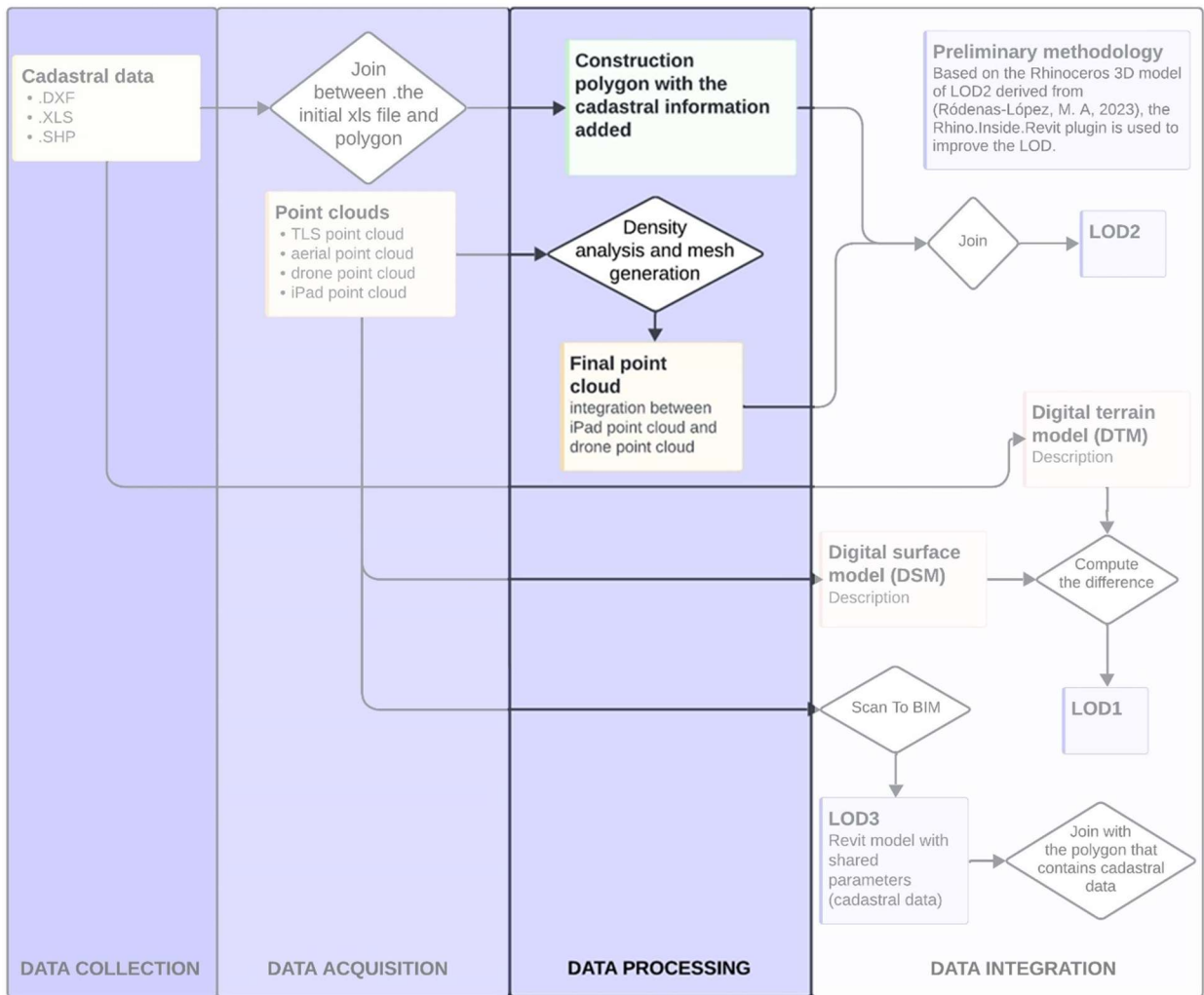


Figure 42 Data processing schema. Source: (Author, 2024)

This section will be divided into two parts. In the first part, an explanation will be provided describing the procedure to obtain the cadastral data on a GIS software. On the contrary, based on density point cloud analysis, the second part will consider the workflow utilized to select the most suitable point cloud for our objectives.

#### 3.3.1. From the cartographic viewer

To be easily integrated into the GIS software, the data obtained from cadastral code was downloaded in DXF format. When the DXF file is opened, it is possible to find the layers: mass, parcel, subparcel and construction, that are discussed in the data collection section. Considering these layers, the construction layer was selected since it defines the building areas relevant to the study, while the remaining layers related to the cadastral parcel were discarded. The “construction” data from cadastre was already in the correct location but it was needed a “define projection” to have the files in the correct projected coordinate system, ETRS 89 UTM 30N.

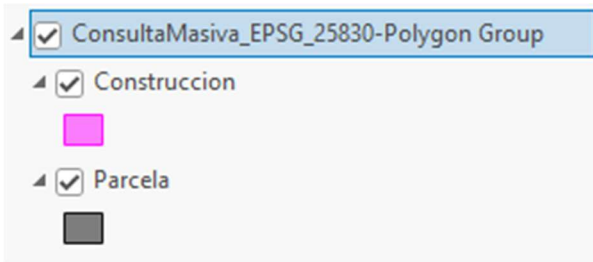


Figure 43 DXF file extracted from the digital cadastre and inserted in ArcGIS Pro. Source: (Instituto Geografico Nacional, n.d.)

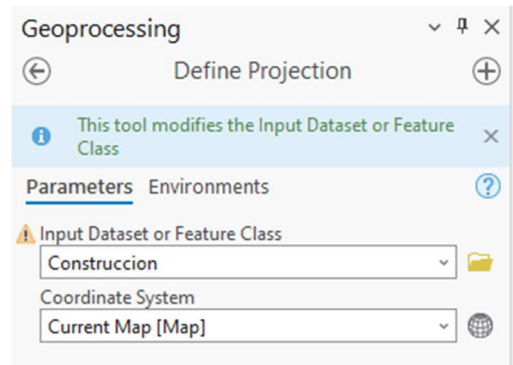


Figure 44 Define projection command. Source: (ArcGIS Pro)

Nevertheless, in terms of information the construction layer didn't have the cadastral data for building under exam, so the data was extracted from an Excel table that was acquired from the cadastral website, as shown in the picture 45 and in the table below. The data contained in the excel table are the building's destination, cadastral code, construction year, address and area.

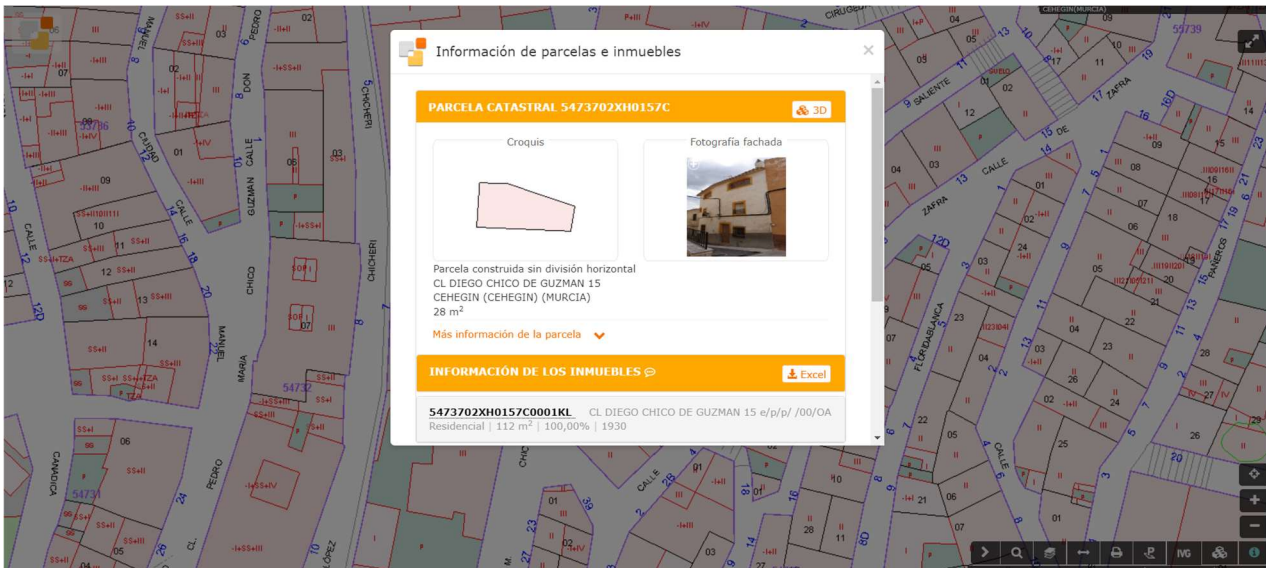


Figure 45 Cadastral information in the excel file. Source: (Spanish cadastre, n.d.)

| REFCAT | DIRECCIÓN      | USO                    | SUP# CONSTRUIDA (m2) | AÑO | PARTICIPACIÓN D |
|--------|----------------|------------------------|----------------------|-----|-----------------|
| 1      | 5473702XH0157C | CL DIEGO CHICO DE G... | Residencial          | 112 | 1930            |
| 2      | 5473702XH0157C | CL DIEGO CHICO DE G... | Residencial          | 112 | 1930            |
| 3      | 5473702XH0157C | CL DIEGO CHICO DE G... | Residencial          | 112 | 1930            |
| 4      | 5473702XH0157C | CL DIEGO CHICO DE G... | Residencial          | 112 | 1930            |
| 5      | 5473702XH0157C | CL DIEGO CHICO DE G... | Residencial          | 112 | 1930            |
| 6      | 5473702XH0157C | CL DIEGO CHICO DE G... | Residencial          | 112 | 1930            |

Figure 46 Excel file extracted from digital cadastre and inserted in ArcGIS Pro. Source: (Instituto Geografico Nacional, n.d.)

The OID identification code of the building and its geographic coordinates were incorporated into the Excel data to create a shapefile of points that accurately represented the vertices of the projected building within the study area.

| X         | Y          | OID |
|-----------|------------|-----|
| 605358,56 | 4217142,56 | 72  |
| 605361,02 | 4217142,49 | 72  |
| 605366,95 | 4217140,49 | 72  |
| 605366,57 | 4217138,29 | 72  |
| 605358,3  | 4217138,65 | 72  |
| 605358,56 | 4217142,56 | 72  |

In the GIS software, the vertices of the projected case study building were created by utilizing the XY Display data command, as shown in the pictures below.

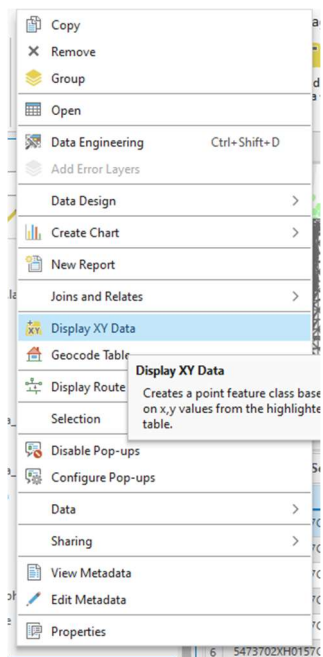


Figure 47 Display XY command. Source: (ArcGIS Pro)

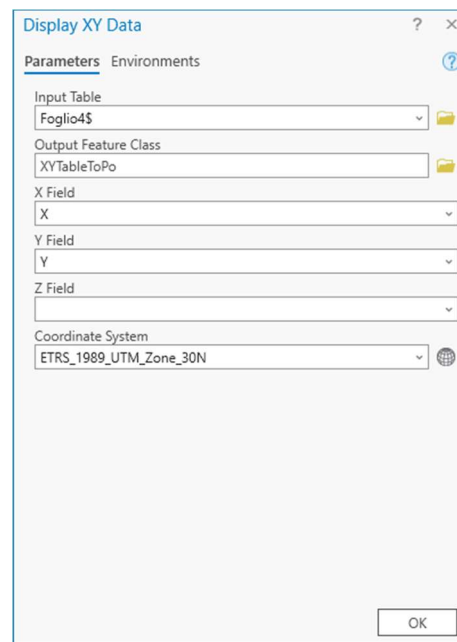


Figure 48 Settings of the Display XY Data. Source: (ArcGIS Pro)

After generating the shapefile of points representing the vertices of the building case study the next step involved generating the line and polygon shapefiles to ultimately create a polygon for our case study. The commands utilized in the GIS software are shown in the images below.

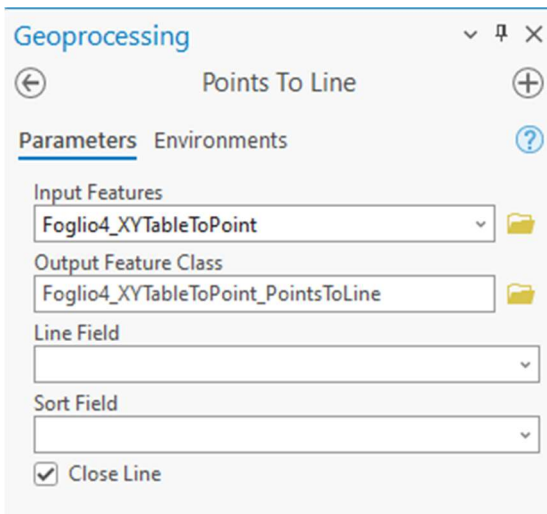


Figure 49 Command to generate the line from the points. Source: (ArcGIS Pro)

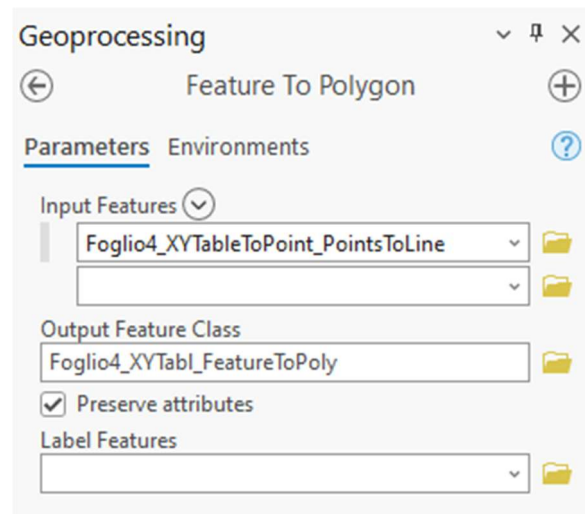


Figure 50 Command to generate the polygon from the lines. Source: (ArcGIS Pro)

The procedure described above was followed with the aim of obtaining a polygon with the excel cadastral data in it. As matter of a fact, since the attribute table of the polygon created contained only the area and the perimeter, as shown in the picture below, two connections have been made using the “join command”.

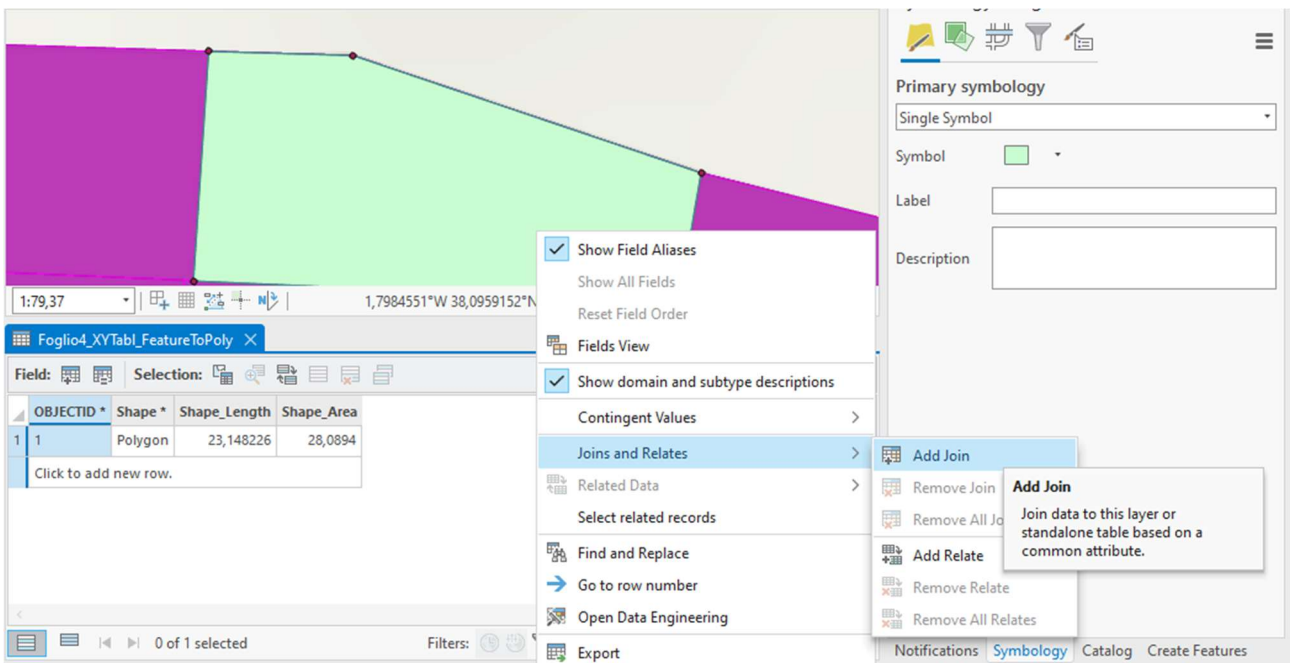


Figure 51 Add join between the construction polygon and the polygon obtained from the excel file. Source: (ArcGIS Pro)

The first connection was between the polygon obtained and the excel table based on ObjectID. The following screen shows that “join” function worked and all the characteristics of the points in the table were transmitted to the polygon.

| OBJECTID * | Shape * | Shape_Length | Shape_Area | REFCAT         | DIRECCIÓN              | USO         |
|------------|---------|--------------|------------|----------------|------------------------|-------------|
| 1          | Polygon | 23,148226    | 28,0894    | 5473702XH0157C | CL DIEGO CHICO DE G... | Residencial |

Figure 52 Results of the join function. Source: (ArcGIS Pro)

Subsequently, a second "add join" was created between the polygon obtained in the step before and the construction polygon that was directly obtained from the cadastre.

Figure 53 Join between the two polygons. Source: (ArcGIS Pro)

The construction polygon contains all the buildings within the study area. As consequence, when creating the "join" between the generated polygon and the "construction" file, only the fields corresponding to the OID of our building will be filled. To clarify, the picture below shows only the building of interest. This result will be considered in the data integration section.

| CAT | DIRECCIÓN   | USO                    | SUP# CONSTRUIDA (m2) | AÑO | PARTICIPACIÓN DEI |
|-----|-------------|------------------------|----------------------|-----|-------------------|
| 1   | 3702XH0157C | CL DIEGO CHICO DE G... | Residencial          | 112 | 1930              |

Figure 54 Results obtained from the join. Source: (ArcGIS Pro)

### 3.3.2. Alignment of Lidar point cloud scans

After the scanning of all point clouds was completed, attention was directed towards the LiDAR point clouds obtained through 3D rapid mapping system. Particularly, all point clouds with a resolution of 5 mm were georeferenced respect the 50 mm resolution point cloud, ensuring a more detailed representation. Georeferencing process was done by matching points from point



clouds through the use of Cloud Compare software. For the georeferencing process, we used a minimum of four homologous points per pair of point clouds. The alignment between these homologous points required that they be well distributed and at differing heights to avoid minimized error between the two point clouds. Below are described the results of georeferencing the 5 mm point clouds using the 50 mm point cloud, with the RMS matrix.

- Georeferencing between “scansione 4\_2\_hd” and “scansione 5\_2\_hd”, with relative matrix.

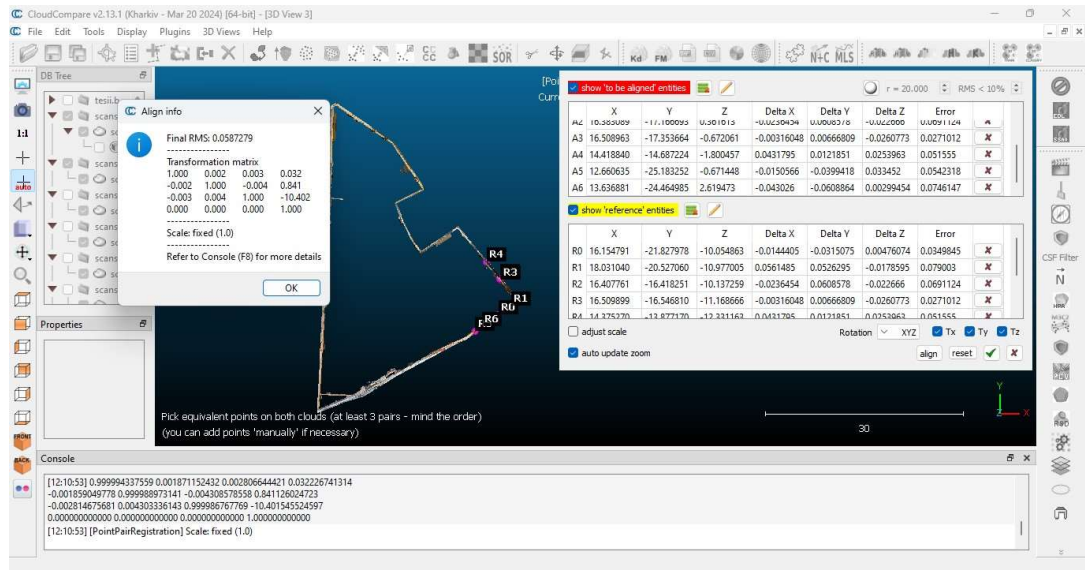


Figure 55 Georeferencing between “scansione 4\_2\_hd” e “scansione 5\_2\_hd”. Source: (Cloud Compare)

- Georeferencing between “scansione 4\_2\_hd” and “scansione 6\_3\_hd”, with relative matrix.

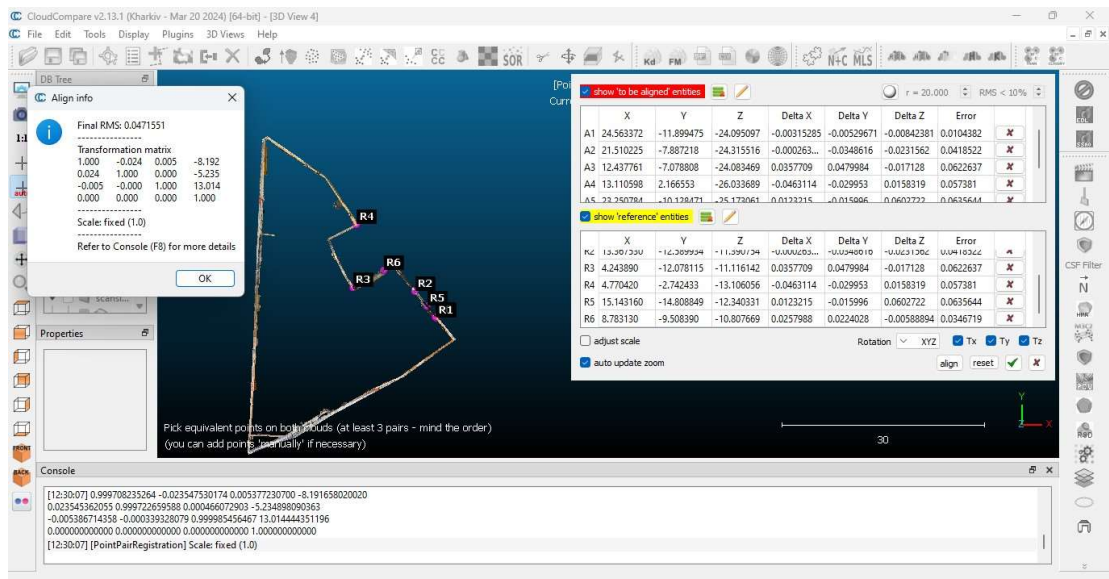


Figure 56 Georeferencing between “scansione 4\_2\_hd” e “scansione 6\_3\_hd”. Source: (Cloud Compare)

- Georeferencing between “scansione 4\_2\_hd” and “scansione 7\_3\_hd”, with relative matrix.

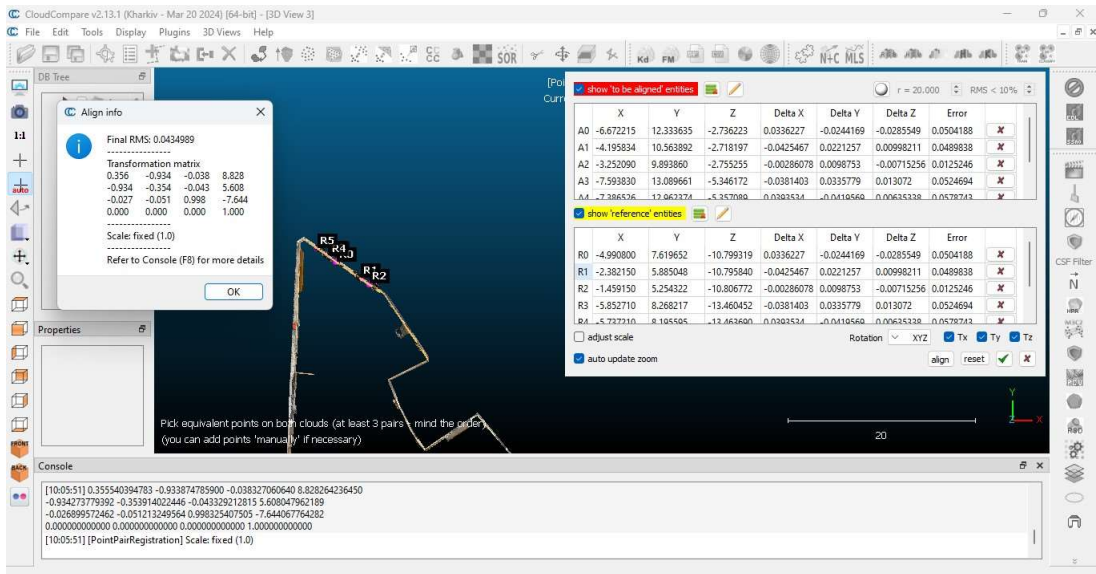


Figure 57 Georeferencing between "scansione 4\_2\_hd" e "scansione 7\_3\_hd". Source: (Cloud Compare)

- Georeferencing between “scansione 4\_2\_hd” and “scansione 8\_2\_hd”, with relative matrix.

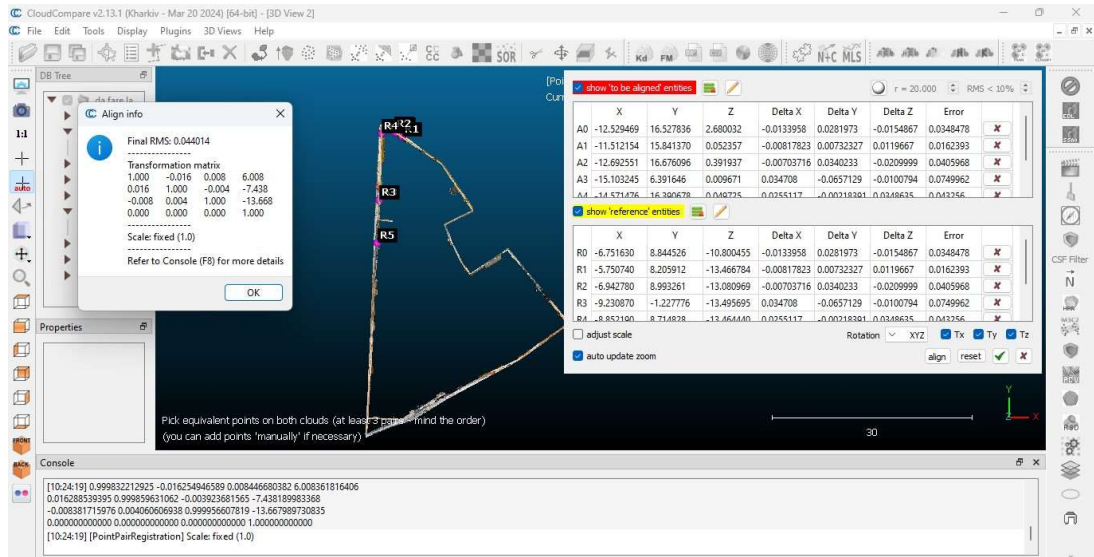


Figure 58 Georeferencing between "scansione 4\_2\_hd" e "scansione 8\_2\_hd". Source: (Cloud Compare)

- Georeferencing between “scansione 4\_2\_hd” and “scansione 9\_2\_hd”, with relative matrix.

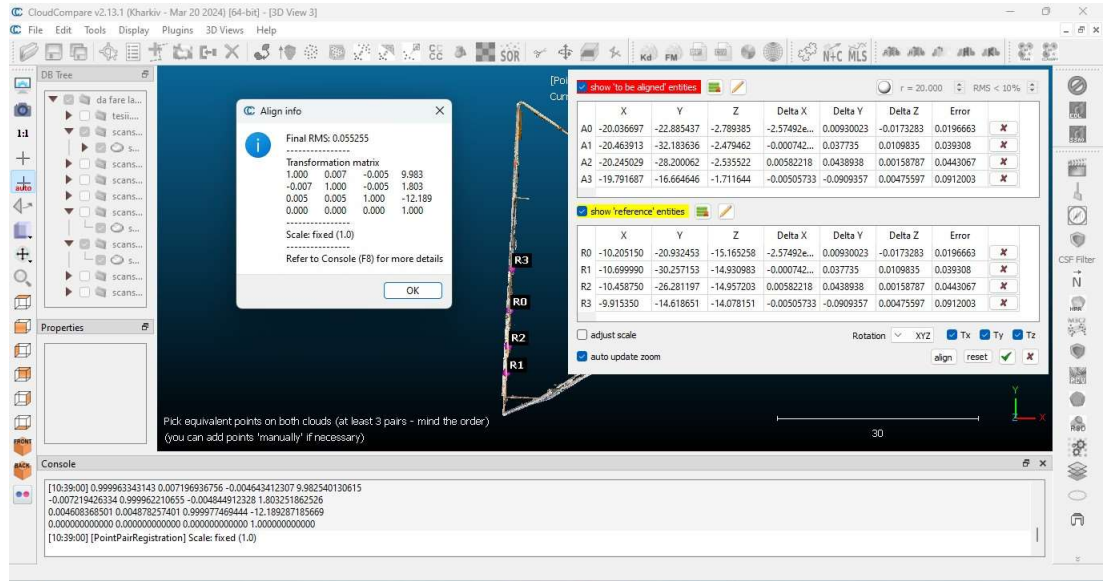


Figure 59 Georeferencing between "scansione 4\_2\_hd" e "scansione 9\_2\_hd". Source: (Cloud Compare)

- Georeferencing between “scansione 4\_2\_hd” and “scansione 10\_2\_hd”, with relative matrix.

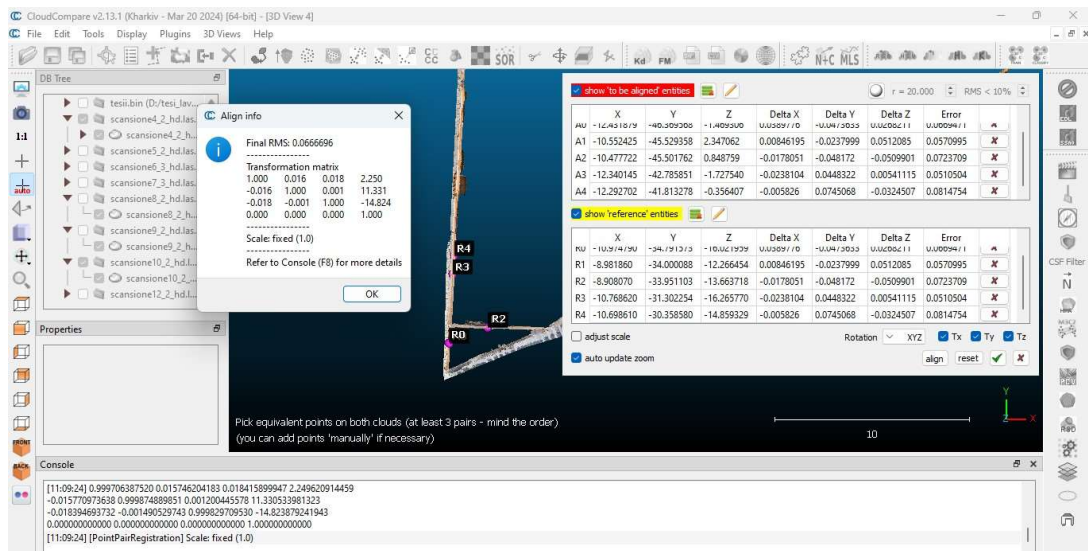


Figure 60 Georeferencing between "scansione 4\_2\_hd" e "scansione 10\_2\_hd". Source: (Cloud Compare)



- Georeferencing between “scansione 4\_2\_hd” and “scansione 12\_2\_hd”, with relative matrix.

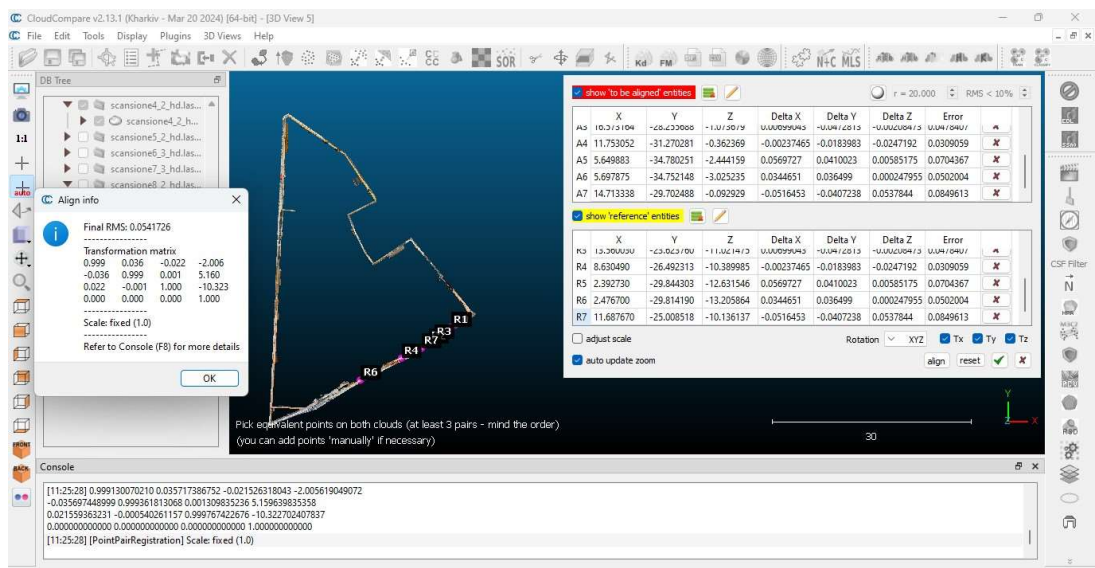


Figure 61 Georeferencing between “scansione 4\_2\_hd” e “scansione 12\_2\_hd”. Source: (Cloud Compare)

By observing the generated matrices, the root mean square (RMS) obtained for the alignment between the 5 mm and 50 mm point clouds was found to be an average of 0.05 m. In other words, each point in the aligned cloud is approximately 5 centimetres from its corresponding point in the reference cloud. Since the final goal is referred to a 3D cadastre, the error of 5 cm still provides a good result for the detailed 3D model. The following picture represents the point cloud obtained along with the outcomes of the aforementioned geoprocessing procedures.

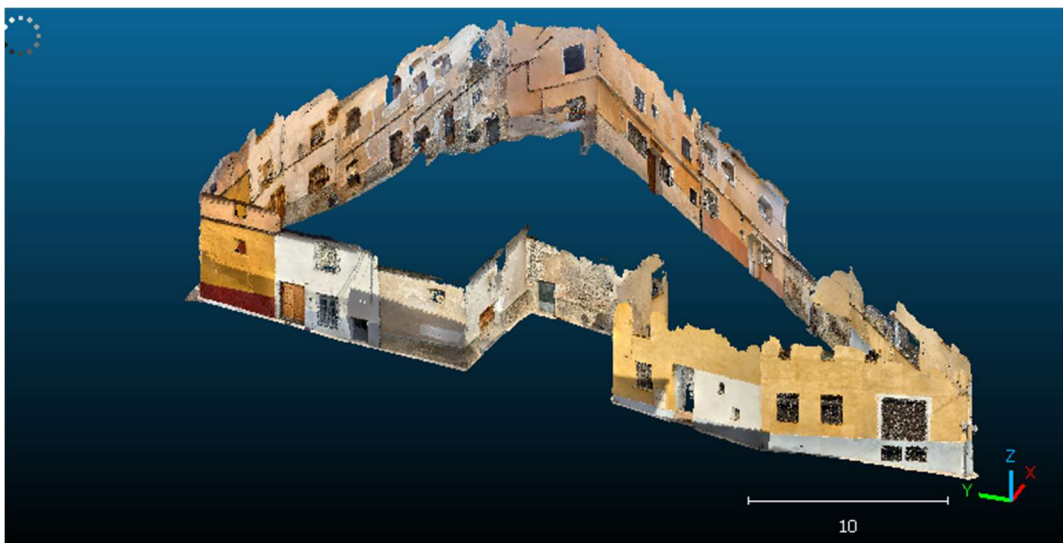


Figure 62 Final point cloud obtained from iPad. Source: (Cloud Compare)

### 3.3.3. Point cloud density analysis

During this research, a density analysis was carried out to determine the quality and level of detail of each point cloud. This analysis was carried out using Cloud Compare software, using the compute geometric feature function (fig. 63). As shown in the accompanying figure, this was used to accurately calculate the number of neighbours of each point within 0.05 meters of sphere. Through the method, the spatial interactions between the points could be examined in detail, which led to a more accurate assessment of the points' overall distribution and aggregation in the cloud. The results produced were the point cloud's density, the Gaussian average, and the standard deviation. This method was applied across all available point clouds, which included two-point cloud captured from the ground level and two-point ground captured from above the ground level.

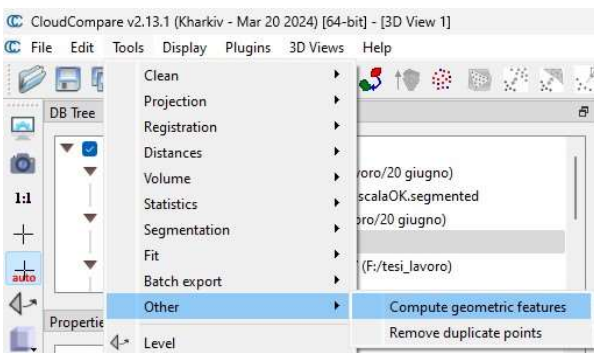


Figure 63 Density calculation. Source: (CloudCompare)

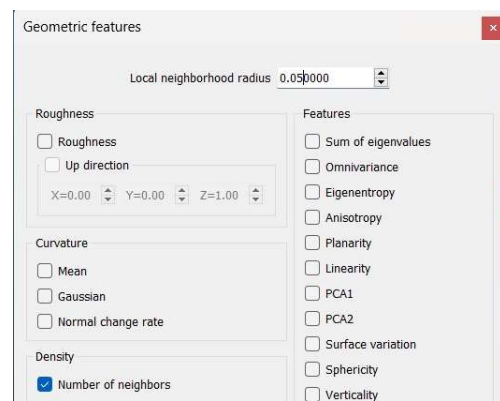


Figure 64 Density calculation: number of neighbors. Source: (CloudCompare)

It is determined that the terrestrial laser scanner that was acquired with the Leica Nova MS50 Total Station had a mean value of 17.3 points and a standard deviation value of 17.14 points. In the first picture shown below there is the value of the surface density instead in the second one there is the value of the Gauss mean and the standard deviation. In both pictures it is evident that the values are higher in the spots where the total station was most likely settled. On the other hand, it is noted that there are some sections of the façade, far from the total station spots, that are either completely absent or have a low density.

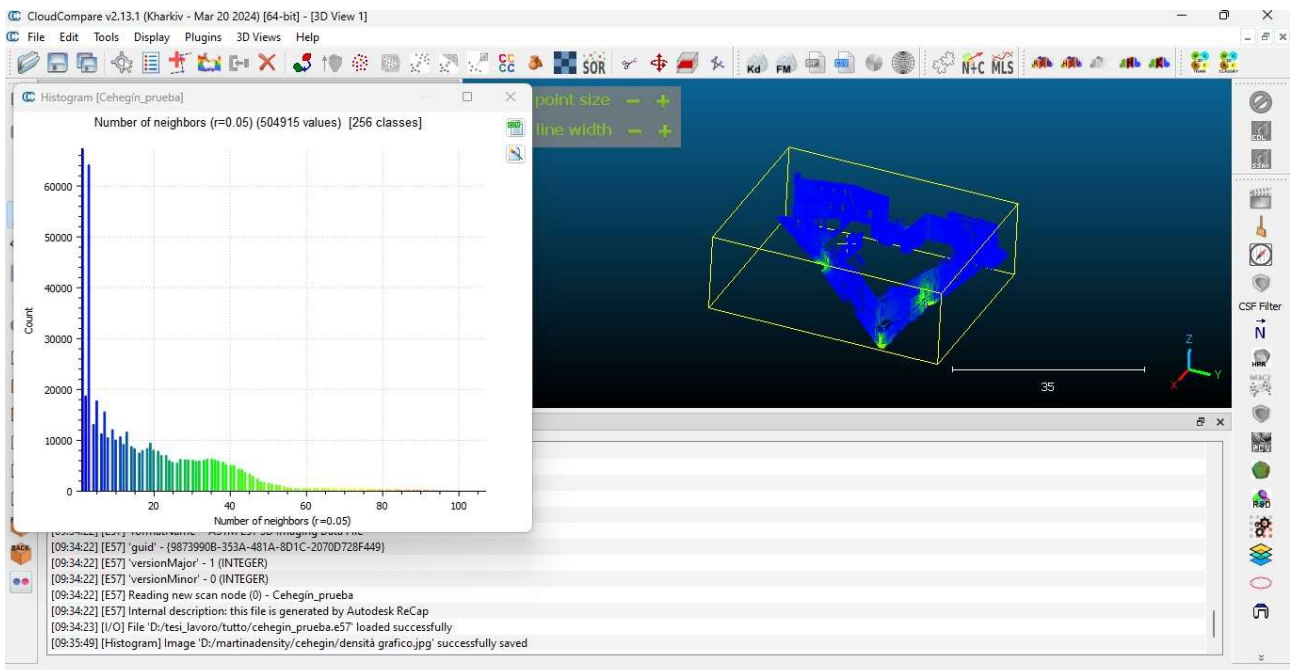


Figure 65 Density calculation for the Total Station Leica Nova MS50. Source: (CloudCompare)

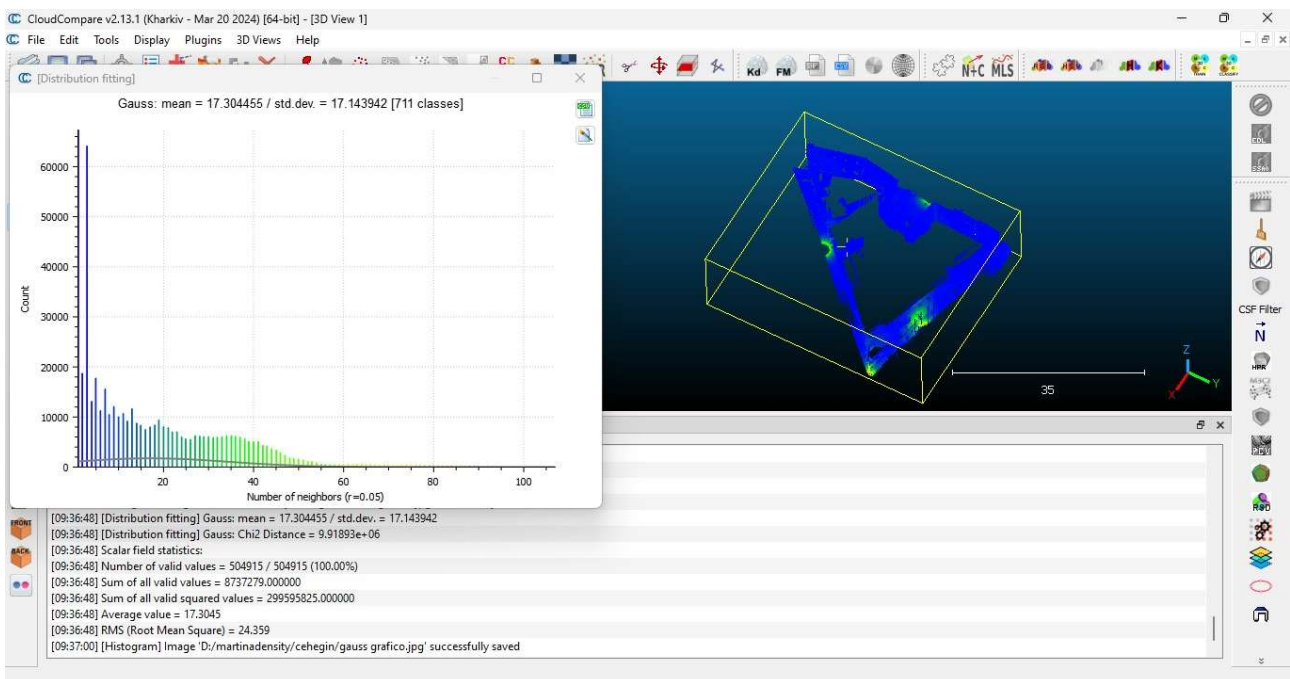


Figure 66 Gaussian density calculation for the Total Station Leica Nova MS50. Source: (CloudCompare)

For the second terrestrial laser scanner point cloud acquired using an iPad Pro Apple 11-inch (2nd generation), the situation is different compared to the previous one since the values are 426.63 for the Gauss mean and 167.75 as standard deviation. As matter of fact, in this case the number of points is higher compared to the previous one and the facades are dense. There are points where the density is particularly high, probably due to the speed at which scans were made, since slower scanning allows to acquire more points. Density is also affected by proximity to the surface. Although efforts have been made to maintain a constant distance of 1

meter from the vertical walls, in some cases physical obstacles have prevented this distance from being maintained. It should also be noted that the iPad is limited to a maximum height for scanning facades, which leads to lower density at the top of the point cloud, as shown in (Murtiyoso et al. 2021). However, since each scanning was done on a sunny afternoon, the weather should not be considered as a discriminant. To sum up, according to the density of the collected point cloud information, this data is suitable for high detail modelling.

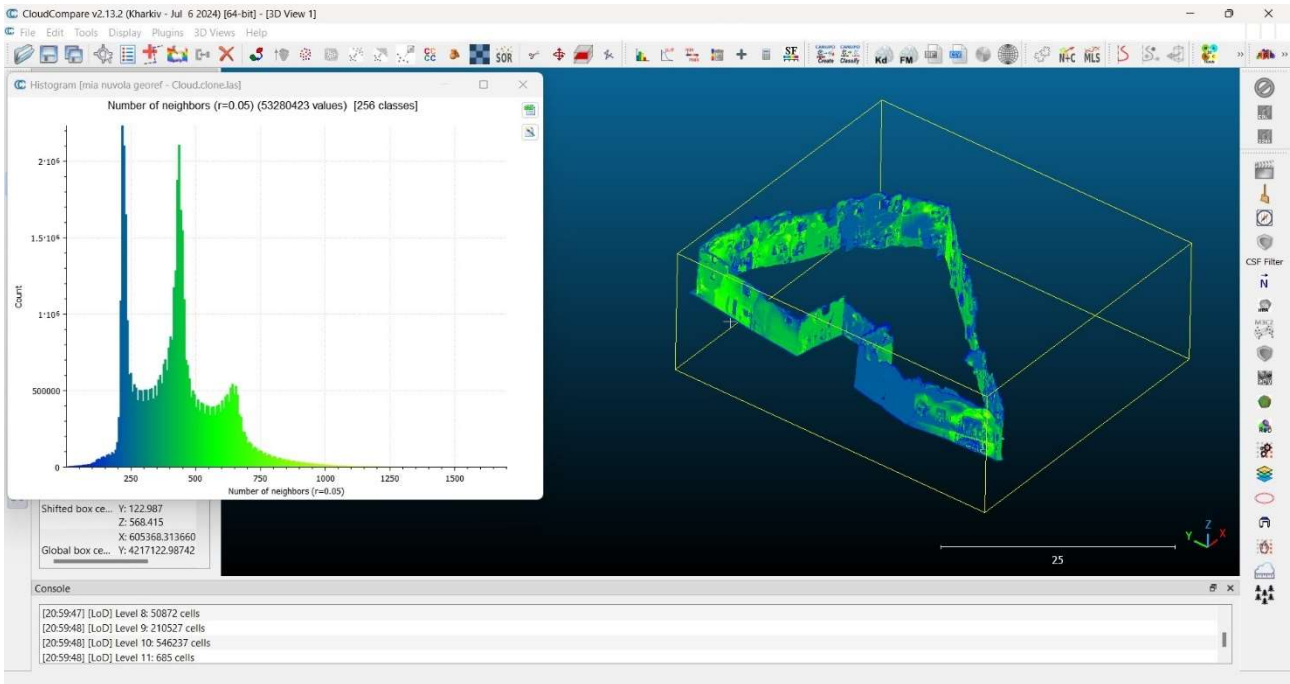


Figure 67 Density calculation for the iPad Pro Apple 11-inch. Source: (CloudCompare)

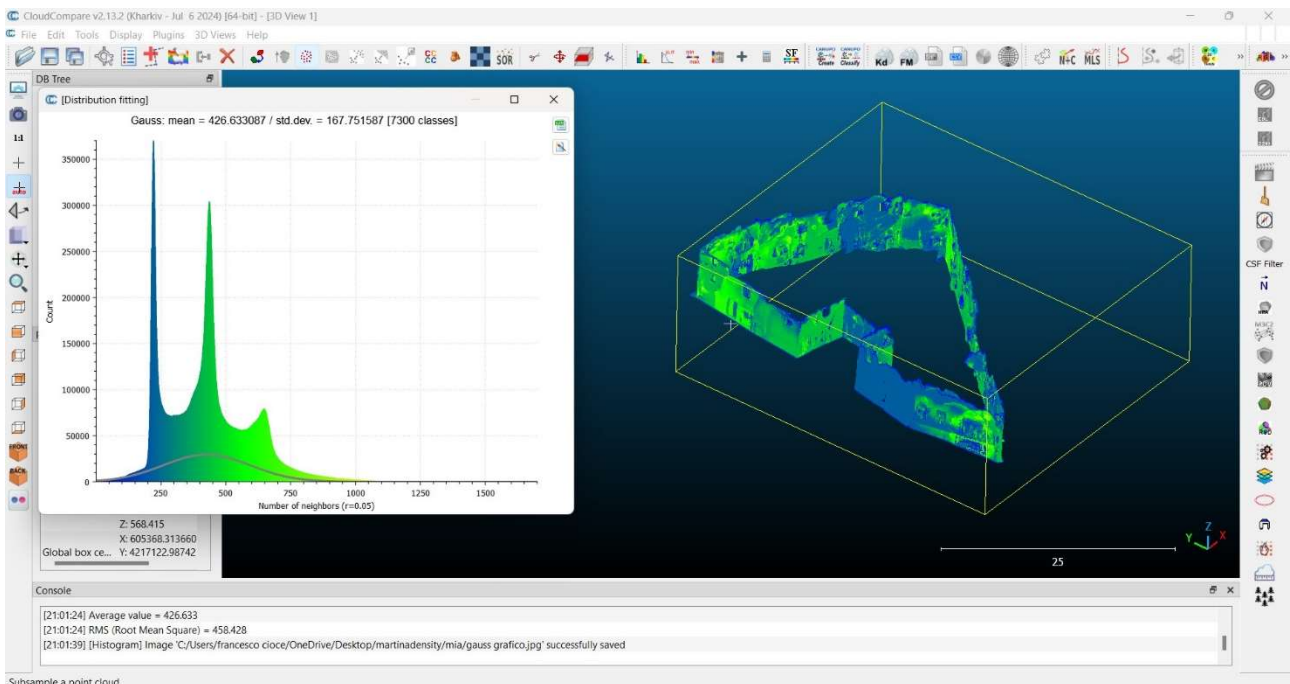


Figure 68 Gaussian density calculation for the iPad Pro Apple 11-inch. Source: (CloudCompare)



In this section, an analysis was conducted on the point cloud captured from aerial vehicles. The first point cloud under consideration is derived from a digital elevation model (DEM) obtained using photogrammetry technique, which operates on a national scale. The specific scan exhibits a point density of 0.5 points per square meter, which quantifies the number of points collected within a designated area. An analysis of the point cloud density in a sphere of 0.05 meters revealed that most points had only one or two neighbouring points within the specified radius. This suggests that there is not a dense clustering of points because of the spatial structure of the point cloud. In the best-case scenario, each point would have exactly one neighbour within the defined radius. However, in less favourable conditions, some points might not have any neighbours within the 0.05-meter sphere. In these cases, the point is considered its own neighbour, resulting in a neighbour count of 1. The low point density, both at the local and global scale corresponds to a constraint in the ability to capture the spatial variability and to determine topological relations among points. In this context, it is essential to highlight that the primary objective of the aerial survey conducted at the national level was large-scale mapping. Consequently, the point density observed in this scan is lower when compared to the densities identified in previously analysed point clouds.

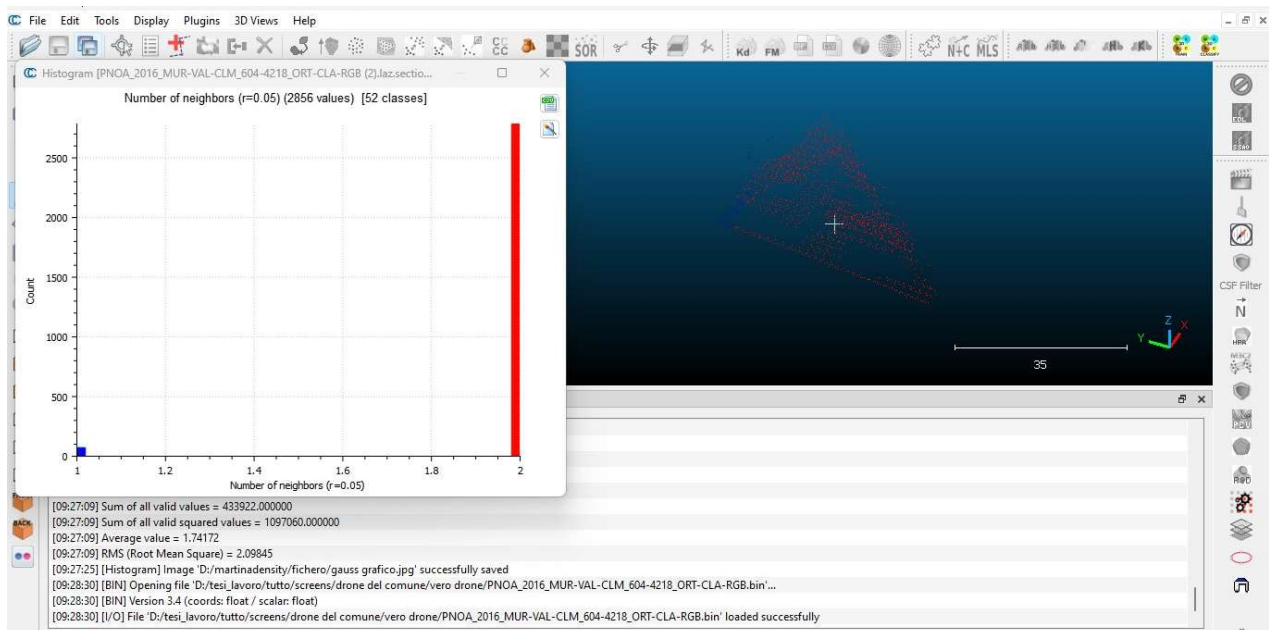


Figure 69 Density calculation for the aerial LiDAR scan conducted by national flight. Source: (CloudCompare)

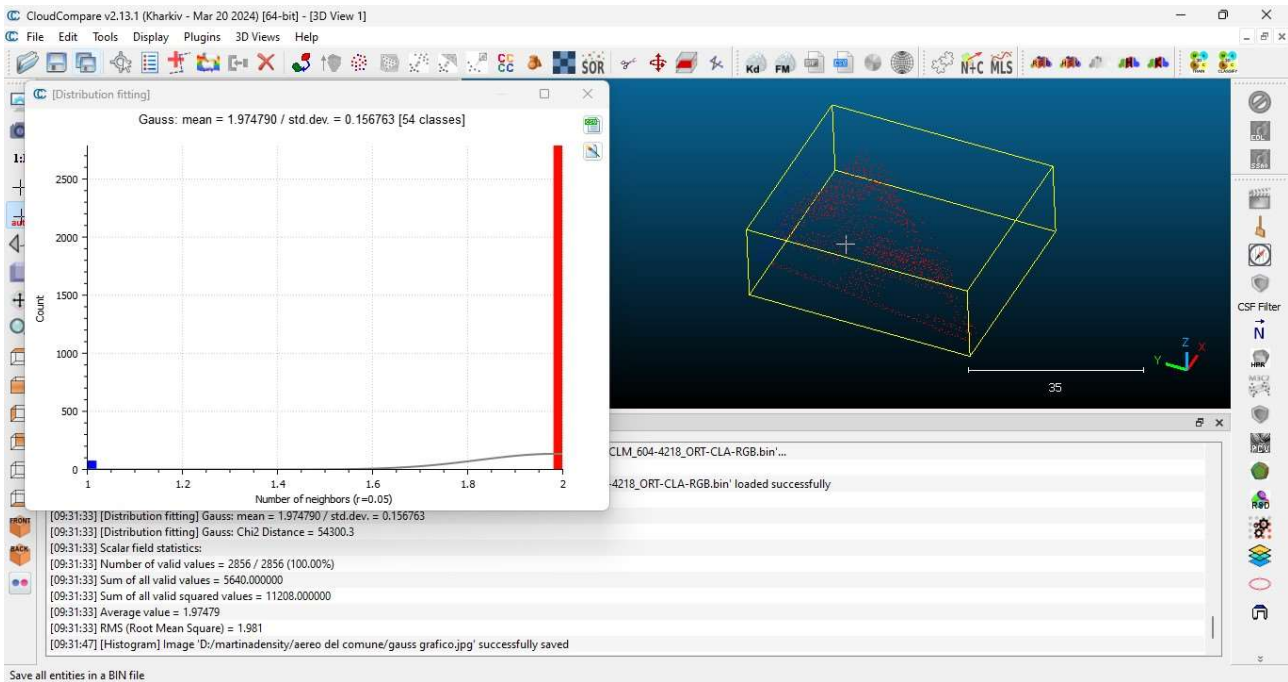


Figure 70 Gaussian density calculation for the aerial LIDAR scan conducted by national flight. Source: (CloudCompare)

In conclusion, the density results for the point cloud generated through photogrammetry using a drone, acquired during the research done by (Ródenas-López, M. A, 2023) are presented. The analysis shows an average point density of 1.74 points and a standard deviation of 1.17 points. Once the point cloud density was calculated, it became evident that certain areas within the point clouds showed higher densities compared to others. This phenomenon is probably produced by more picture overlap in that region, which is the consequence of the intricate geometries that characterize the study area. Specifically, the need to create additional points to accurately represent the intricate surfaces because of the terrace, may have played a role in the increased density. The drone software can identify more details and create a denser point cloud when the drone flies closer to a structure because the images it takes have a greater resolution. The point cloud generated can be utilised for roof modelling because to its higher density when compared to the previous aerial point cloud.

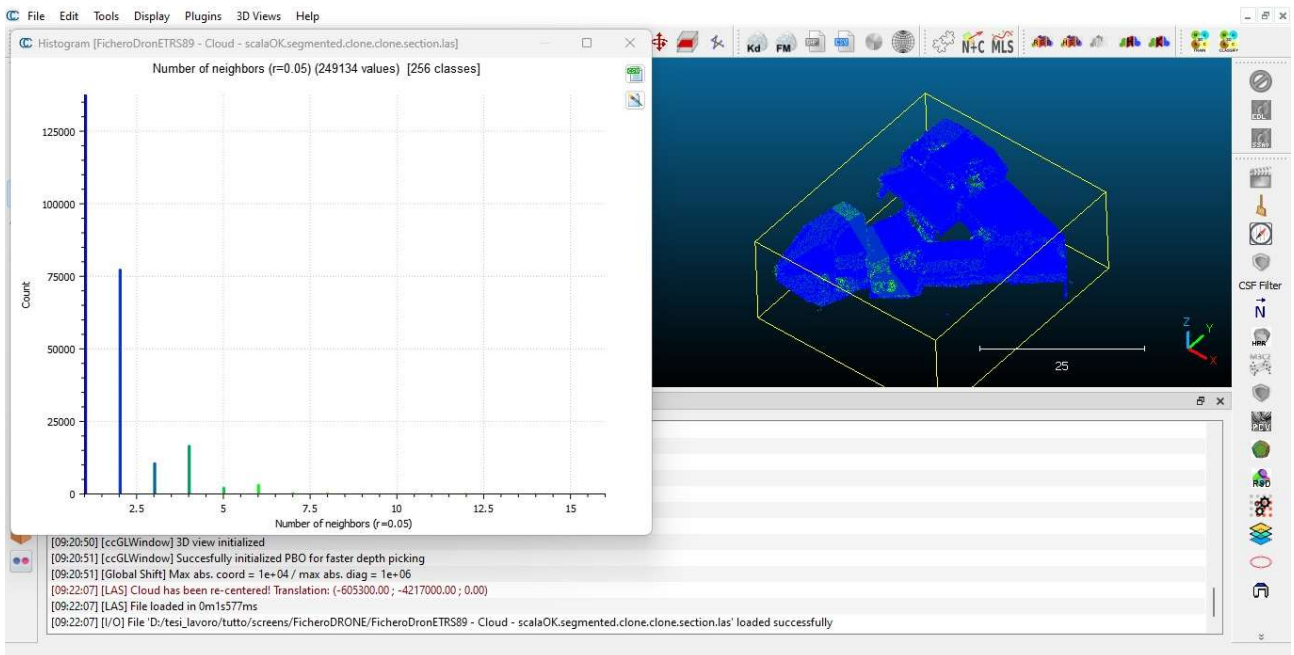


Figure 71 Density calculation for the drone point cloud generated through photogrammetry. Source: (CloudCompare)

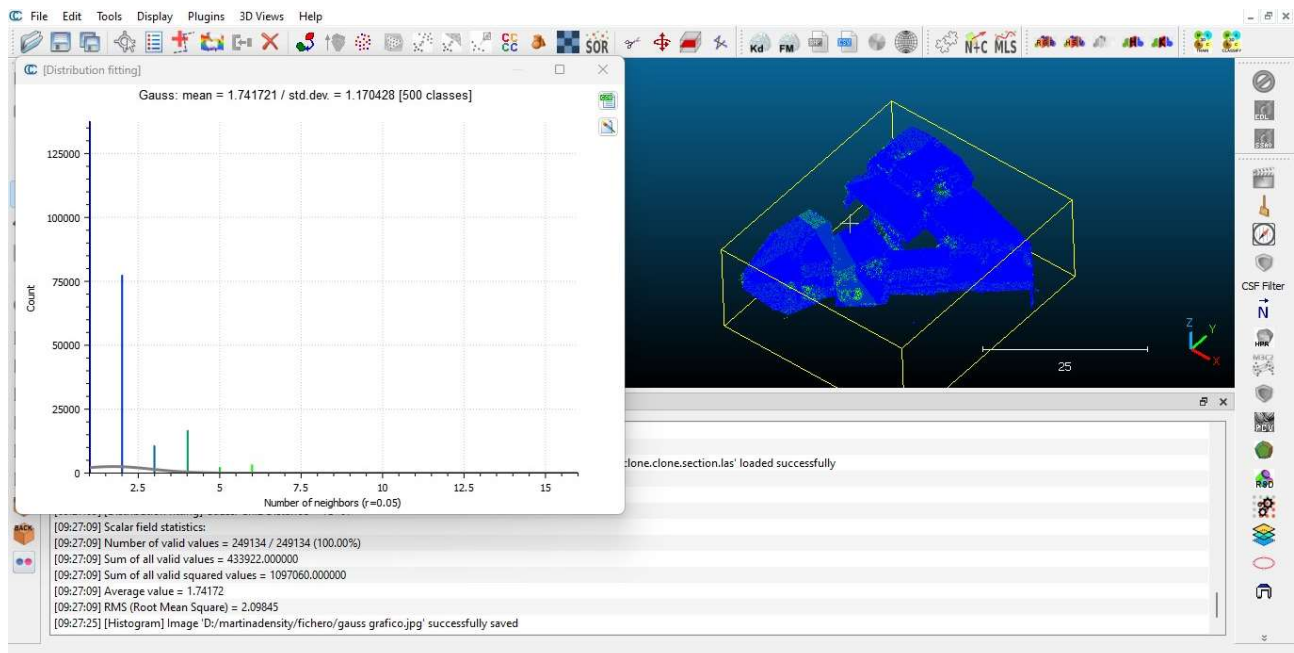


Figure 72 Gaussian density calculation for drone point cloud generated through photogrammetry. Source: (CloudCompare)

The density computation produced the following values:

| Point cloud                             | N° of points | File size | Average value | Standard deviation |
|---|--------------|-----------|---------------|--------------------|
| Leica Nova MS50 Total Station           | 504915       | 13,5 MB   | 17.30         | 17.14              |
| iPad Pro Apple 11-inch (2nd generation) | 53280423     | 1,29 GB   | 426.63        | 167.75             |
| Aerial flight                           | 2856         | 208 KB    | 1.97          | 0.16               |
| University drone                        | 249134       | 6,17 MB   | 1.74          | 1.17               |

A comparative analysis of the point clouds revealed that those acquired using the rapid mapping and the drone, used during the research of (Ródenas-López, M. A, 2023), exhibited a markedly superior level of detail. To augment the model's precision, it was deemed appropriate to merge these two point cloud.

| Point cloud                 | N° of points | File size |
|-----------------------------|--------------|-----------|
| iPad Pro + University drone | 53529557     | 2,49 GB   |

To successfully integrate the two point clouds, two preliminary steps were required: data cleaning and data geolocating. Specifically, the point clouds have been subjected to a cleaning process in Cloud Compare software to remove any extraneous points that were not relevant for analysis. Additionally, the point cloud generated using LiDAR technology was georeferenced in relation to the point cloud derived from drone photogrammetry, to be correctly geolocated. A correct alignment and an overall quality of the final point cloud was obtained.



### 3.3.4. Georeferencing process for the Lidar point cloud

The LiDAR point cloud was georeferenced to the ETRS 89 UTM 30N coordinate system by identifying homologous points between the point cloud and reference drone point cloud. This process allowed for a precise transformation of the point cloud from the local coordinate system to the global coordinate system, ensuring accurate spatial representation of the data.

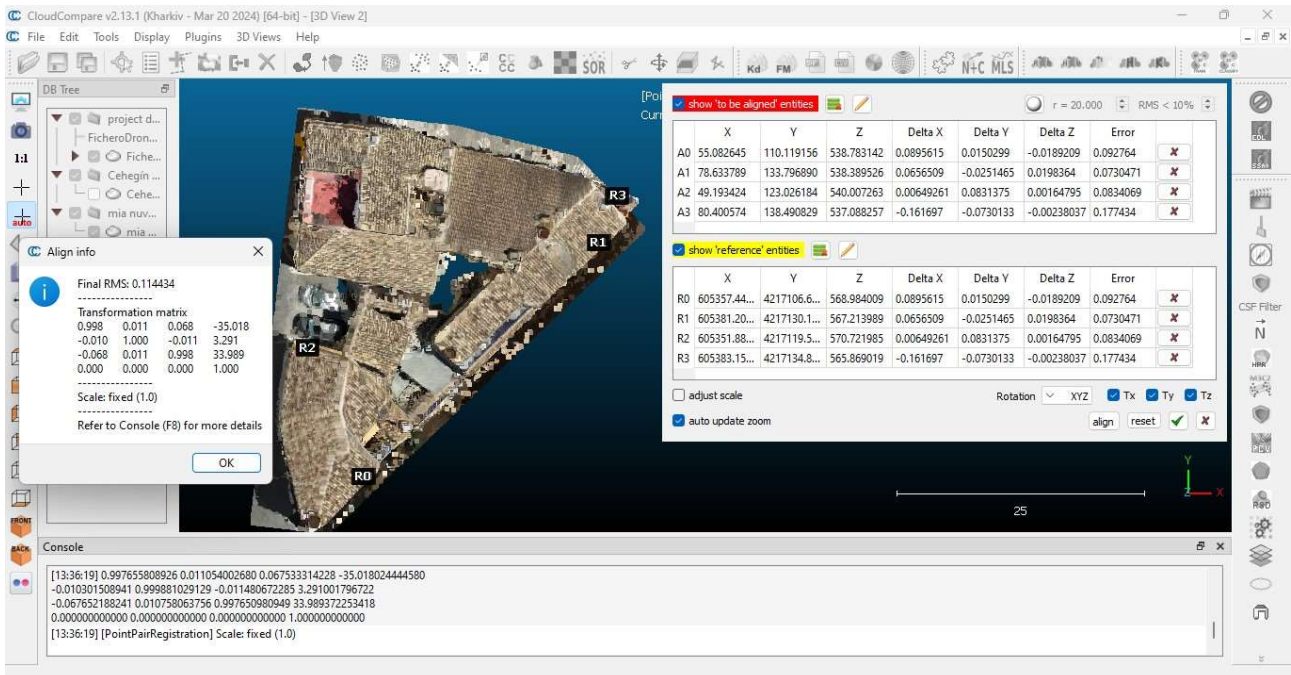


Figure 73 Georeferencing process of the iPad point cloud with the drone point cloud. Source: (Cloud Compare)

As result of the georeferencing process, the final RMS error was 0.11 meters, indicating that the distance between the two point clouds was relatively large. This higher error, compared to previous georeferencing efforts, can be attributed to the lower precision of the point cloud generated by the drone, which has caused a difficulty in selecting points. As seen in the image below, certain distortions are noticeable in the windows and other sections of the facade.

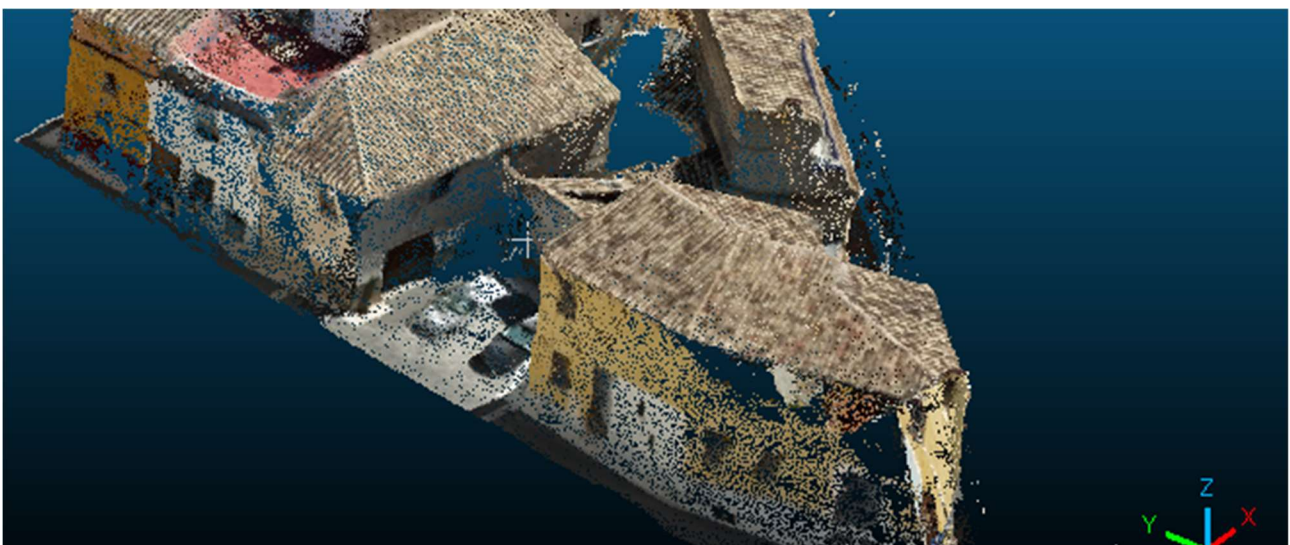


Figure 74 Distortion of the drone point cloud. Source: (Cloud Compare)

These distortions are most likely due to inaccuracies during the photogrammetric process in Metashape, or possibly errors introduced by the LiDAR scanner during the on-site survey.

### 3.3.5. Mesh generations

Prior to mesh generation, the point cloud underwent a normal computation process using the 'compute normal' command. This step was essential for establishing the surface orientation of the point cloud data. The mesh was subsequently generated from the point cloud using the PoissonRecon command, with a processing time of 1.2 seconds, resulting in a mesh with 75.923 faces and 38.315 points.

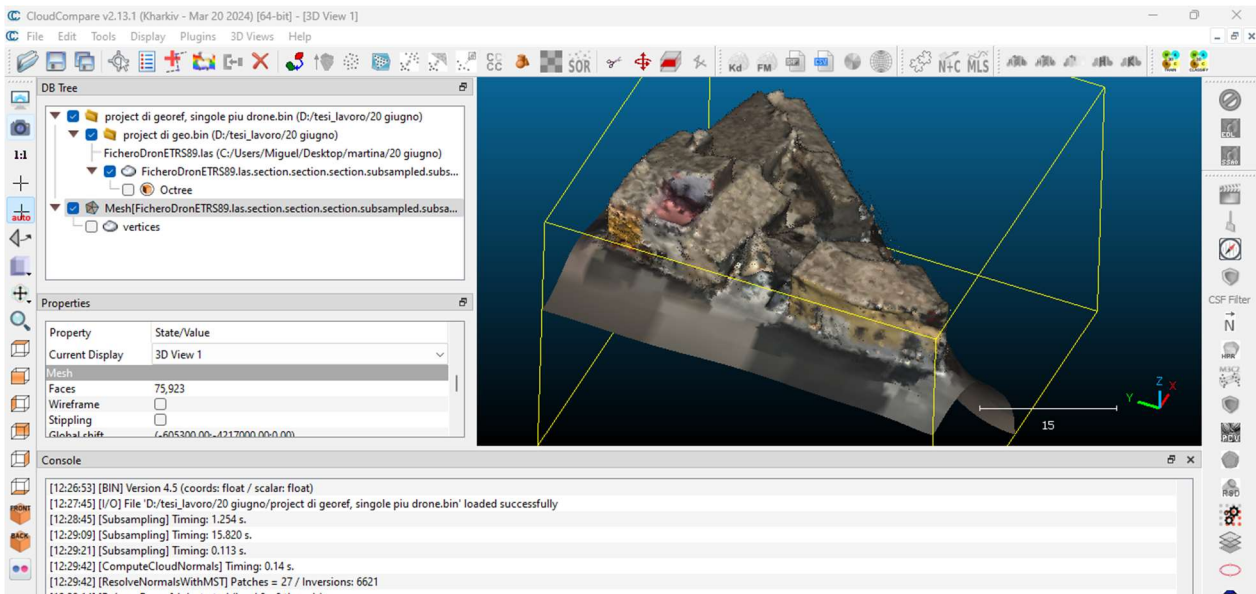


Figure 75 Mesh generated. Source: (Cloud Compare)

For the mesh generated, using the segment command, it was possible to delete all the points that were external to the study area. The final mesh has 68.636 faces and 34.831 points.

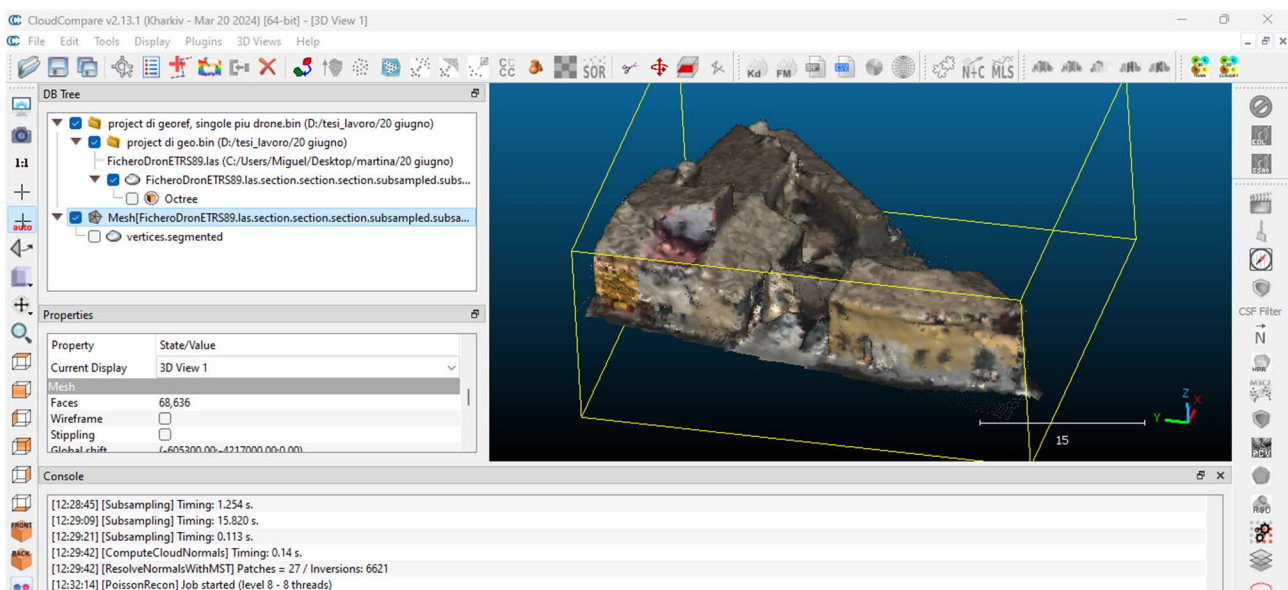


Figure 76 Cleaning mesh. Source: (Cloud Compare)

This procedure was applied consistently to all point clouds, regardless of their point density, to facilitate a comparative analysis of geometric characteristics and processing time. The results will be mentioned in the following table.

| Point cloud                             | Mesh pictures   | Initial nº of points | Initial nº of faces | Normal time computing | Mesh time computing | Final nº of points | Final nº of faces |
|---|---|----------------------|---------------------|-----------------------|---------------------|--------------------|-------------------|
| Leica Nova MS50 Total Station           |    | 59.584               | 118.927             | 10,93 s               | 3 s                 | 42.550             | 83.295            |
| iPad Pro Apple 11-inch (2nd generation) |    | 49.488               | 98.839              | 6 h                   | 10,6 s              | 35.911             | 69.930            |
| Aerial flight                           |  | 5.441                | 10.712              | 0,05 s                | 0,5 s               | 2.901              | 5.593             |
| University drone                        |  | 105.573              | 201.875             | 2,55 s                | 2,6 s               | 99.693             | 198.312           |
| iPad Pro + University drone             |  | 98.342               | 196.576             | 7 h                   | 17,6 s              | 93.886             | 186.814           |

### 3.4. Data integration and model development

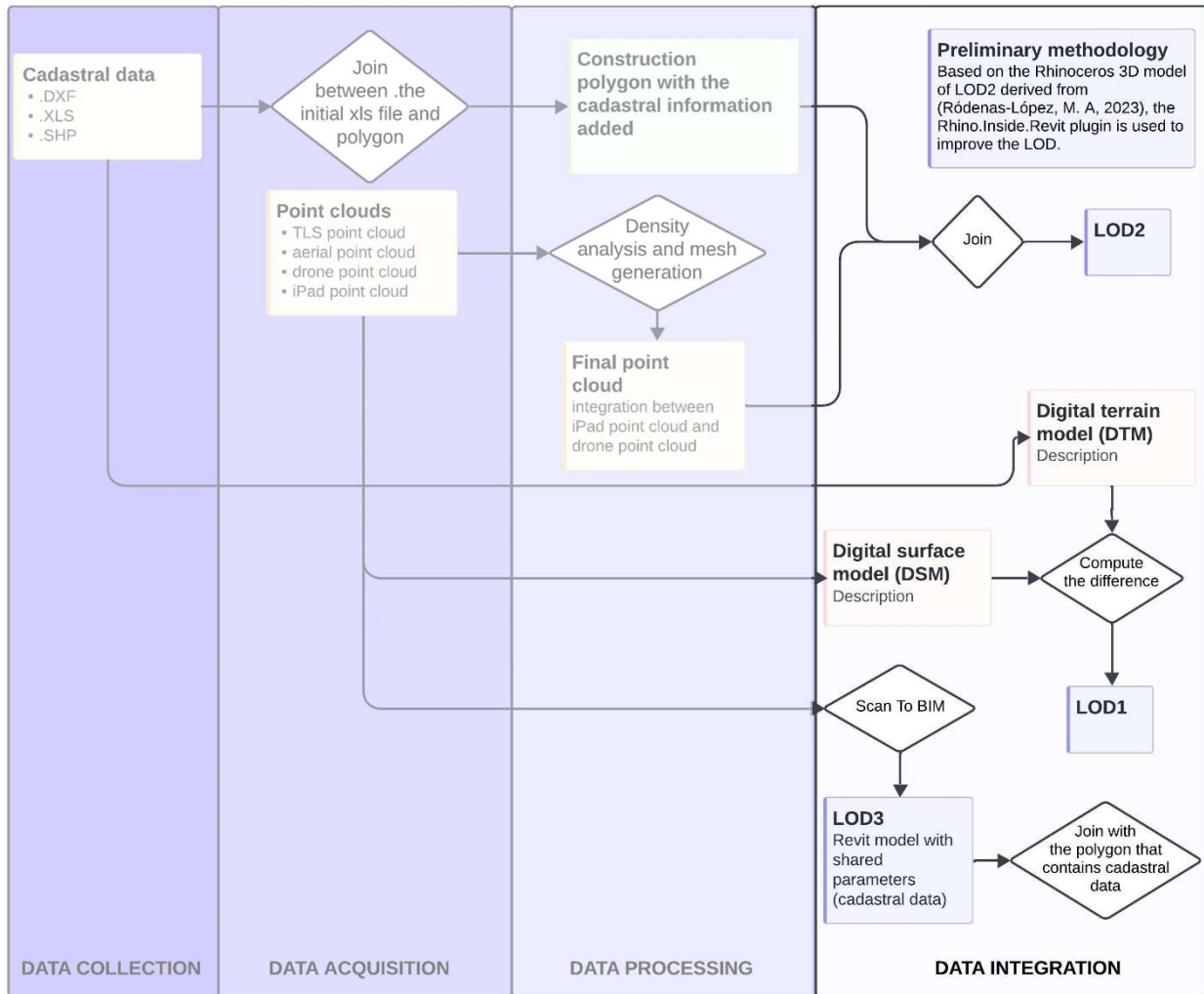


Figure 77 Data integration schema. Source: (Author, 2024)

This chapter outlines a methodology to produce a detailed 3D model of the case study, based on BIM and GIS integration, using cadastral data and point clouds. Furthermore, a preliminary methodology was introduced that could potentially make use of the Rhinoceros model derived from the (Ródenas-López, M. A, 2023) research study. This chapter is divided in three main sections in accordance with the models obtained at varying levels of details (LOD). By combining diverse data sources, the study aims to give a faithful representation of the case study. In this regard, the thesis's last section included a study on the integration of BIM and GIS, which was founded on the integration of the different data gathered from the approach.



### 3.4.1. Preliminary methodology

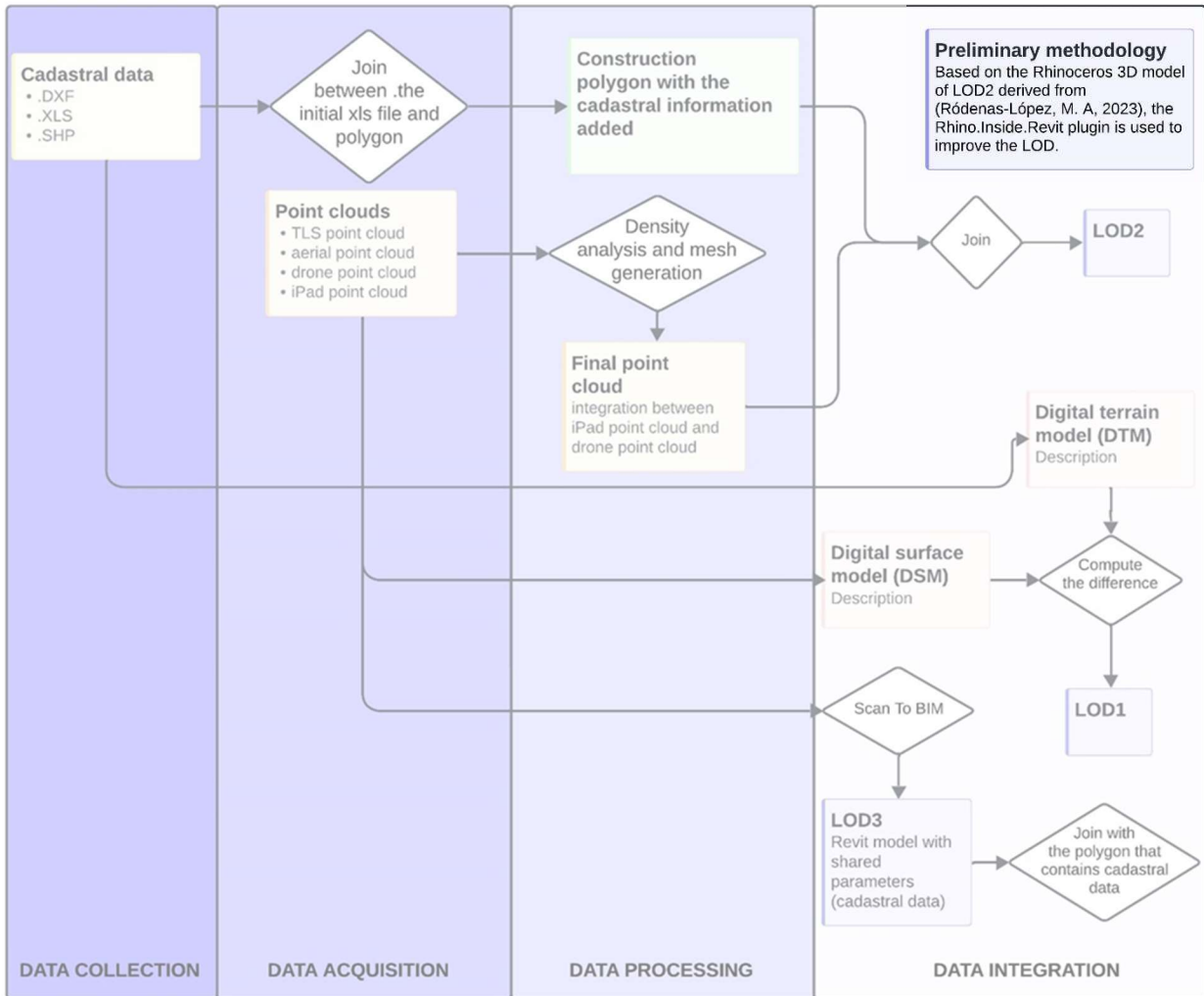


Figure 78 Preliminary methodology schema. Source: (Author, 2024)

It is important to consider that to enhance the level of detail and improve BIM-GIS interoperability, it was tested an approach using the Rhino.Inside.Revit plugin. This method was selected to allow the Rhinoceros 3D model of LOD2 from prior research by (Ródenas-López, M. A, 2023) to function as if it were a native Revit model. Nevertheless, it became clear that the BIM model was imported as a generic object, considering all the neighbour of Cehegín as a unique model. Since every building should be a distinct object with distinct information stored in it, this result was a limitation in terms of 3D cadastre. The limitation of this result allows to study a different strategy.

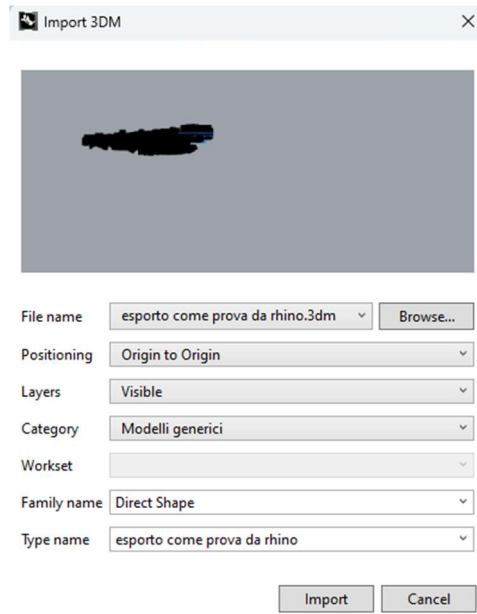


Figure 79 Import command using the plugin. Source: (Revit Autodesk)

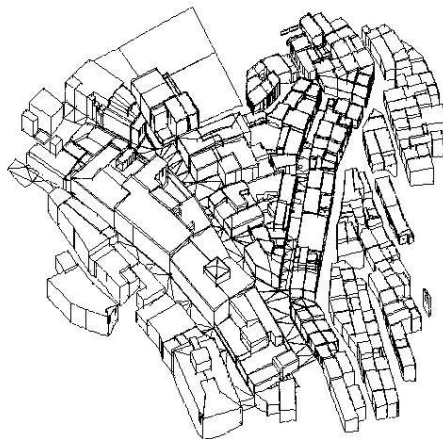


Figure 80 Screenshot of the result on Revit software. Source: (Revit Autodesk)





The data obtained from the download data section of the digital cadastre is the source of the initial component of the integration between cadastral data and point clouds. In particular, the data utilised are "ALTIPUN," a shapefile that contains the altitude points of the topography, and the point cloud acquired during the aerial survey, from which the roof points were extrapolated. The data selected was necessary to generate the digital terrain model (DTM) and the digital surface model (DSM). The DTM and the DSM were computed to provide an accurate and precise representation of the soil and the surfaces above it. As a matter of a fact, digital terrain model (DTM) represents the development of the soil surface in the absence of vegetation and human components. Instead, the digital surface model (DSM) is the surface includes these kinds of components. Specifically, the digital terrain model was computed on ArcGIS software, using the "3d Analyst tools" and selecting the "natural neighbour" interpolation, as shown in the picture 82. The Natural Neighbour interpolation tool's technique locates the selected group of input samples that is closest to a query point and weights them according to proportionate regions to interpolate a value. Specifically, the "natural neighbour" interpolation was based on the "cota", which represents the elevation points within the ALTIPUN shapefile, and a cell size of 10. This cell size is the result of the average distance between points in the point cloud.

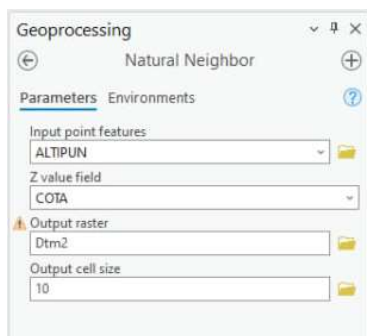


Figure 82 Natural Neighbor command.  
Source: (ArcGIS Pro)

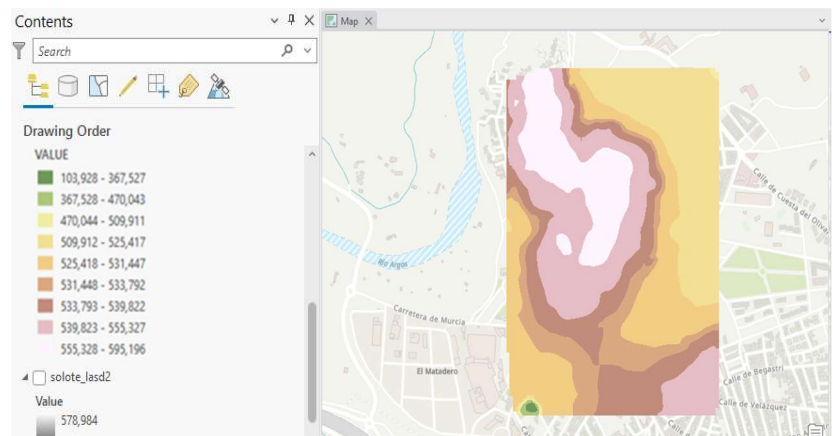


Figure 83 DTM. Source: (ArcGIS Pro)

The digital surface model was computed using the command "LAS Dataset to Raster" and selecting the point cloud "solo tetto" with only roof points, which were extracted from the aerial point cloud. This process was based on the elevation of the maximum value for each cell, since we are considering the maximum height of the point cloud.

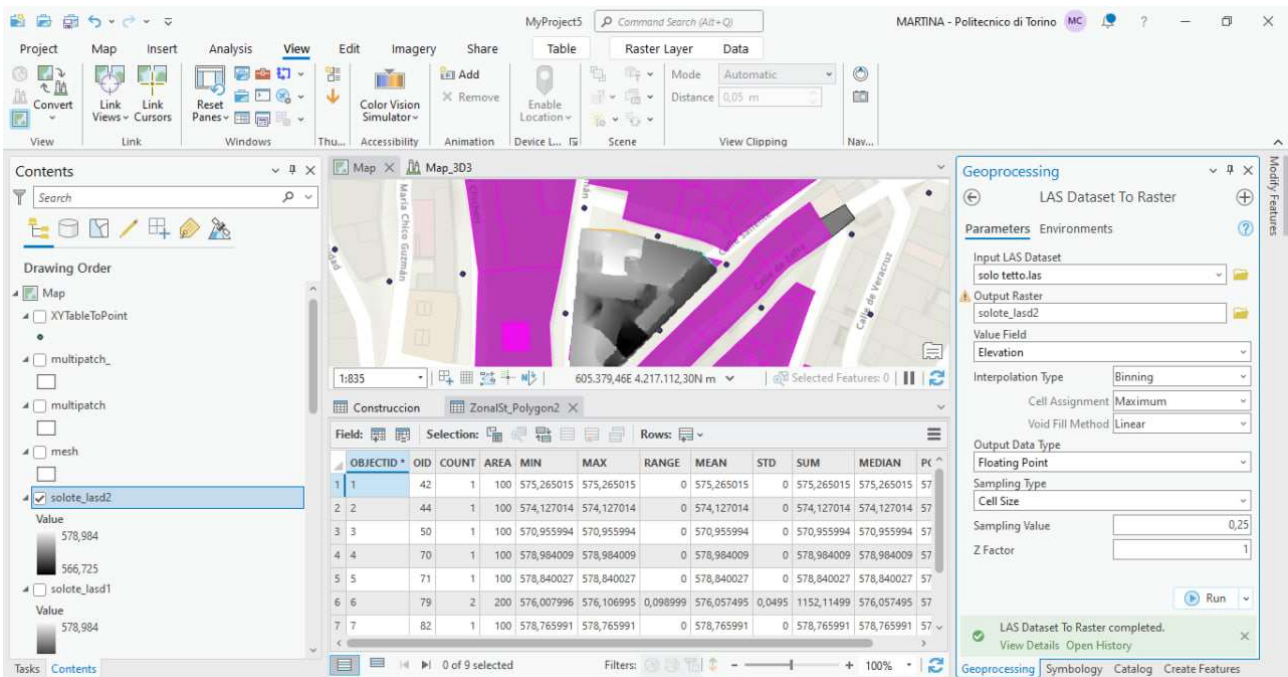


Figure 84 DSM settings. Source: (ArcGIS Pro)

After performing raster computation, a table containing all the maximum values for each polygon in the "construction" file was obtained using the "zonal statistics as table" command and a join field command was used those values in the construction file. However, a warning is displayed because, during the process, not all construction polygons are covered by the DSM, as shown in the image below.

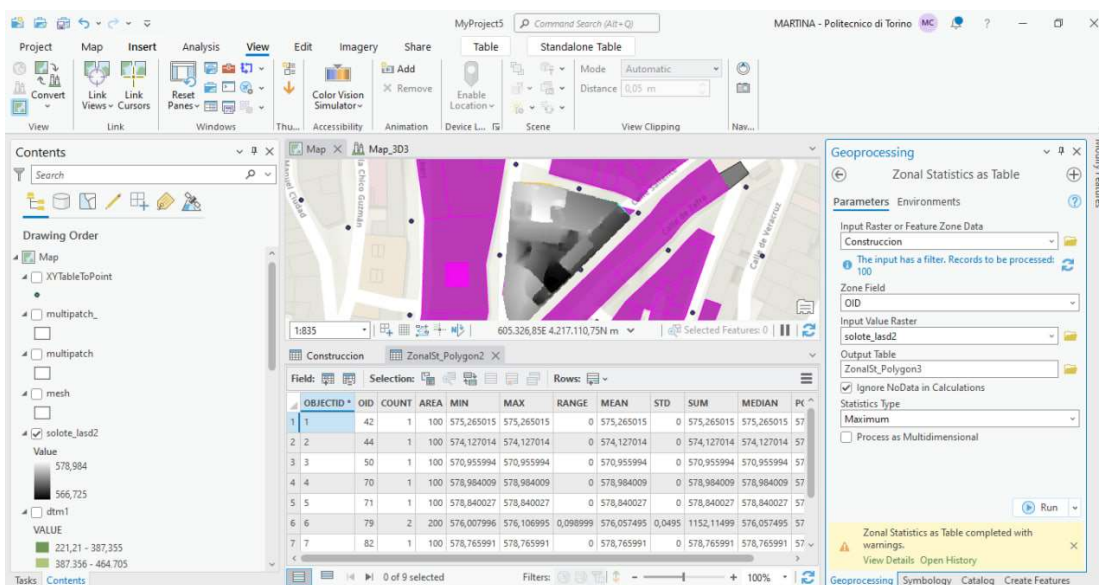


Figure 85 Zonal statistics as Table command. Source: (ArcGIS Pro)

This is because some regions are not within the scope of our investigation. It is advised to choose just the polygons pertinent to our case study and store them in a different shapefile in order to prevent receiving any more alerts. Consequently, the command "feature class to feature class" was used to extract the only polygons in the study region from the "construction" shapefile. Only the polygons having a value max that is not null are taken into consideration to create the "triangle" shapefile containing the case study buildings.

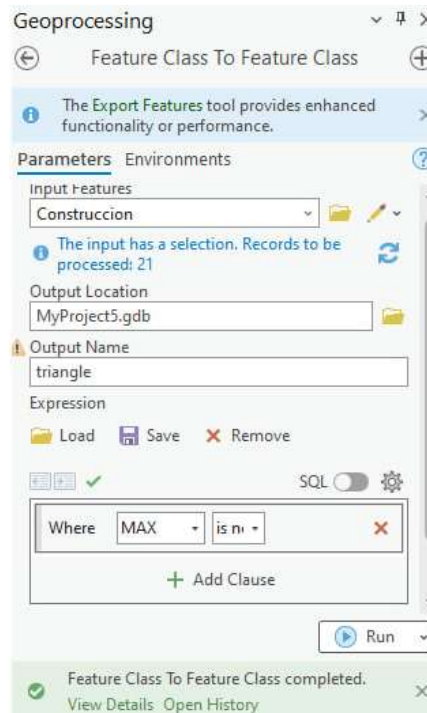


Figure 86 Generation of "triangle" shapefile. Source: (ArcGIS Pro)

To determine the true height of the buildings, the heights from the DTM were also connected to the same polygons after the heights from the DSM were assigned to them. To correlate DTM values with polygons, the centroids were generated using the 'Feature to Point' command, to which the elevation values are linked using the "extract values to points" command.

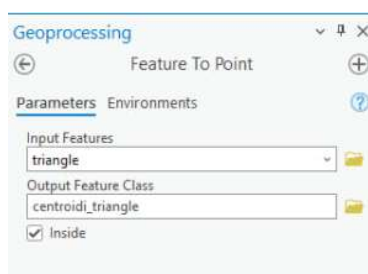


Figure 87 Generation of centroids of the new shapefile. Source: (ArcGIS Pro)

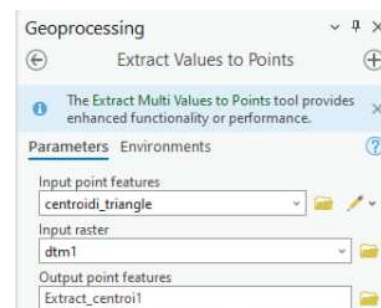


Figure 88 Extract values to points command. Source: (ArcGIS Pro)

Using “join field” command all the DTM elevations were inserted in the “triangle” table based on the common field “OID”.

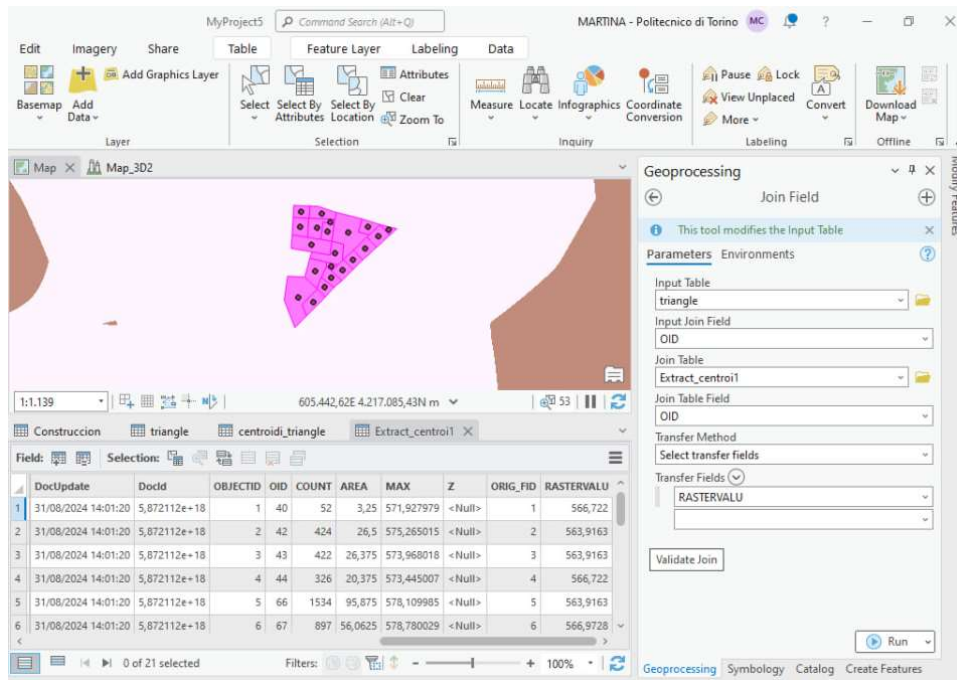


Figure 89 Adding elevation data to the centroids of the polygons. Source: (ArcGIS Pro)

Building heights are computed using the difference between the two elevation values extracted from the DTM and the DSM, and the resulting data are used to create the 3D model in ArcGIS software.

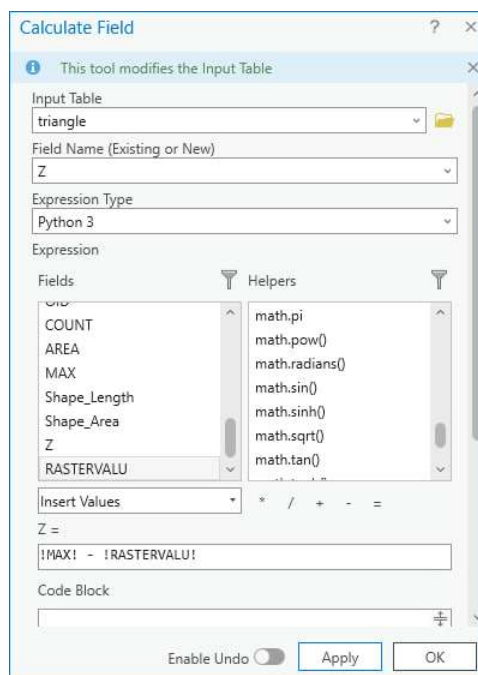


Figure 90 Difference between the elevations. Source: (ArcGIS Pro)

To create the 3D model in ArcGIS, we utilized the “triangle” shapefile and the associated building height data. The process began by opening the “local scene”, where the extrusion is carried out using the base height as the starting point and the building height to determine the elevation.



Figure 91 LOD1 model. Source: (ArcGIS Pro)

A three-dimensional solution to the 3D cadastre is demonstrated by the observed level of detail 1 and the digital surfaces produced, which are an improvement above the polygons generated by the digital cadastre. This improvement is associated with the potential to use a three-dimensional model that incorporates cadastral data and the potential to obtain information on the land's structure, which is crucial information for understanding how the natural and built environments interact. Efforts will be made to further enhance the level of detail in the following sections.

### 3.4.3. From the point clouds to LOD2

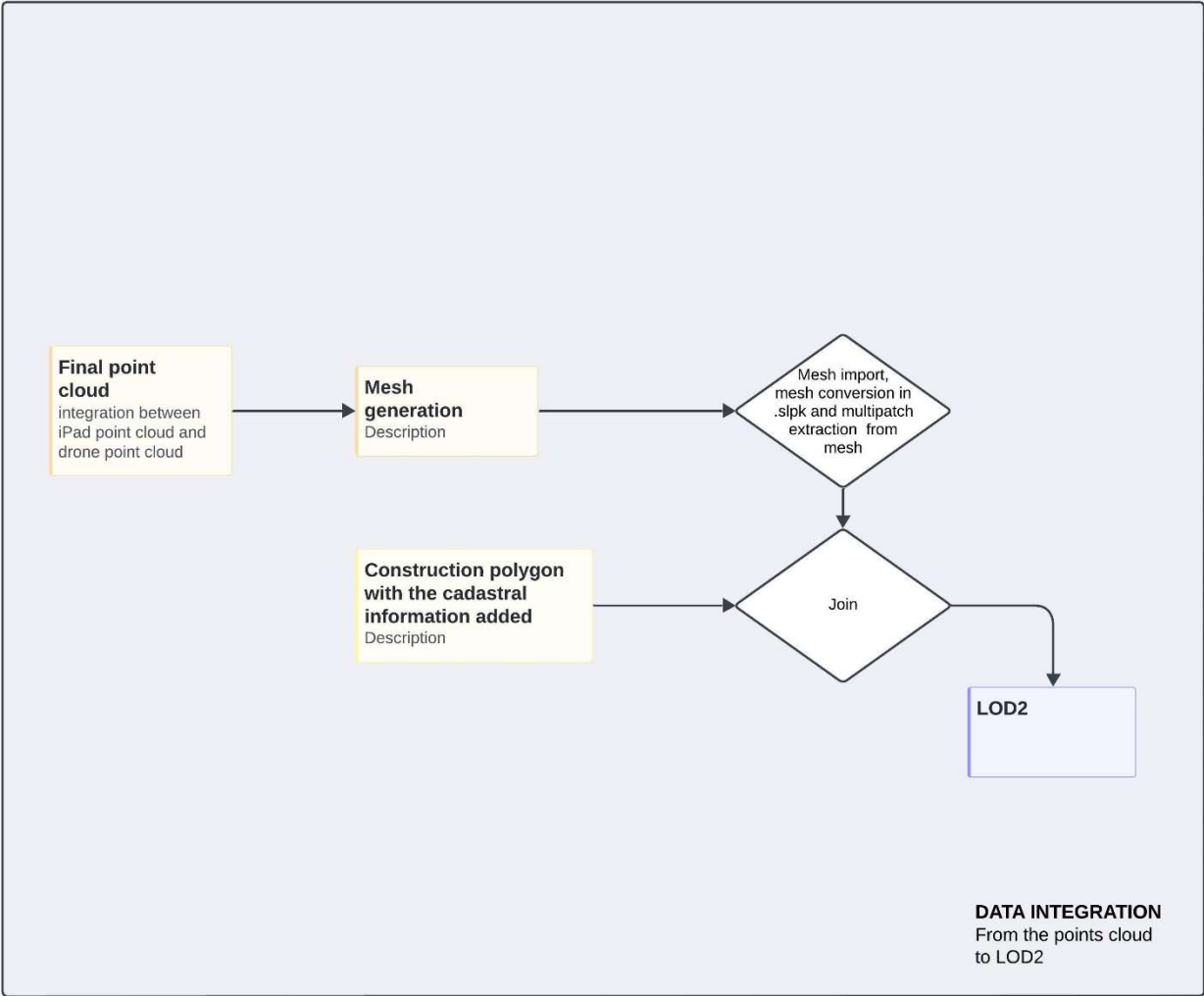


Figure 92 From the points cloud to LOD2. Source: (Author,2024)



With the purpose of increasing the level of detail obtained in the previous section, the mesh created from the point clouds was integrated in the GIS software. Although the mesh generation, which was used in the data processing section, was successful, the file size was quite large. As matter of a fact, when the mesh was imported into ArcGIS Pro, this caused the application crash. To streamline the analysis and prevent computational overload, a subsample of the union of georeferenced point clouds was created in Cloud Compare software. This involved strategically selecting a subset of points while preserving the overall spatial distribution. This step was crucial for optimizing processing time and ensuring computational stability during the integration of the point cloud in the ArcGIS software. In particular, a distance of 0.3 meters was chosen as minimum space between points. Iterative tests led to the decision to lower the point cloud to 0.3. Actually, another minimum distance between points might possibly be selected for other computers, but the features of the one that was used, precluded the usage of a file that was notably heavy.

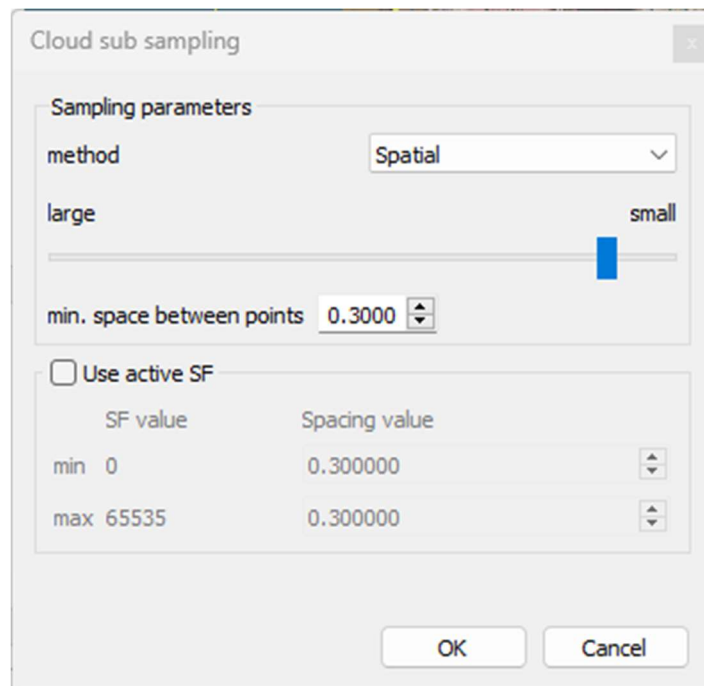


Figure 93 Subsample command. Source: (Cloud Compare)

The final result has a size of 997 KB and can be observed in the figure below.

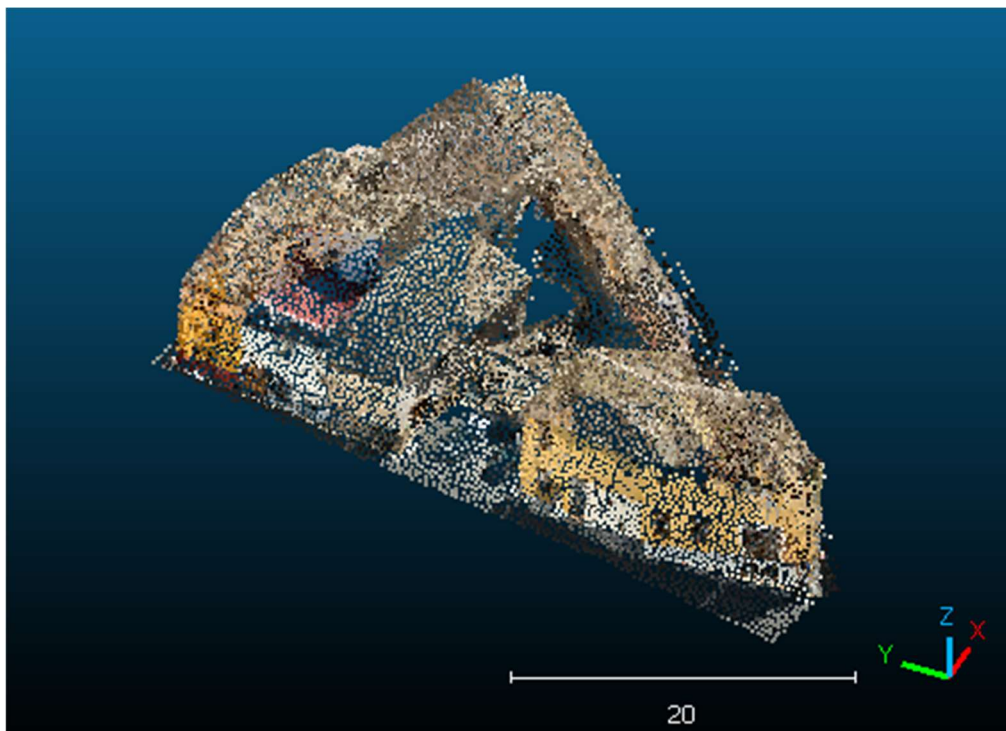


Figure 94 Final result of the two point clouds merged. Source: (Cloud Compare)

Once the issue was fixed, the mesh was imported in GIS software using the command “import 3D files”. This step was essential to gain a clearer understanding and representation of the building structure, which could not have been achieved using only cadastral data.

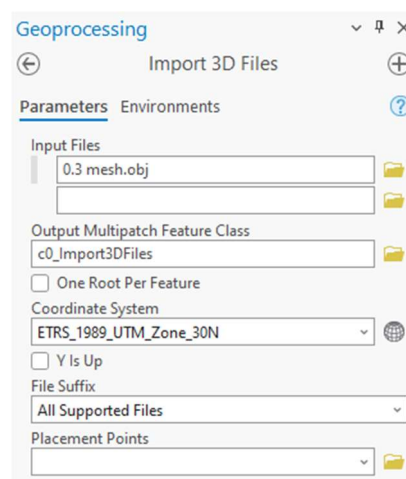


Figure 95 Import of the mesh in ArcGIS Pro. Source: (ArcGIS Pro)

The findings of the research can be seen in the 2D and 3D maps below.

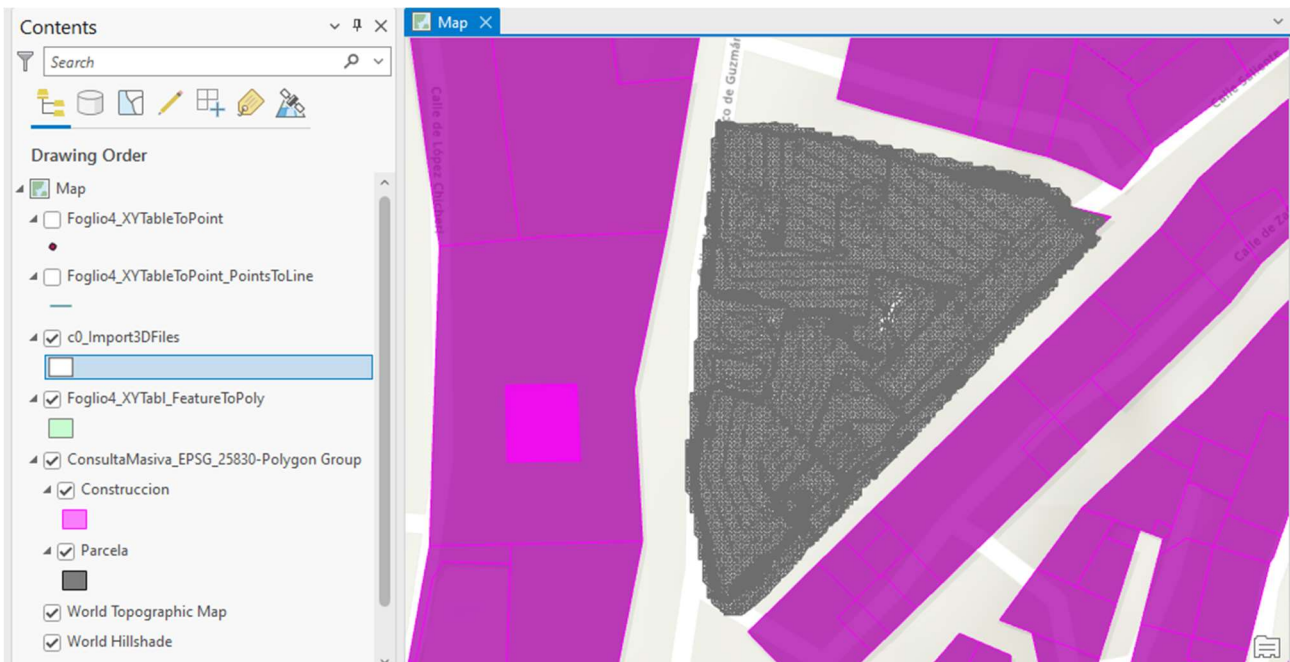


Figure 96 Visualization of the mesh in 2D Map. Source: (ArcGIS Pro)

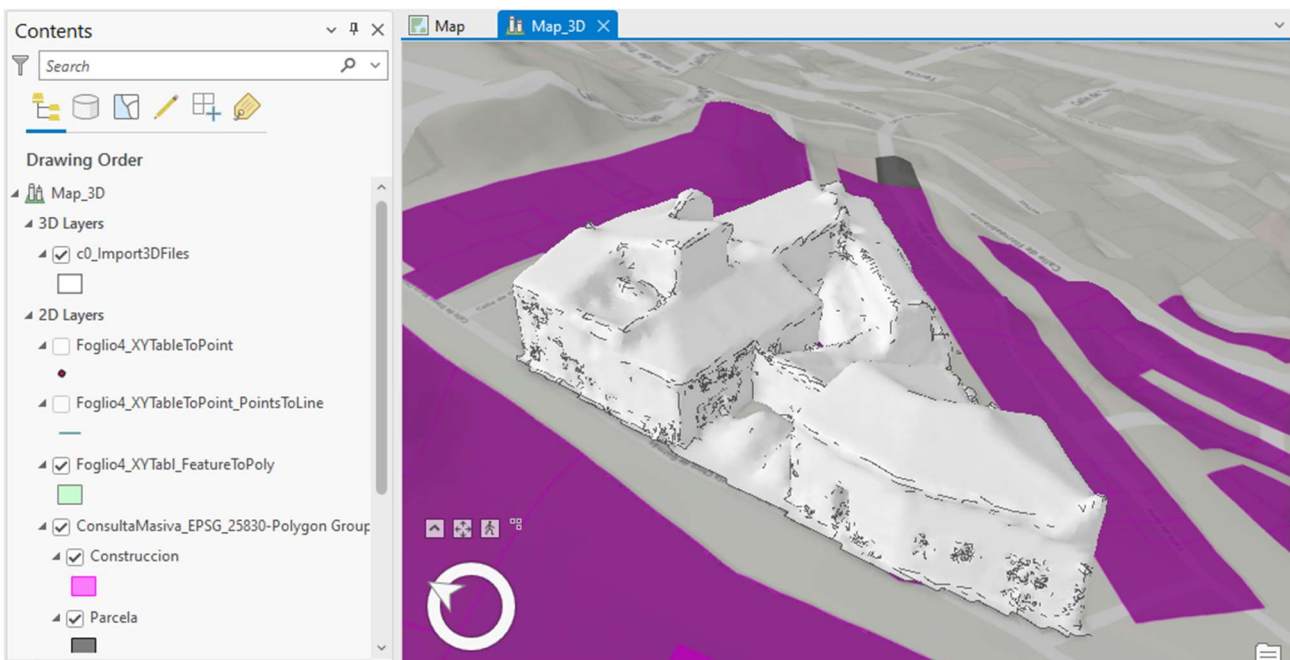


Figure 97 Visualization of the mesh in 3D Map. Source: (ArcGIS Pro)

The extension of the mesh file was changed from .obj to .slpk (scene layer package file) to convert it into a multipatch. From a theoretical perspective, the mesh is a surface that describes the building, while the multipatch is a 3D geometry used in GIS software to represent surfaces and volumes closed in a tridimensionality way (Esri, n.d.).

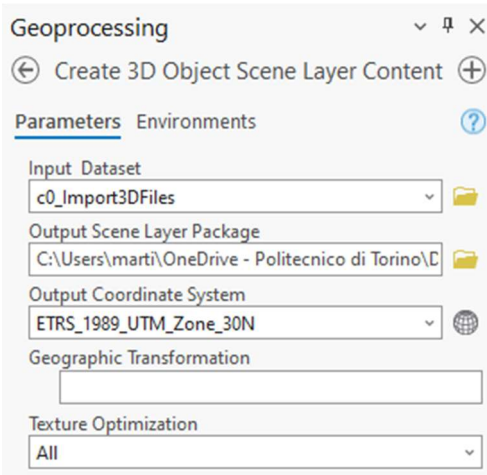


Figure 98 Create 3D object scene layer content. Source: (ArcGIS Pro)

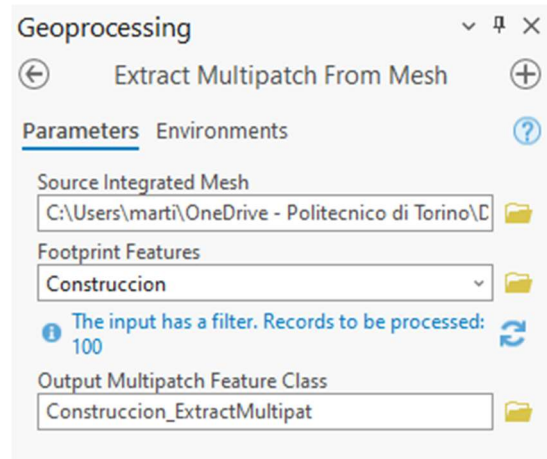


Figure 99 Extract multipatch from mesh. Source: (ArcGIS Pro)

As shown in the picture 100, the construction polygon was employed as the "footprint feature" in the extraction method from the mesh to the multipatch. Consequently, many sections of a multipatch feature are obtained. Each section is linked to every building in the construction layer.



Figure 100 Visualization of the multipatch. Source: (ArcGIS Pro)



A last 'add join' between the multipatch and the construction polygon was performed. It consistently referenced the building of our interest, in order to connect the cadastral data to the multipatch feature. The pictures below show the results in 2D and 3D.

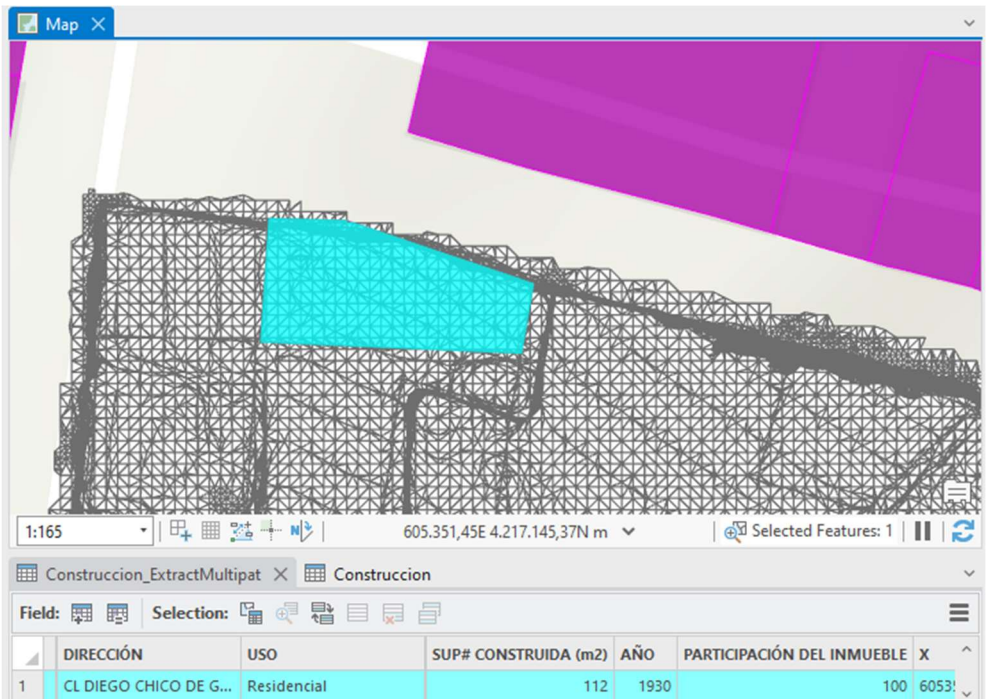


Figure 101 Result of the join in 2D. Source: (ArcGIS Pro)

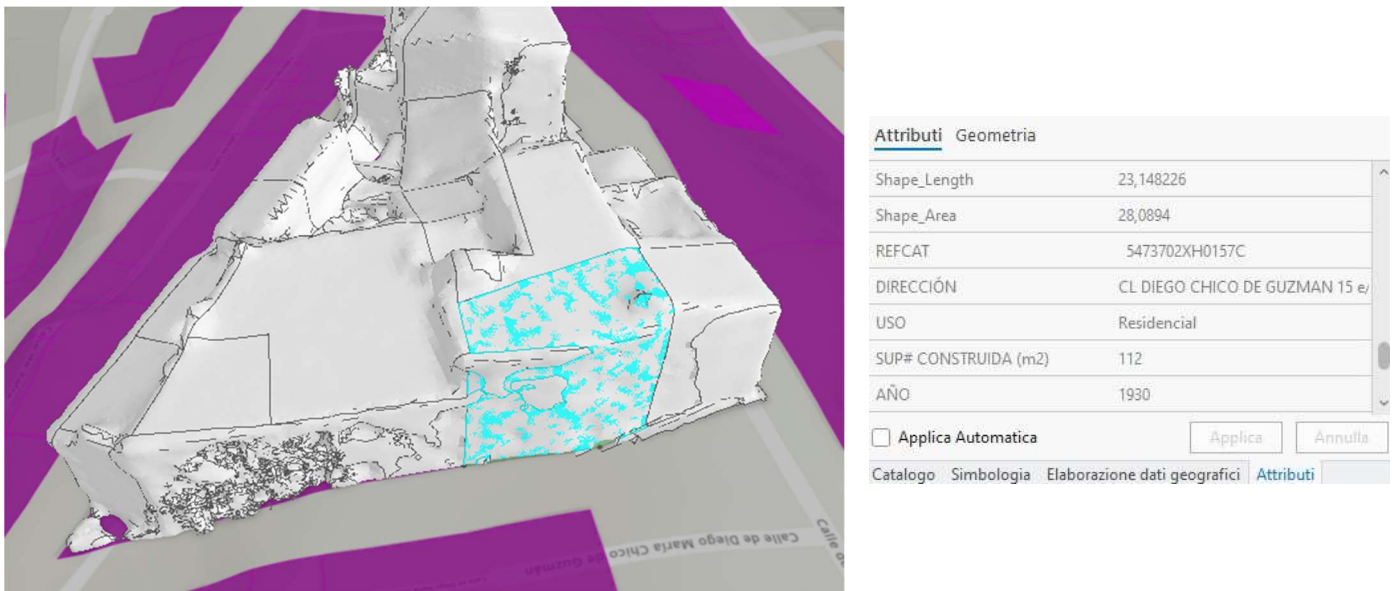


Figure 102 Result of the join in 3D. Source: (ArcGIS Pro)

A three-dimensional solution to the 3D cadastre is demonstrated by the observed level of detail 2, which is an improvement above the previous section since it is generated from the mesh representing the correct altitudes and coverings of the buildings. However, despite these improvements, the representation is not optimal. The reason can be searched in the limited number of points utilized, which was a necessary compromise for procedural efficiency, but also can be find in the process of conversion of a mesh file into a multipatch format that may

have further affected the quality of the initial point cloud. Efforts will be made to further enhance the level of detail in the following section.

### 3.4.4. From the scan to BIM to LOD3

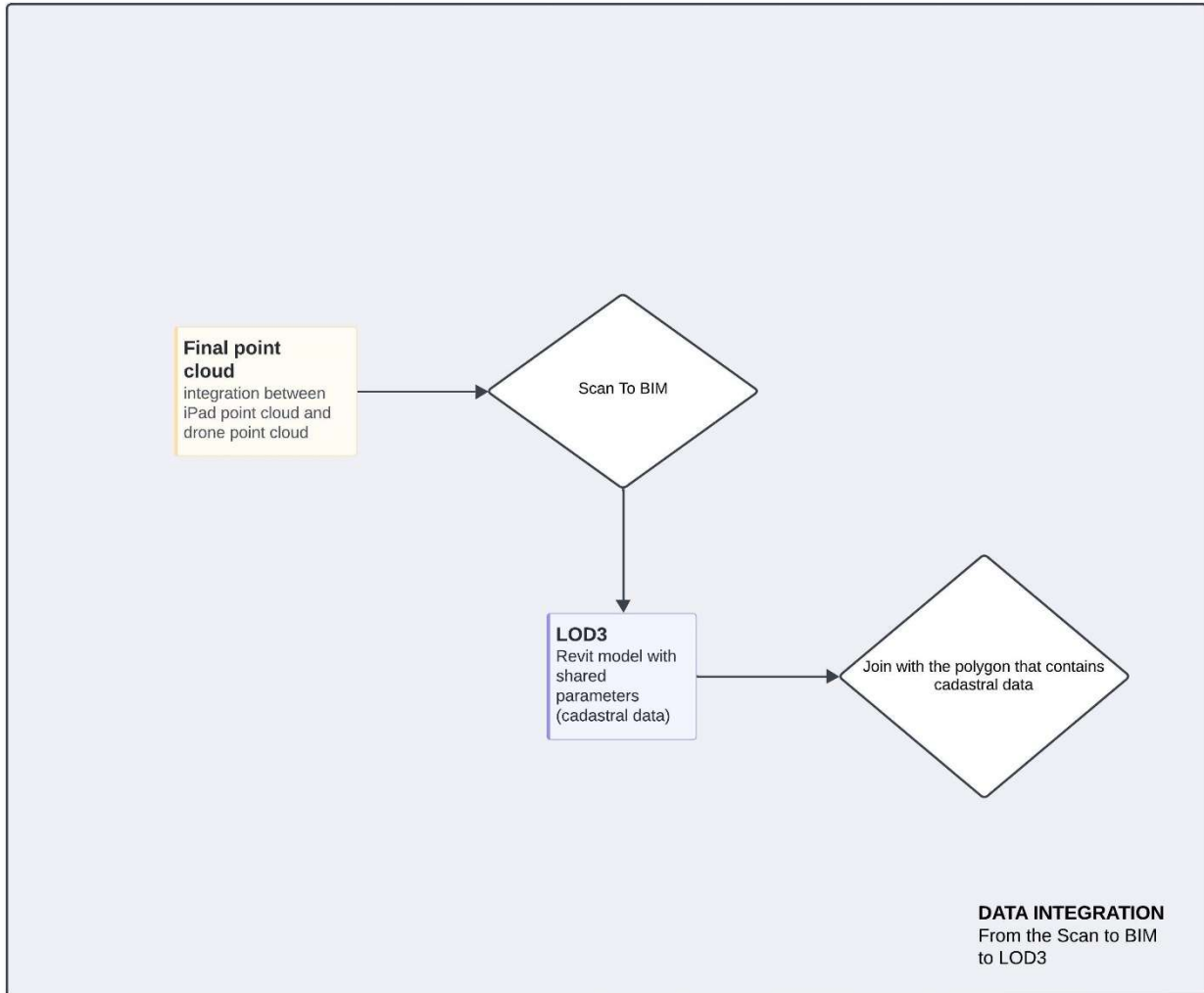


Figure 103 From the Scan to BIM to LOD3. Source: (Author,2024)



This section of the thesis includes an additional integration aimed at enhancing the level of detail. In this context, Revit software is utilized to create a 3D model, with the goal of improving the detail achieved through the previously discussed method. Specifically, the point cloud is imported and accurately geolocated using the project north and shared coordinates, as shown in the pictures below.

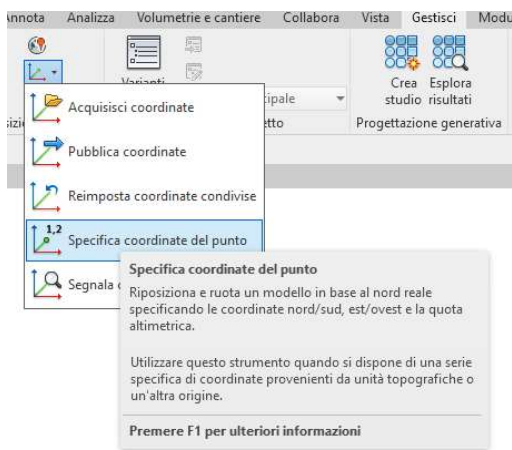


Figure 104 Point coordinates settings. Source: (Revit Autodesk)

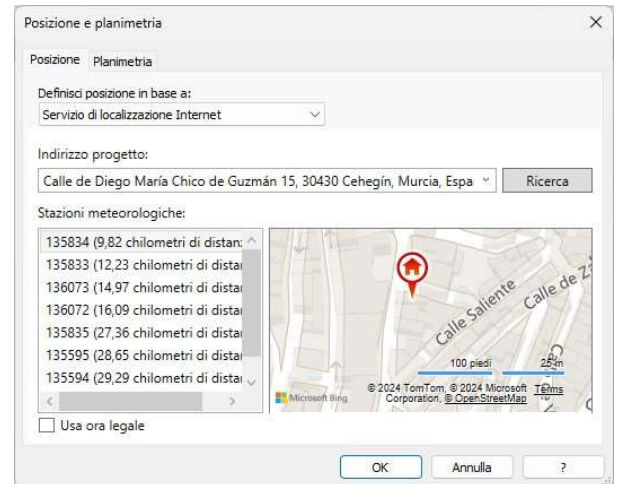


Figure 105 Model address. Source: (Revit Autodesk)

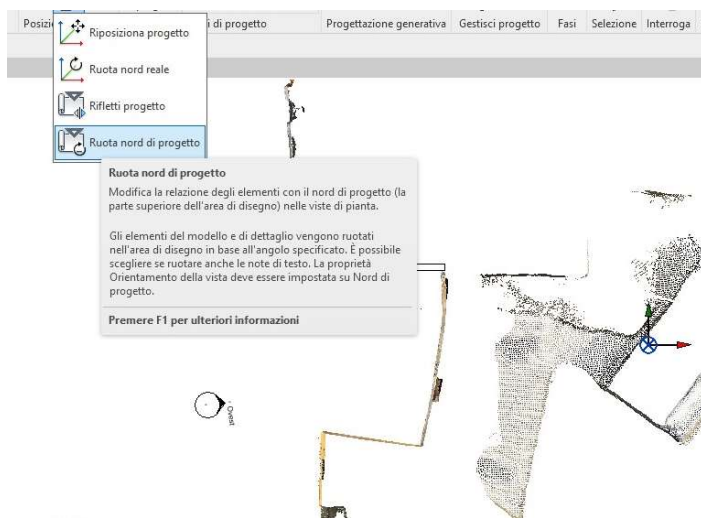


Figure 106 North of the project. Source: (Revit Autodesk)

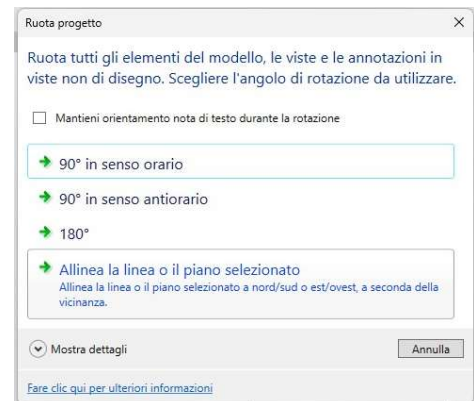


Figure 107 Rotation of the north. Source: (Revit Autodesk)

Shared parameters were incorporated into the entrance wall element of the 3D model to include qualitative and quantitative additional information analysed from the site survey, beyond what is directly sourced from the digital cadastre.

The shared parameters incorporated into the model are:

- Colour façade: it is the colour of the façade recorded during the site survey in April 2024. It is a qualitative attribute given to the wall. This information is useful for an accurate visual representation of the building, that represents a connection between the 3D model and the reality.
- Conservation status: It derives from a visual analysis made during the site survey in April 2024. It is a qualitative description based on three values: low, medium, high. Where the highest level, “high” identifies a perfect state of the conservation of the property, whereas the lowest level “low” indicates the need for urgent maintenance. This information could be used for the sale of real estate value.
- Floors code: it is a codification of the building floors, derived from the digital cadastre, analysed in the data collection section. It represents the number of floors that are above and below the ground level.
- Medium price: As stated in the data collection section, it is an economic assessment of the area where the building is placed and is taken from the digital cadastre. This information could be useful for the economic evaluation of the building.
- Orientation: It is the orientation of the main façade of the building respect to the cardinal points, useful information in terms of building identification and building energy performance, and it was determined through the analysis based on google earth website.
- Construction material: This parameter identifies the building construction elements of the building. In particular, due to lack of information, it was identified based on a visual study and estimates related to the historical period of construction.
- Terrace: The presence or absence of terraces was recorded, based on a visual analysis and on the consultation of cadastral data.
- Municipality\_code: it is a codification of the municipality of Cehegín, derived from the digital cadastre.
- Balcony: The presence or absence of balconies was recorded, based on a visual analysis and on the consultation of cadastral data.

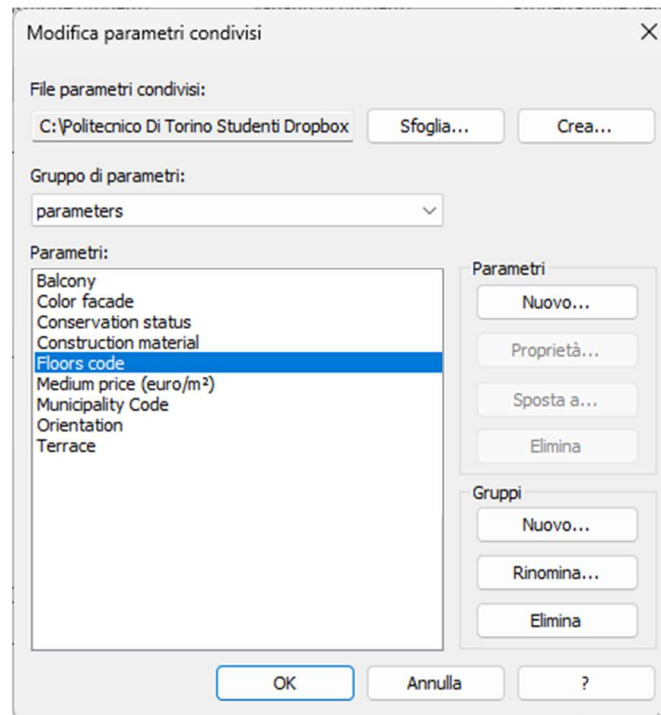


Figure 108 Shared parameters selected for the 3D model. Source: (Revit Autodesk)

The decision to utilise "shared parameters per instance" was taken due to their increased accuracy and flexibility. This kind of parameter is adaptable to different families or projects, enabling the assignment of distinct values to separate element instances. This feature improves the specificity and detail of the model, offering a more customised method of information management within the 3D model.

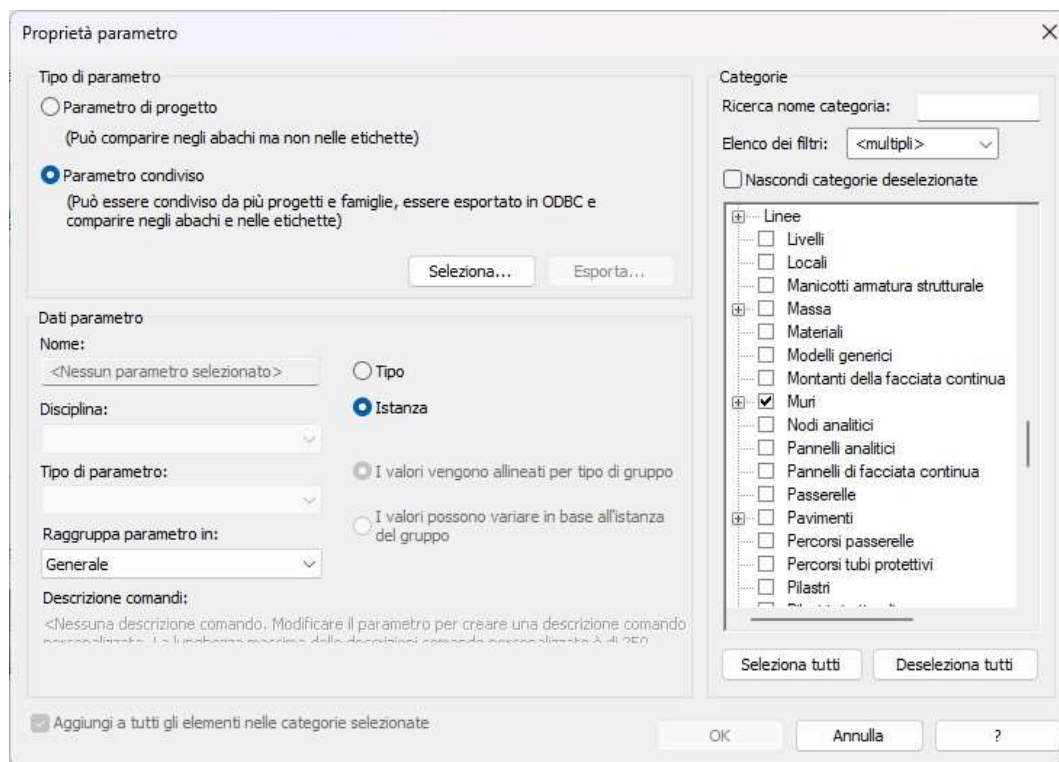


Figure 109 Shared parameters. Source: (Revit Autodesk)

The integration of the shared parameters to the model and the scan to BIM procedure, permit to the model to achieve a Level of Detail (LOD) 3. The model with an extraction of the properties table is presented below.

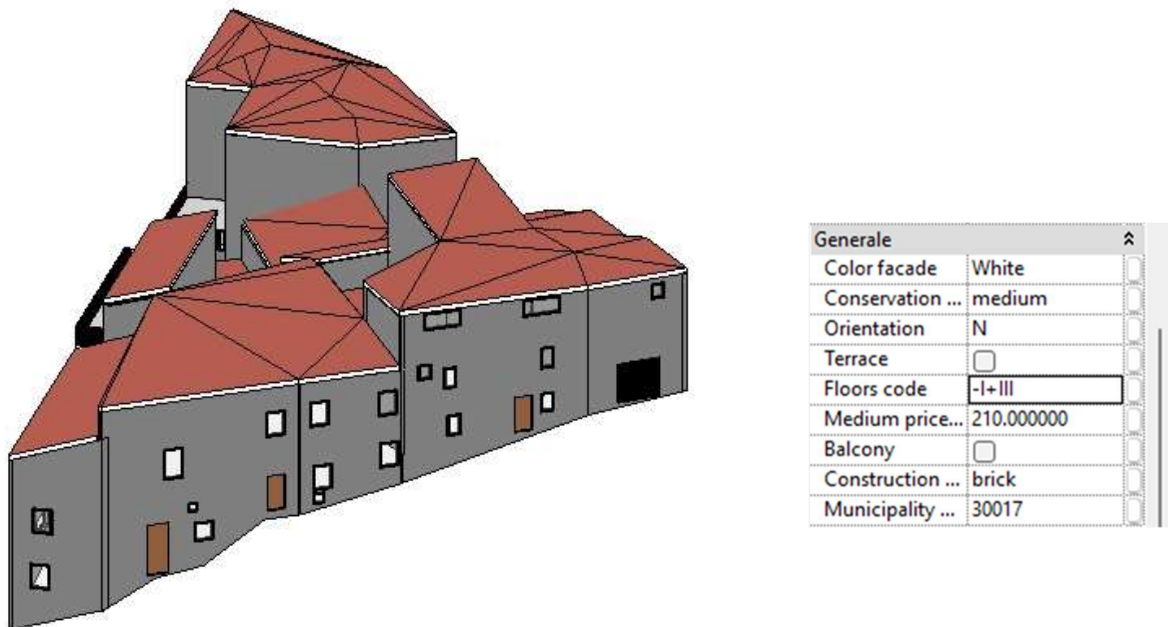


Figure 110 Shared parameters and 3D model. Source: (Revit Autodesk)

### 3.4.5. Integration analysis

After the Revit model was completed, it was imported into the GIS program. This has led to numerous considerations in the field of integration between BIM and GIS fields. As shown in the (fig.111) the first consideration that can be made is that the elements of the imported BIM model are read according to the categorization present within the IFC standard and according to the subdivision present within the BIM software. These factors have been an obstacle in the transfer of cadastral data from the polygon into the BIM model, recognized as multipatch.

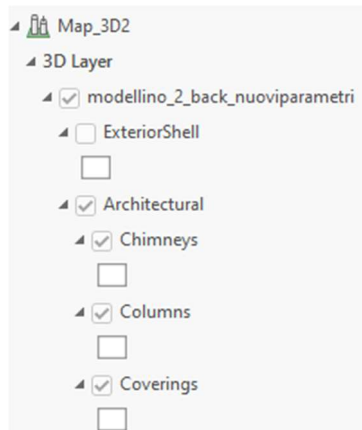


Figure 111 Revit's layers imported in the GIS software. Source: (ArcGIS Pro)

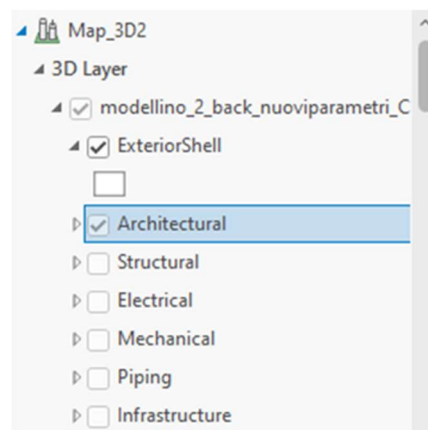


Figure 112 Subdivision of the Revit model. Source: (ArcGIS Pro)

Furthermore, the multipatch file has also led to some difficulties during the process, given its complex geometry and the impossibility of using commands like "Spatial join", "join" and "join features" in GIS software. The impossibility of using these commands is probably because the GIS software works mainly on shapefile of points, lines and polygons. The integration between BIM and GIS was conducted between the BIM model and the polygon generated with all the cadastral information derived from the official site of the land registry. During the procedure, it was chosen to work with the "Walls" layer of the Revit model, which refers to the walls of the building. The explanation for the use of "Walls" layers is based on the decision to establish a correspondence between the building and the wall housing the main door. The "Walls" layer was exported in a new shapefile and in a new geodatabase, because it was observed that this layer could not be modified. As consequence, it was impossible to insert the cadastral data in it. At this point, a join has been made between the new layer extracted and the polygon containing all the cadastral information, based on the municipality code.

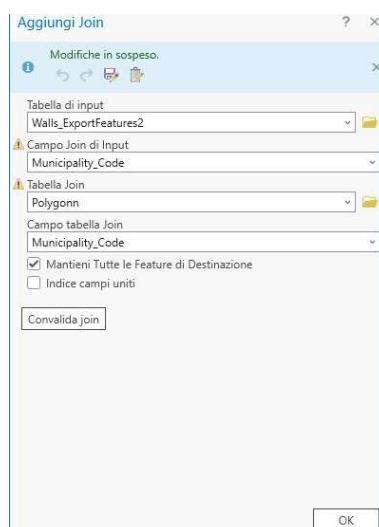


Figure 113 Join command between the walls of the Revit model and the polygon with the cadastral data embedded in it. Source: (ArcGIS Pro)

Since the municipality code was not included in the original cadastre data that was downloaded as an Excel file, it was manually added to the polygon shapefile to enable the join function between the polygon and the new shapefile. This join has led to the following results. Although the union between the two layers was made, the values were not reported. This can be attributed to the difficult interoperability between BIM and GIS, as the imported Revit model in ArcGIS was not editable and the resulting difficulty of interoperability between the two standard formats. Also, it should be considered that the shapefile was still considered as a multipatch and therefore this may have led to difficulties in the union of the Revit model, displayed in multipatch, and the polygon.

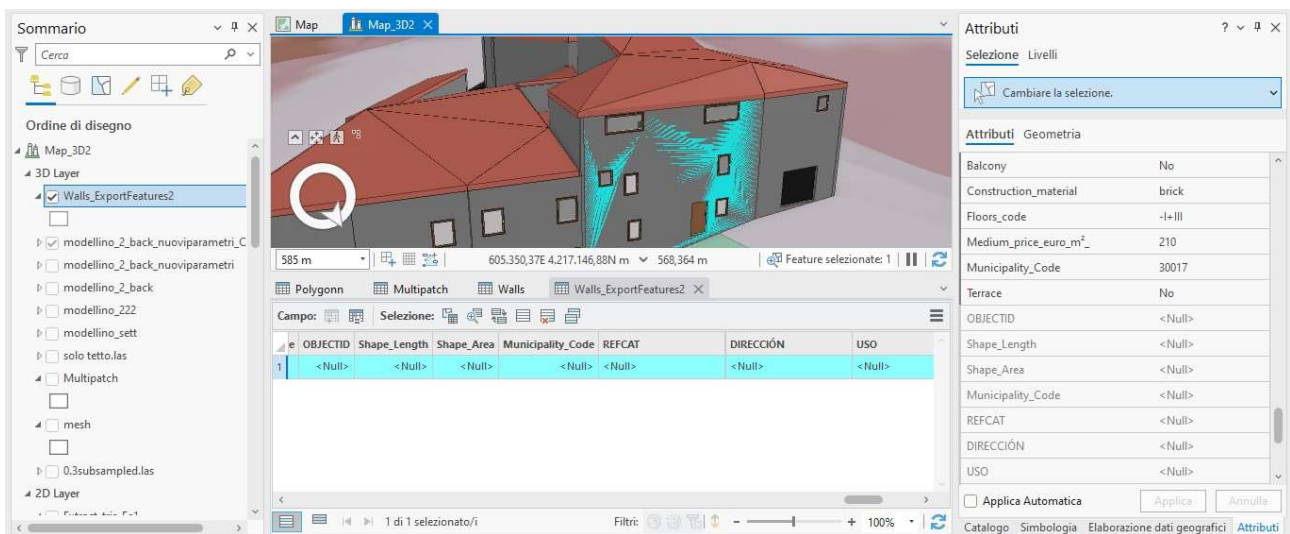


Figure 114 Results of the join between Revit walls and the polygon. Source: (ArcGIS Pro)

To show the integration between different sources, the point cloud with a subsample size of 0.3 meters, the DTM, and the Revit model exported via IFC were imported into ArcGIS software. Specifically, the colourful points depict the point cloud with a 0.3-meter subsample size.



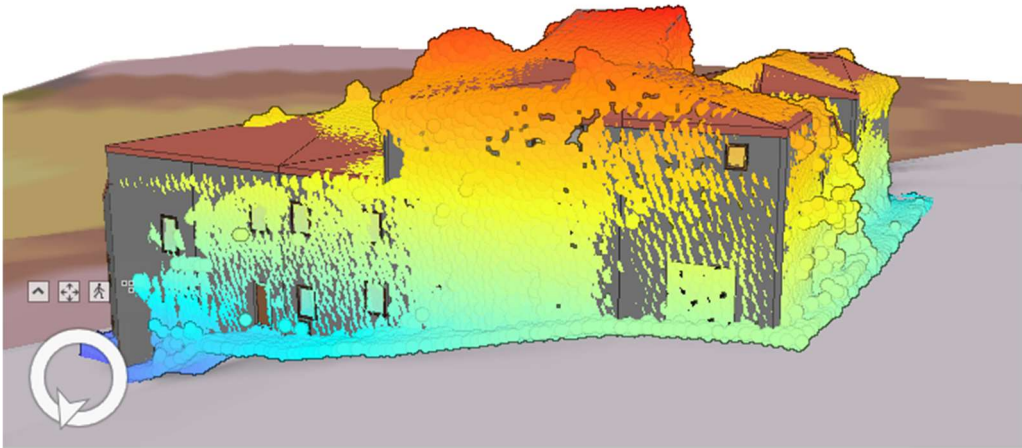


Figure 115 Integration between different sources. Source: (ArcGIS Pro)

An explanatory graph was created to illustrate the progression of the data integration section of this thesis, with the main work carried out using ArcGIS software. Starting from a Level of Detail (LOD) 0, which only included the building footprints in the DXF file and cadastral information in Excel format, it was possible to advance to LOD1 using a point cloud, that defines the roof of the buildings, and a digital terrain model. Additionally, the procedure for obtaining the LOD2 and LOD3 was distinct, even though the initial data information was identical. In essence, LOD2 was produced utilising the mesh generated by the union between the LIDAR point cloud and the drone point cloud, whereas LOD3 was created through scan to BIM process in Revit software. Furthermore, the main difference between these levels of detail can be seen in the informative data. In fact, LOD3 contains additional information like the number of floors, orientation, and other features that have made it possible to improve the 3D model's level of detail in comparison to LOD2.

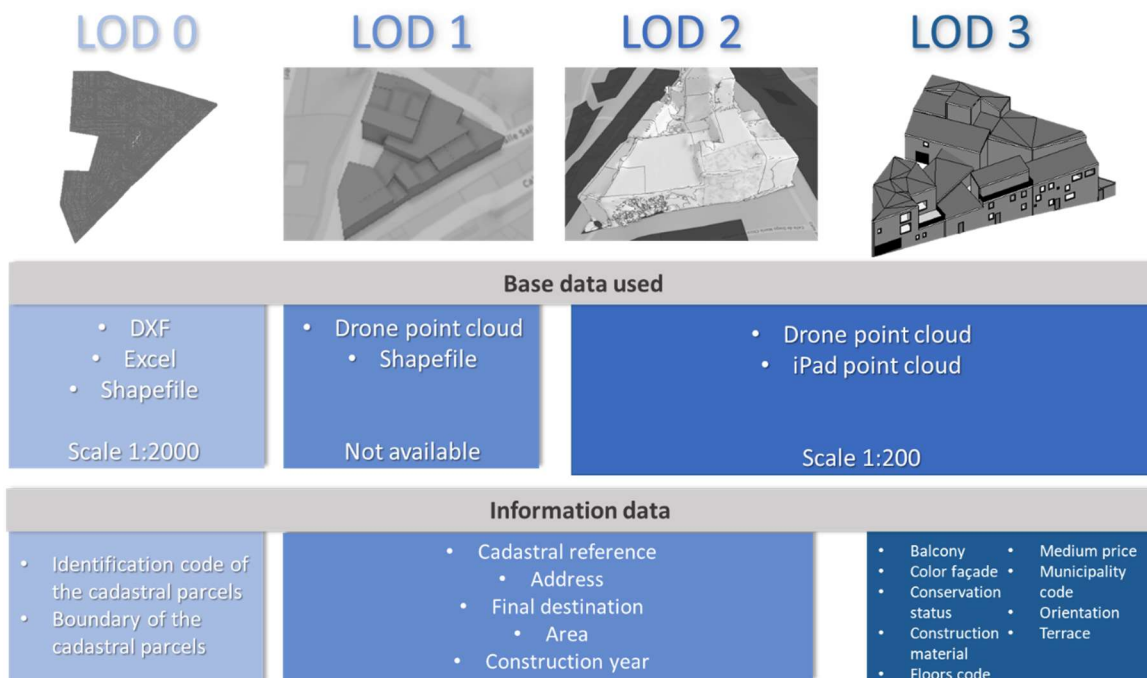


Figure 116 Workflow and LODs. Source: (Author, 2024)

## 4. Analysis and discussion of the results

The purpose of this research was to develop a methodology integrating BIM and GIS to provide a suitable three-dimensional representation of a building in the historic district of Cehegín. Additionally, this thesis involved the use of an iPad Pro to facilitate scans and accelerate the 3D cadastral transformation process. Below is a brief summary of the results obtained during each phase of the methodology. During the data collection phase, the proposed process enabled us to gather information that should be inserted in the building under investigation, downloaded from the Spanish cadastre as Excel and DXF files. An improvement suggested for this phase is to use shapefiles, which are already georeferenced and do not require additional integration, unlike the procedure used. It should be noted that the decision not to use shapefiles was made because they are not freely available to the public. This led to the need to establish a methodology based on accessible data, to ensure transparency and repeatability for other users. For data acquisition, all point clouds obtained during the scans were listed, and the scanning procedure for the point cloud obtained with the iPad Pro was analysed. A general scan of the neighbour and smaller scans represented parts of the neighbour were conducted to form the overall point cloud. During scanning, some errors were detected, probably due to a shift in the instrument's alignment. Moreover, from the point cloud texturing process, it was observed that one cloud was too large, likely due to the high density of points, and we had to exclude it due to application crashes. For data processing, two different processes were followed, starting from the cadastral data and the point clouds. The first process, related to cadastral data, involved georeferencing the data and generating a polygon that contains the cadastral data. The second process entailed creating the iPad's point cloud by aligning it in Cloud Compare and analysing the density of all available point clouds. This analysis led to selecting the iPad's point cloud to represent the lower part of the building, while the drone's point cloud represented the building's roof. An important decision was to reduce the number of points when merging the drone and iPad Pro clouds, as the high point density made it incompatible with the GIS software due to hardware limitations. In this section, we also assessed the potential of the iPad Pro and the limitations of traditional tools, mostly visible from the density analysis. During data integration, cadastral data and point clouds were integrated to create a three-dimensional model. Based on this integration, the levels of detail were progressively improved until achieving a three-dimensional model at LOD3 through BIM software. In this case, it should be noted that a preliminary study was conducted to enable the reuse of a 3D model generated on Rhinoceros by (Ródenas-López, M. A, 2023) as part of their research. This reuse was based on the "Rhino for Revit" plugin, which allowed the Rhinoceros model to be used on the Revit platform, with potential modifications. However, this procedure was considered ineffective for cadastral purposes, as the entire district was treated as a single model, which made it impossible to select an individual building. A final section was related to the interoperability between BIM and GIS standards and multipatch feature that didn't allow a correct integration of cadastral data in LOD3.

| Opportunities   | Threats   |
|---|---|
| <ul style="list-style-type: none"> <li>• Use of cadastral data accessible</li> <li>• Transparency and repeatability of the process</li> <li>• Implementation and integration of cadastral data with point clouds</li> <li>• Progressive BIM-GIS Integration into a 3D Model of LOD3</li> <li>• Faster and economic scanning procedure</li> <li>• Highly detailed point cloud obtained from 3D rapid scanning</li> </ul> | <ul style="list-style-type: none"> <li>• Limitations in cadastral data format available</li> <li>• Issues during scanning survey with iPad Pro</li> <li>• High density points of the final point cloud</li> <li>• Limitations of "Rhino for Revit" plugin</li> <li>• Interoperability issues between BIM and GIS</li> <li>• Necessity to merge and to georeference the iPad point cloud with drone point cloud</li> </ul> |

Figure 117 Table of the opportunities and of the threats of the thesis. Source: (Author, 2024)

## Conclusions

In a context of profound change and transformation of the land register, the integration between BIM and GIS assumes a central role. These two systems, although representing different realities - one on an architectural scale and the other on a territorial scale - allow a more effective and precise representation of the cadastral reality. This research examined the current state of cadastre in Europe, mainly in Italy and in Spain, and looked at the integration of BIM and GIS, closely linked to scanning techniques such as photogrammetry and LiDAR, which are key tools for moving from 2D to 3D cadastres. To meet the need to facilitate this transition, it was chosen an iPad Pro for scanning the case study. This solution allowed the building facades to be quickly acquired, bringing numerous advantages despite the height limit of the instrument. These include the speed of capture and completeness of scanning thanks to LiDAR, the low cost compared to other relevant instruments, and the ease of use, which makes the device accessible to users without specific training. These features are important for the 3D cadastre, since they facilitate a capillary collection of point clouds in a fast time, allowing municipalities to equip themselves with an economical and accessible tool. Furthermore, the iPad Pro could be considered an ideal tool for scanning building interiors, providing a more detailed representation of cadastral features. By capturing the internal subdivision, it enables a more precise analysis of interior spaces, leading to improved economic appraisals and a clearer subdivision of cadastral rights within the property. However, some difficulties have emerged, such as scanning the coverings and georeferencing the point clouds, for which a drone has been used. The combined use of drone and iPad Pro has helped overcome these limitations, suggesting an integrated solution that can facilitate widespread adoption of 3D survey technologies. Using iPad scanning, a method was developed for the 3D reconstruction of a building in the historic centre of Cehegín, creating an accurate model through the integration of BIM and GIS, with a progressive increase in detail. Although there have been problems of interoperability between BIM and GIS, linked to the different data structure, it is hoped that future studies can progress in this direction, providing an increasingly optimal solution for the definition of a 3D cadastre.

## Bibliography

Abbas, S.F., & Abed, F.M. (2024). Evaluating the Accuracy of iPhone Lidar Sensor for Building Façades Conservation. In: Bezzeghoud, M., et al. Recent Research on Geotechnical Engineering, Remote Sensing, Geophysics and Earthquake Seismology. MedGU 2022. Advances in Science, Technology & Innovation. Springer, Cham. [https://doi.org/10.1007/978-3-031-48715-6\\_31](https://doi.org/10.1007/978-3-031-48715-6_31)

Amirebrahimi, S., Rajabifard, A., Mendis, P., & Ngo, T. (2016). A BIM-GIS integration method in support of the assessment and 3D visualisation of flood damage to a building. *Journal of Spatial Science*, 61, 1-34. <https://doi.org/10.1080/14498596.2016.1189365>

Bahram Saeidian, Abbas Rajabifard, Behnam Atazadeh, Mohsen Kalantari (2023) A semantic 3D city model for underground land administration: Development and implementation of an ADE for CityGML 3.0, <https://doi.org/10.1016/j.tust.2023.105267>

Borrmann, A., Beetz, J., Koch, C., Liebich, T., & Muhic, S. (2018). Industry Foundation Classes: A Standardized Data Model for the Vendor-Neutral Exchange of Digital Building Models. In: Borrmann, A., König, M., Koch, C., & Beetz, J. (Eds.), *Building Information Modeling*. Springer, Cham.

Borrmann, A., Kolbe, T.H., Donaubaue, A., Steuer, H., Jubierre, J.R., & Flurl, M. (2014). Multi-Scale Geometric-Semantic Modeling of Shield Tunnels for GIS and BIM Applications. *Computer-Aided Civil and Infrastructure Engineering*, 30. <https://doi.org/10.1111/mice.12090>

Cannarozzo, A., Cucchiarini, S., & Meschieri, M. (2012). *Principi e strumenti di fotogrammetria*. Bologna, Italia: Zanichelli Editore. Estensione online del corso *Misure, rilievo, progetto*.

Carnevali, L.; Lanfranchi, F.; Russo, M. (2019) Built Information Modeling for the 3D Reconstruction of Modern Railway Stations. *Heritage*, 2, 2298-2310. <https://doi.org/10.3390/heritage2030141>

Döllner, J., Baumann, K., & Buchholz, H. (2006). Virtual 3D city models as foundation of complex urban information spaces. In *Proceedings of CORP 2006 & Geomultimedia06*. Vienna, Austria.



Eastman, C.M., Eastman, C., Teicholz, P., Sacks, R., & Liston, K. (2011). BIM Handbook: A Guide to Building Information Modeling for Owners, Managers, Designers, Engineers and Contractors. John Wiley & Sons: Hoboken, NJ, USA.

Fabrizi, C. (2024). Il Sistema Catastale dati al 31 dicembre 2023. Divisione Servizi Direzione Centrale - Servizi Catastali, Cartografici e di Pubblicità Immobiliare, Agenzia delle entrate.

Fronza, A., Dalla Torre, S., & Agugiario, G. (2013). Docfa 4, rappresentazione grafica vettoriale e integrazione 3D. In Atti della 17a Conferenza Nazionale ASITA, 5–7 novembre 2013, Riva del Garda, Italia.

Gruppo di Lavoro 2 “DB Geotopografici” dell'Agenzia per l'Italia Digitale coordinato dal CISIS con il supporto della struttura tecnica del Comitato Permanente per i Sistemi Geografici (2015). CATALOGO DEI DATI TERRITORIALI Specifiche di contenuto per i DataBase Geotopografici versione 2.0. [https://geodati.gov.it/geoportale/images/Specifica\\_GdL2\\_09-05-2016.pdf](https://geodati.gov.it/geoportale/images/Specifica_GdL2_09-05-2016.pdf)

Hajji, R., Yaagoubi, R., Meliana, I., Laafou, I., & Gholabzouri, A.E. (2021). Development of an Integrated BIM-3D GIS Approach for 3D Cadastre in Morocco. ISPRS International Journal of Geo-Information, 10, 351. <https://doi.org/10.3390/ijgi10050351>

Harshit, Pallavi Chaurasia, Sisi Zlatanova, and Kamal Jain (2024) Low-Cost Data, High-Quality Models: A Semi-Automated Approach to LOD3 Creation, ISPRS International Journal of Geo-Information 13, no. 4: 119. <https://doi.org/10.3390/ijgi13040119>

Henssen, J. (1995). Basic Principles of the Main Cadastral Systems in the World. Paper presented at the Seminar Modern Cadastres and Cadastral Innovations. In Proceedings of the One Day Seminar held during the Annual Meeting of Commission 7, Cadastre and Rural Land Management, of the International Federation of Surveyors (FIG), May 16, Delft, The Netherlands. Working Group “Cadastre 2014”

International Federation of Surveyors. (1995). FIG publication no. 11: The FIG statement on the cadastre – FIG policy statement. The International Federation of Surveyors (FIG).

Konde, A., Tauscher, H., Biljecki, F., Crawford, J., (2018): Floor plans in CityGML. In: Proceedings of the 13th 3D GeoInfo Conference 2018, ISPRS Annals of the Photogrammetry, Remote Sensing and Spatial Information Sciences, Vol. IV-4/W6, 25–32, ISPRS. <https://doi.org/10.5194/isprs-annals-IV-4-W6-25-2018>

Kutzner, T.; Kolbe, T.H. CityGML 3.0: Sneak Preview. In Proceedings of the PFGK18—Photogrammetrie Fernerkundung Geoinformatik Kartographie, 37. Jahrestagung in München, München, Germany, 23 February 2018.

Lemmen C., van Oosterom P.J. M., Bennett R.M. (2015). “The land administration domain model”. Land use policy, 49, 535-545. <https://doi.org/10.1016/j.landusepol.2015.01.014>

Murtiyoso, A., Grussenmeyer, P., Landes, T., & Macher, H. (2021). First assessments into the use of commercial-grade solid-state LiDAR for low-cost heritage documentation. International Archives of Photogrammetry, Remote Sensing and Spatial Information Sciences, XLIII-B2-2021, 599–604. <https://doi.org/10.5194/isprs-archives-XLIII-B2-2021-599-2021>

Nagel, C., & Kolbe, T.H. (2007). *Conversion of IFC to CityGML*. Department of Geoinformation Science, Institute for Geodesy and Geoinformation Science, Technische Universität Berlin. Presented at OGC 3DIM WG, Paris, July 10, 2007.

Olivares García, J.M., Virgós Soriano, L.I., & Velasco Martín-Varés, A. (2011). 3D Modeling and Representation of the Spanish Cadastral Cartography. In Proceedings of the 2nd International Workshop on 3D Cadastres, 16-18 November 2011, Delft, the Netherlands.

Ródenas-López, M.A., García-León, J., Jiménez-Vicario, P.M., & El Ghomari-Bakhat, S. (2023). Three-dimensional urban models in complex rural environments: Proposal for automation in the historical centre of Cehegín. DISEGNARECON, 30. <https://doi.org/10.20365/disegnarecon.30.2023.14>

Spreafico, A., Chiabrando, F., Teppati Losè, L., & Tonolo, F.G. (2021). The iPad Pro built-in LiDAR sensor: 3D rapid mapping tests and quality assessment. International Archives of Photogrammetry, Remote Sensing and Spatial Information Sciences, XLIII-B1-2021, 63–69. <https://doi.org/10.5194/isprs-archives-XLIII-B1-2021-63-2021>

Stoter, J., Ploeger, H., Roes, R., van der Riet, E., Biljecki, F., & Ledoux, H. (2016). First 3D cadastral registration of multi-level ownership rights in the Netherlands. In Proceedings of the 5th International FIG 3D Cadastre Workshop, 18-20 October 2016, Athens, Greece.

Sun J., Mi, S., Olsson, P.-O., Paulsson, J., & Harrie, L. (2019). Utilizing BIM and GIS for Representation and Visualization of 3D Cadastre. *ISPRS International Journal of Geo-Information*, 8, 503. <https://doi.org/10.3390/ijgi8110503>

Sun J., Paulsson J., Harrie L., Eriksson K., Paasch J., Tarandi V. (2022) BIM-based 3D Cadastral Management, report is a delivery from the Smart Built Environment project “BIM-based 3D Cadastral Management” (SWE: BIM-baserad hantering av 3Dfastighetsinformation). Department of Real Estate and Construction Management KTH (Sweden), Department of Physical Geography and Ecosystem Science Lund University (Sweden), University of Gävle (Sweden), Lantmäteriet (Sweden), V Tarandi AB (Sweden).

Tontini, Alessandro, Leonardo Gasparini, and Matteo Perenzoni (2020) "Numerical Model of SPAD-Based Direct Time-of-Flight Flash LIDAR CMOS Image Sensors" *Sensors* 20, no. 18: 5203. <https://doi.org/10.3390/s20185203>

United Nations Department of Economic and Social Affairs/Population Division. (2011). *World Urbanization Prospects: The 2011 Revision*. New York.

van Oosterom, P. (Ed.). (2018). *Best Practices 3D Cadastres - Extended version*. (FIG Publication Series). International Federation of Surveyors (FIG). [http://www.gdmc.nl/publications/2018/FIG\\_3DCad.pdf](http://www.gdmc.nl/publications/2018/FIG_3DCad.pdf)

## Sitography

AgID (n.d.). RNDT - Dati Territoriali. [online] Available at: <https://www.agid.gov.it/it/dati/dati-territoriali> [Accessed 29 October 2024].

Ayuntamiento de Cehegín (n.d.). Plan de ordenación Urbana 2021. [online] Available at: <https://cehegin.es/plan-de-ordenacion-urbana-2021/#10iGuckZmFdUkvFli4EMdDVmdJ-CKL5Uh> [Accessed 10 March 2024].

Esri (n.d.). Multipatches - ArcGIS 3D Analyst. [online] Available at: <https://desktop.arcgis.com/en/arcmap/latest/extensions/3d-analyst/multipatches.htm> [Accessed 29 October 2024].

Esri (n.d.). What is LiDAR? - ArcGIS Pro. [online] Available at: <https://pro.arcgis.com/en/pro-app/latest/help/data/las-dataset/what-is-lidar-.htm> [Accessed 29 October 2024].

Google Earth (n.d.). [online] Available at: <https://www.google.it/earth/> [Accessed 19 April 2024].

Instituto Geográfico Nacional (IGN) (n.d.). Portal IGN. [online] Available at: <https://www.ign.es/web/ign/portal> [Accessed 29 October 2024].

Ingeoexpert (n.d.). Conocimiento previo del área a cartografiar. [online] Available at: <https://ingeoexpert.com/articulo/conocimiento-previo-del-area-a-cartografiar/> [Accessed 23 March 2024].

Italian Cartography Geoportal (n.d.). Geoportale Cartografico Italiano. [online] Available at: <https://geoportale.cartografia.agenziaentrate.gov.it/age-inspire/srv/ita/catalog.search#/home?pg=> [Accessed 10 October 2024].

Open Geospatial Consortium (OGC) (n.d.). GML Standard. [online] Available at: <https://www.ogc.org/publications/standard/gml/> [Accessed 3 October 2024].

Open Geospatial Consortium (OGC) (n.d.). WMS Standard. [online] Available at: <https://www.ogc.org/publications/standard/wms/> [Accessed 3 October 2024].

PNOA (n.d.). Presentación PNOA LiDAR. [online] Available at: <https://pnoa.ign.es/web/portal/pnoa-lidar/presentacion> [Accessed 15 September 2024].

Spanish Cadastre (n.d.). Ayuda Bi Cartografia. [online] Available at: [https://www.catastro.hacienda.gob.es/ayuda/ayuda\\_bi.htm#cartografia](https://www.catastro.hacienda.gob.es/ayuda/ayuda_bi.htm#cartografia) [Accessed 29 October 2024].

Spanish Cadastre (n.d.). Cartografia Spagnola. [online] Available at: <https://www1.sedecatastro.gob.es/Cartografia/mapa.aspx?buscar=S> [Accessed 29 October 2024].

Spanish Cadastre (n.d.). Guia de servicios SEC para ciudadanos. [online] Available at: [https://www.catastro.hacienda.gob.es/ayuda/Guia\\_de\\_servicios\\_SEC\\_ciudadanos.pdf](https://www.catastro.hacienda.gob.es/ayuda/Guia_de_servicios_SEC_ciudadanos.pdf) [Accessed 29 October 2024].

Spanish Cadastre (n.d.). Manual de descargas de Shapefile. [online] Available at: [https://www.catastro.hacienda.gob.es/ayuda/manual\\_descargas\\_shapefile.pdf](https://www.catastro.hacienda.gob.es/ayuda/manual_descargas_shapefile.pdf) [Accessed 29 October 2024].

Spanish Cadastre (n.d.). Manual descriptivo de Shapefile. [online] Available at: [https://www.catastro.hacienda.gob.es/ayuda/manual\\_descriptivo\\_shapefile.pdf](https://www.catastro.hacienda.gob.es/ayuda/manual_descriptivo_shapefile.pdf) [Accessed 29 October 2024].

UNI (2017). UNI 11337-4:2017. [online] Available at: <https://store.uni.com/uni-11337-4-2017> [Accessed 6 November 2024].

# List of figures

Figure 1 Description of the cadastral system. Source: (Henssen J., 1995)..... 8

Figure 2 Schema of Rete nazionale dati territoriali. Source: (Gruppo di Lavoro 2 “DB Geotopografici” dell’Agenzia per l’Italia Digitale, 2015) ..... 10

Figure 3 Cadastral map. Source: (Italian Cartography Geoportal, n.d.)..... 11

Figure 4 Cadastral information. Source: (Spanish Cadastre, n.d.)..... 12

Figure 5 Orientation system of the building. Source: (Fronza et al., 2013)..... 13

Figure 6 Polygons construction of the real estate unit. Source: (Fronza et al., 2013)..... 14

Figure 7 Markers of the subalterno. Source: (Fronza et al., 2013) ..... 14

Figure 8 Representation of the net and gross areas. Source: (Fronza et al., 2013) ..... 15

Figure 9 Lines and points of modeling. Source: (Fronza et al., 2013) ..... 15

Figure 10 On the left: A three-dimensional representation of the interior of the building derived from Docfa 4 data. On the right: A combined representation of the building’s façade (derived from topographic data) and interior (derived from Docfa data). Source: (Fronza et al., 2013) 16

Figure 11 The two layers and the superposition of digital cadastre. Source: (Olivares García et al., 2011) ..... 17

Figure 12 Superposition of the layers with the orthophoto. Source: (Olivares García et al., 2011)..... 17

Figure 13 3D model based on parcel extrusion. Source : (Olivares García et al., 2011) ..... 18

Figure 14 3D representation of the internal parts of the building. Source: (Olivares García et al., 2011) ..... 18

Figure 15 Representation of the different rights. Source: (Stoter J. et al., 2016) ..... 19

Figure 16 3D model representation based on the different rights. Source: (Stoter J. et al., 2016) ..... 19

Figure 17 The Land Administration Domain Model. Source: (Lemmen, C. et al., 2015) ..... 20

Figure 18 BIM LOD. Source:(Carnevali L. et al., 2019) ..... 23

Figure 19 The IFC hierarchical structure and entities mostly integrated with 3D cadastre. Source: (Borrmann et al., 2018) ..... 23

Figure 20 GIS LODs. Source: (Harshit P.C. et al., 2024)..... 25

Figure 21 CityGML 3.0 space concepts Source: (Bahram S. et al., 2023) ..... 26

Figure 22 CityGML vs IFC. Source: (Nagel, C. et al., 2007) ..... 26

Figure 23 Photogrammetry. Source: (Cannarozzo et al., 2012)..... 27

Figure 24 Spain map. Source: (Google Earth, n.d.)..... 30

Figure 25 Murcia region map. Source: (Google Earth, n.d.) ..... 30

Figure 26 Archaeological map of the study area. Source: (Ayuntamiento de Cehegin, n.d) ... 31

Figure 27 In the middle: Cadastral map of the study area. Source: (Sede Electronica del Catastro, n.d.). On the boundary: Picture of the onsite survey. Source: (Author’s image, 2024) ..... 31

Figure 28 Methodology schema. Source: (Author’s schema, 2024)..... 32

Figure 29 Data collection schema. Source: (Author, 2024) ..... 34



|  |    |
|--|----|
| Figure 30 Spanish cadastre website. Source: (Spanish cadastre, n.d.) .....   | 35 |
| Figure 31 Data download subdivision in the Spanish cadastre. Source: (Spanish cadastre, n.d.).....   | 35 |
| Figure 32 Explanation of the cadastral code in Spain. Source: (Ingeoexpert, n.d.) .....  | 36 |
| Figure 33 Area of the case study. Source: (Spanish cadastre, n.d.).....  | 37 |
| Figure 34 Building under investigation. Source: (Spanish cadastre, n.d.) .....   | 38 |
| Figure 35 Cartographic viewer of the Spanish cadastre. Source: (Spanish cadastre, n.d.).....   | 38 |
| Figure 36 Economic map of the Cehegin municipality. Source: (Spanish cadastre, n.d.).....  | 39 |
| Figure 37 Data acquisition schema. Source: (Author, 2024) .....  | 40 |
| Figure 38 Lidar Point cloud, obtained by public Lidar sensor flights from 2015 onwards, excluded due to the scarcity of density. Source: (Instituto Geografico Nacional, n.d.) ..... | 41 |
| Figure 39 Terrestrial laser scanner acquired using Leica Nova MS50. Source: Cloud Compare .....  | 42 |
| Figure 40 Final drone point cloud. Source: (Cloud Compare) .....   | 42 |
| Figure 41 Final point cloud obtained from iPad. Source: (Cloud Compare) .....  | 44 |
| Figure 42 Data processing schema. Source: (Author, 2024).....  | 45 |
| Figure 43 DXF file extracted from the digital cadastre and inserted in ArcGIS Pro. Source: (Instituto Geografico Nacional, n.d.) .....   | 46 |
| Figure 44 Define projection command. Source: (ArcGIS Pro).....   | 46 |
| Figure 45 Cadastral information in the excel file. Source: (Spanish cadastre, n.d.) .....  | 46 |
| Figure 46 Excel file extracted from digital cadastre and inserted in ArcGIS Pro. Source: (Instituto Geografico Nacional, n.d.) .....   | 46 |
| Figure 47 Display XY command. Source: (ArcGIS Pro).....  | 47 |
| Figure 48 Settings of the Display XY Data. Source: (ArcGIS Pro).....   | 47 |
| Figure 49 Command to generate the line from the points. Source: (ArcGIS Pro) .....   | 48 |
| Figure 50 Command to generate the polygon from the lines. Source: (ArcGIS Pro) .....   | 48 |
| Figure 51 Add join between the construction polygon and the polygon obtained from the excel file. Source: (ArcGIS Pro).....  | 48 |
| Figure 52 Results of the join function. Source: (ArcGIS Pro).....  | 49 |
| Figure 53 Join between the two polygons. Source: (ArcGIS Pro) .....  | 49 |
| Figure 54 Results obtained from the join. Source: (ArcGIS Pro).....  | 49 |
| Figure 55 Georeferencing between "scansione 4_2_hd" e "scansione 5_2_hd". Source: (Cloud Compare) .....  | 50 |
| Figure 56 Georeferencing between "scansione 4_2_hd" e "scansione 6_3_hd". Source: (Cloud Compare) .....  | 50 |
| Figure 57 Georeferencing between "scansione 4_2_hd" e "scansione 7_3_hd". Source: (Cloud Compare) .....  | 51 |
| Figure 58 Georeferencing between "scansione 4_2_hd" e "scansione 8_2_hd". Source: (Cloud Compare) .....  | 51 |
| Figure 59 Georeferencing between "scansione 4_2_hd" e "scansione 9_2_hd". Source: (Cloud Compare) .....  | 52 |

|   |    |
|---|----|
| Figure 60 Georeferencing between "scansione 4_2_hd" e "scansione 10_2_hd". Source: (Cloud Compare) .....                    | 52 |
| Figure 61 Georeferencing between "scansione 4_2_hd" e "scansione 12_2_hd". Source: (Cloud Compare) .....                    | 53 |
| Figure 62 Final point cloud obtained from iPad. Source: (Cloud Compare) .....   | 53 |
| Figure 63 Density calculation. Source: (CloudCompare).....  | 54 |
| Figure 64 Density calculation: number of neighbors. Source: (CloudCompare) .....  | 54 |
| Figure 65 Density calculation for the Total Station Leica Nova MS50. Source: (CloudCompare) .....                           | 55 |
| Figure 66 Gaussian density calculation for the Total Station Leica Nova MS50. Source: (CloudCompare) .....                  | 55 |
| Figure 67 Density calculation for the iPad Pro Apple 11-inch. Source: (CloudCompare) .....                                  | 56 |
| Figure 68 Gaussian density calculation for the iPad Pro Apple 11-inch. Source: (CloudCompare) .....                         | 56 |
| Figure 69 Density calculation for the aerial LiDAR scan conducted by national flight. Source: (CloudCompare) .....          | 57 |
| Figure 70 Gaussian density calculation for the aerial LIDAR scan conducted by national flight. Source: (CloudCompare) ..... | 58 |
| Figure 71 Density calculation for the drone point cloud generated through photogrammetry. Source: (CloudCompare) .....      | 59 |
| Figure 72 Gaussian density calculation for drone point cloud generated through photogrammetry. Source: (CloudCompare) ..... | 59 |
| Figure 73 Georeferencing process of the iPad point cloud with the drone point cloud. Source: (Cloud Compare).....           | 61 |
| Figure 74 Distortion of the drone point cloud. Source: (Cloud Compare).....   | 61 |
| Figure 75 Mesh generated. Source: (Cloud Compare).....  | 62 |
| Figure 76 Cleaning mesh. Source: (Cloud Compare) .....  | 62 |
| Figure 77 Data integration schema. Source: (Author, 2024) .....   | 64 |
| Figure 78 Preliminary methodology schema. Source: (Author, 2024) .....  | 65 |
| Figure 79 Import command using the plugin. Source: (Revit Autodesk) .....   | 66 |
| Figure 80 Screenshot of the result on Revit software. Source: (Revit Autodesk) .....  | 66 |
| Figure 81 From the cadastral data to LOD1 schema. Source: (Author, 2024).....   | 67 |
| Figure 82 Natural Neighbor command. Source: (ArcGIS Pro).....   | 68 |
| Figure 83 DTM. Source: (ArcGIS Pro).....  | 68 |
| Figure 84 DSM settings. Source: (ArcGIS Pro) .....  | 69 |
| Figure 85 Zonal statistics as Table command. Source: (ArcGIS Pro) .....   | 69 |
| Figure 86 Generation of "triangle" shapefile. Source: (ArcGIS Pro) .....  | 70 |
| Figure 87 Generation of centroids of the new shapefile. Source: (ArcGIS Pro) .....  | 70 |
| Figure 88 Extract values to points command. Source: (ArcGIS Pro) .....  | 70 |
| Figure 89 Adding elevation data to the centroids of the polygons. Source: (ArcGIS Pro) .....                                | 71 |
| Figure 90 Difference between the elevations. Source: (ArcGIS Pro).....  | 71 |

|   |    |
|---|----|
| Figure 91 LOD1 model. Source: (ArcGIS Pro) .....  | 72 |
| Figure 92 From the points cloud to LOD2. Source: (Author,2024) .....  | 73 |
| Figure 93 Subsample command. Source: (Cloud Compare) .....  | 74 |
| Figure 94 Final result of the two point clouds merged. Source: (Cloud Compare) .....  | 75 |
| Figure 95 Import of the mesh in ArcGIS Pro. Source: (ArcGIS Pro) .....  | 75 |
| Figure 96 Visualization of the mesh in 2D Map. Source: (ArcGIS Pro) .....   | 76 |
| Figure 97 Visualization of the mesh in 3D Map. Source: (ArcGIS Pro) .....   | 76 |
| Figure 98 Create 3D object scene layer content. Source: (ArcGIS Pro) .....  | 77 |
| Figure 99 Extract multipatch from mesh. Source: (ArcGIS Pro) .....  | 77 |
| Figure 100 Visualization of the multipatch. Source: (ArcGIS Pro) .....  | 77 |
| Figure 101 Result of the join in 2D. Source: (ArcGIS Pro) .....   | 78 |
| Figure 102 Result of the join in 3D. Source: (ArcGIS Pro) .....   | 78 |
| Figure 103 From the Scan to BIM to LOD3. Source: (Author,2024) .....  | 79 |
| Figure 104 Point coordinates settings. Source: (Revit Autodesk) .....   | 80 |
| Figure 105 Model address. Source: (Revit Autodesk) .....  | 80 |
| Figure 106 North of the project. Source: (Revit Autodesk) .....   | 80 |
| Figure 107 Rotation of the north. Source: (Revit Autodesk) .....  | 80 |
| Figure 108 Shared parameters selected for the 3D model. Source: (Revit Autodesk) .....  | 82 |
| Figure 109 Shared parameters. Source: (Revit Autodesk) .....  | 82 |
| Figure 110 Shared parameters and 3D model. Source: (Revit Autodesk) .....   | 83 |
| Figure 111 Revit's layers imported in the GIS software. Source: (ArcGIS Pro) .....  | 84 |
| Figure 112 Subdivision of the Revit model. Source: (ArcGIS Pro) .....   | 84 |
| Figure 113 Join command between the walls of the Revit model and the polygon with the cadastral data embedded in it. Source: (ArcGIS Pro) ..... | 84 |
| Figure 114 Results of the join between Revit walls and the polygon. Source: (ArcGIS Pro) ....   | 85 |
| Figure 115 Integration between different sources. Source: (ArcGIS Pro) .....  | 86 |
| Figure 116 Workflow and LODs. Source: (Author, 2024) .....  | 87 |
| Figure 117 Table of the opportunities and of the threats of the thesis. Source: (Author, 2024)  | 89 |

# Acknowledgments

Mi piacerebbe esprimere un grande ringraziamento alla mia relatrice Prof.ssa Villa Valentina e alla mia correlatrice Prof.ssa Matrone Francesca, sempre pronte a guidarmi e a consigliarmi in ogni fase della realizzazione della tesi. Grazie a Voi ho accresciuto le mie conoscenze e le mie competenze. Inoltre, ringrazio il Prof. Jimenez Vicario Pedro Miguel che mi ha seguito durante la parte iniziale di questa tesi, svoltasi durante la mia esperienza Erasmus. Ringrazio tutti i professori che hanno preso parte alla mia carriera universitaria, è grazie a voi se oggi sono quella che sono.

Ringrazio la mia famiglia, che mi ha sempre sostenuta incondizionatamente, facendomi sentire amata anche quando la distanza e le difficoltà della vita ci mettevano alla prova. A voi devo tantissimo, ma più di ogni altra cosa vi ringrazio per avermi insegnato ad essere ambiziosa e a credere nei miei sogni, incoraggiandomi a perseguirli con determinazione. Grazie a mamma e a papà che dopo tanti sacrifici e tante privazioni, hanno reso possibile tutto ciò. Grazie a mio fratello, la persona più importante della mia vita, che è e sempre sarà una parte insostituibile della mia vita, grazie Ciocino. Ringrazio i miei parenti che mi hanno sempre ricordata quali fossero le mie origini e mi hanno sempre portato a riflettere sulla vita, professionale e personale.

Un ringraziamento speciale lo dedico anche ai miei amici. Agli amici di “giù” che da anni ormai sono pronti a sostenermi e a incoraggiarmi sempre. Agli amici di Torino, ormai mia seconda famiglia che mi hanno accolta dal primo anno e non mi hanno più lasciata, mi riferisco a Cops, Luca, Fra, Gra, Auror, Zimo, Nick, Ernesta, a voi devo tanto.

Ai miei amici e colleghi universitari che mi hanno fatto capire quanto sia importante avere delle persone vere, sincere e divertenti al proprio fianco nei momenti di difficoltà, ringrazio nello specifico Sara, Nadia, Martina, Edoardo, Eros, Sam, Lucrezia e Aurora. Ringrazio Diana che in quest’ultimo periodo mi è stata molto vicina, mi hai capita e sostenuta, come una grande amica. Ringrazio a tutti gli amici che ho conosciuto durante la mia esperienza Erasmus per avermi fatto capire quanto sia importante saper equilibrare la vita professionale con la vita privata. Ringrazio i miei coinquilini, nello specifico mi riferisco ad Emmanuel ed a Miriam che mi hanno seguita durante il mio percorso magistrale e mi sono stati vicini spronandomi a dare il massimo. E come non potrei, non ringraziare i miei coinquilini spagnoli Sandra e Miguel che mi hanno accolto come se fossi una sorella, mi hanno spronato a dare sempre il massimo e a prendere le giuste pause quando servivano. È grazie a voi che ho imparato a ritrovare me stessa.

Un ultimo ringraziamento speciale va a voi, Cops e Luca: sin dal primo anno, mi avete trasmesso il valore della determinazione e della perseveranza nel perseguire i propri sogni. Mi avete insegnato a restare autentica, a non perdere mai l'entusiasmo, e ad affrontare le sfide con resilienza, mantenendo sempre la stessa umiltà di fronte agli obiettivi raggiunti. Vi sono grata per il vostro esempio e per aver reso questo percorso indimenticabile.